High Density Shielding Concrete for Neutron Radiography

Mokgobi Andrew Ramushu

A research report submitted to the Faculty of Engineering and the Built Environment, University of the Witwatersrand, Johannesburg, in partial fulfilment of the requirements for the degree of Master of Science in Engineering.

Johannesburg, 2014

Declaration

I, Mokgobi Andrew Ramushu, declare that this research report is my own unaided work. It is being submitted for the degree of Masters of Science in Civil Engineering to the University of the Witwatersrand, Johannesburg. It has not been submitted before for any degree or examination at this or any other University.

.....

.....day of....., 2014

Abstract

In this research report, special High Density-Shielding Concrete (HDSC) was developed. The objective of this research was to investigate, design and test HDSC to be used to construct the newly upgraded South African Neutron Radiography (SANRAD) facility situated at the South African Nuclear Energy Corporation (NECSA).

To understand the concept of radiation shielding in detail, a literature review on several aspects surrounding radiation shielding and interaction of radioactive energies and matter was conducted. This involved aspects such as the types of radiation, theory of radiation shielding, different materials used for radiation shielding and several other topics. Based on the compiled literature and the availability of materials that could be used, concrete was selected as the best shielding material and further undertakings were carried out to develop a specific mixture that would shield the radioactive energies. The main contributing factors in the decision making with regard to the use of concrete were the already existing knowledge and technology, the local availability of most high density concrete aggregates needed, the versatility and composite nature of the material, the economic benefits of using the material, low maintenance and ease of manufacture, and the structural integrity of the material.

The final mixture produced in this research was workable and cohesive with average 28- day compressive cube strength of 29.9 MPa, water to cement ratio of 0.51 and density of 4231 kg/m^3. The concrete was made to be of high slump with a height and spread of 230 mm and 510 mm respectively. The final mixture was composed of CEM I 52.5 N, silica fume, water, hematite sand, hematite stone, steel shot, colemanite and chemical admixtures.

Dedication

This work is mainly dedicated to my beloved mother, Mmakgorong Sophia Thobakgale-Ramushu for being my rock and pillar of strength in everything that I do. Thank you *“Mogoshadi”* for being an inspiration throughout my entire education. You have been my strength when I was weak, you believed in me when I had doubts and most importantly, you identified my strengths and invested in them when I was not aware. *“Ke a leboga Ngwan’a kgoro”*

Acknowledgements

First and foremost, I would like to thank the Lord almighty for His guidance and wisdom during the challenging times of carrying out this work. He has indeed been the *"Jehovah Shammah"* throughout this research project. There were also many great minds that contributed immensely to the success of this project, without which, this project wouldn't have been a success it turned out to be. Your heartfelt and fond contributions, big or small, are sincerely acknowledged because without them, I would have given up long time ago. I would like to express my sincere gratitude to the following individuals and organisations for contributing tangibly to this project

- My supervisor, Dr. Stephen Okurut Ekolu for his guidance, constructive criticism and encouragement while I conducted the research presented in this report.
- The South African Nuclear Energy Corporation (NECSA) and the National Research Foundation (NRF) for their financial support.
- Miss. Nobuhle Mlambo, Mr. Martin Groenewald (both from ore and metal company), Mr. Eddie Correia, Mr Brenton Bouward (both from Chryso South Africa) and Mr. Charles Dominion (from simple active tactics) for providing free samples to conduct the required experiments and testing.
- Miss. Magda MCajigas from MCV enterprise in the United States of America for her compliance in supplying colemanite material.
- Lafarge Industries for allowing me to use their facilities.
- Mr. Tankiso Modise for his continued support on the project.
- Mr. Sergio Korochinsky for performing the Monte Carlo Neutron Particle (MCNP) simulation on the shielding concrete.
- Mr. Josias Mokgawa of Pelindaba Analytical Laboratories (PAL) for conducting chemical analyses on the raw aggregates of the mixtures.
- Mr. Mabuti Jacob Radebe and Mr. Frikkie de Beer for conducting radiation shielding experiments to validate the developed mixtures.

Contents

List of Figures

List of Tables

List of Definitions and Abbreviations

Activation:	The process in which neutron radiation induces radioactivity in materials.
ALARA:	As Low As Reasonably Achievable.
ANTARES:	Advanced Neutron Tomography and Radiography Experimental System.
ASTM:	American Society for Testing and Materials.
Atom:	A basic unit of a chemical element.
Au:	Gold.
Cc:	Coarse Colemanite.
CCD:	Charged-Coupled Device.
Co:	Cobalt.
Colemanite:	Colourless or white glassy mineral consisting of hydrated calcium borate in monoclinic crystalline form.
Creep Room:	Curing room kept at a constant room temperature of ± 23°C and relative humidity of ± 65%.
Cst:	Coarse Stone.
DST:	Department of Science and Technology.
Electron:	A stable subatomic particle with a charge of negative electricity, found in all atoms.
Fission:	A nuclear reaction in which an atomic nucleus, especially a heavy nucleus such as an isotope of uranium, splits into fragments usually two fragments of comparable mass, releasing from 100 million to several hundred million electron volts of energy.
FRM-II:	Forschungsreaktor München Two.
Galena:	A bluish, grey, or black mineral of metallic appearance, consisting of lead sulphide. It is the chief ore of lead.
HAC:	High Aluminate Cement.
HDSC:	High Density Shielding Concrete.
Hematite:	An ore of iron which is reddish-black in colour.
HPGe:	High-Purity Germanium

IAEA:	International Atomic Energy Agency
ICP:	Inductively Coupled Plasma.
ICRP:	International Commission on Radiological Protection
In:	Indium
Ionizing radiation:	Radiation consisting of particles, X-rays, Neutrons or gamma rays with sufficient energy to cause ionization in the medium through which it passes.
Isotopes:	Each of two or more forms of the same element that contain equal numbers of protons but different numbers of neutrons in their nuclei.
LEU:	Low Enriched Uranium.
Magnetite:	A greyish-black magnetic mineral that consists of an oxide of iron and is an important form of iron ore.
Mev:	Mega Electron Volt.
MCNP:	Monte Carlo N-Particles.
MCNP-X:	Monte Carlo N-Particles eXtended.
Mn:	Manganese.
MPa:	Mega Pascal.
NaI:	Sodium Iodide.
NDT:	Non Destructive Testing.
NDIFF:	Neutron Diffraction.
NECSA:	South African Nuclear Energy Corporation.
NNR:	National Nuclear Regulator
NR:	Neutron Radiography.
NRS:	Natural River Sand.
Nucleus:	The positively charged central core of an atom, containing most of its mass.
PAL:	Pelindaba Analytical Laboratories.
Pb:	Lead.
PC:	Portland cement.

Photons:	A particle representing a quantum of light or other electromagnetic radiation (e.g. gamma rays).
Proton:	A stable subatomic particle occurring in all atomic nuclei, with a positive electric charge equal in magnitude to that of an electron.
Radioactivity:	Spontaneous emission of ionizing radiation particles
Radiographs:	2D image generated by radiography.
RRT:	Reaction and Reactor Theory.
SDD:	Source to Detector Distance.
SAFARI-1:	South African Fundamental Atomic Research Installation one.
SANRAD:	South African Neutron Radiography.
SANS:	South African National Standards.
SANS facility:	Small Angle Neutron Scattering facility.
Tomogram:	3D image generated by radiography by rotating the analysed sample.
Uranium-235:	An Isotope of uranium element.
USNR:	Unites States Nuclear Regulator
W:	Tungsten
W/C:	Water to Cement ratio.
XRF:	X-Ray Fluorescene.

Nomenclature

$^{235}_{92}U$: Uranium 235

n : Neutron

FP : Fission product

E : Energy

γ : Gamma rays

σ : Absorption cross-section [cm^2]

X : Incident or emitted particles

µSv/h : Measurement of dose rate

I : Beam intensity [$n/cm^2/s$]

Σ : Attenuation coefficient

x : Thickness [mm]

σ_{pe} : Photon absorption by photoelectric effect

σ_{pp} : Photon absorption by pair production

σ_{cs} : Photon absorption by compton scattering

Sr : Strontium

Xe : Xenon

Chapter 1 Introduction

1.1 Background

This research was initiated as a result of the necessary upgrading of the SANRAD facility at the South African Fundamental Atomic Research Installation One (SAFARI-1) research reactor in Pelindaba-NECSA .One major component of this upgrade was the development of the shielding material around the newly proposed facility presented in Figure 1.1.This report discusses how this part of the project was addressed and how the solution has been reached.

There are several reasons why shielding of operating facilities is required in nuclear installations. The main and most important primary reason for radiation shielding is to protect people, equipment and structures from the harmful effects of radiation. When ionising radiation penetrates living tissues, it can change the chemical structures of the living cells. Exposure to moderate and high levels of radiation may therefore result in absorption of enough radiation that could alter and destroy living cells which can later develop into cancer and in some cases even cause genetic damage or birth defects. Since radiation installations are operated by people, studies have been carried out to determine levels of exposure permissible to human bodies. These levels of exposures are referred to as dose rates and measured in Sieverts [Sv]. The limits are enforced into legislation by the United Nations' International Atomic Energy Agency (IAEA) through the International Commission on Radiological Protection (ICRP) advisory board (ICRP publication 103, 2007) .South Africa as a member state is required to adhere to these limits. The dose limits as outlined in the ICRP publication 103 of 2007 are given in Table 1.1 and 1.2. In terms of radiation shielding design, the most important limit is that of occupational exposure of any worker which must be controlled to ensure that the limit of effective dose rate of 20 mSv per annum averaged over five years is not exceeded. In South Africa, the dose limits are incorporated into national legislation and the National Nuclear Regulator (NNR) is responsible for regulating this legislation by ensuring that all nuclear based entities are in compliance with the stipulated limits. As part of the upgrade of the SANRAD facility, NECSA as the owner of the facility was required to

obtain the license to construct and operate it from the NNR. It was therefore necessary to demonstrate to the NNR that every measure has been taken to ensure that adequate shielding has been provided and that the facility is in compliance with the legislation. The developmental process and procedure presented in this report was therefore one of the vital submissions to the NNR. The secondary reason for providing adequate shielding was to ensure that the radiation levels (i.e. radiation noise) emerging from the SANRAD facility does not affect other neighbouring facilities which are the Small Angle Neutron Scattering (SANS) and the Neutron Diffraction (NDIFF) facilities as shown in Figure 1.2. The reason for providing adequate shielding for the SANRAD facility was therefore to ensure that the facility complies with the requirements of the legislation for license purposes and also that levels emerging from the facility do not affect the neighbouring facilities.

Table 1.1: ICRP recommended dose limit for occupational exposure to ionising radiation

Type of dose	Dose Limit
Effective dose (excluding pregnant women)	20 mSv per year
Dose to skin, hands and feet	500 mSv per year
Dose lens to lens of an eye	150 mSv per year
Effective dose to pregnant women	1 mSv from diagnosis of pregnancy to its end
Radionuclide intake by pregnant woman	1/20 of regular limiting annual limit on intake for duration of pregnancy

Table 1.2: ICRP recommended dose limit for exposure of the public to ionising radiation

Type of dose	Dose Limit
Effective dose (excluding pregnant women)	1mSv per year
Dose to skin, hands and feet	50 mSv per year
Dose lens to lens of an eye	15 mSv per year

Kaplan (1989) describes radiation shield as a physical barrier placed between a source of ionizing radiation and the object to be protected so as to reduce the radiation level at the position of the object. There are many potential materials that can be used as shielding for radiation but over the years, concrete has been proven not only to be

effective and versatile, but also economical. Unlike materials such as lead which may lack structural integrity, and water that might cause complications such as rusting and leakage on the containers, concretes of normal and special types have many advantages for permanent shielding installations (Kaplan, 1989).

The use of HDSC as shielding material allows for installation of reasonable wall thicknesses which are capable to attenuate neutrons and photons. This is an advantage because the radiation absorption process normally required very thick shields to ensure that the required dosage levels are achieved after the radiation has passed through the shield. Some of the many advantages of using concrete as a shielding material is that it can be cast into almost any complex shape (Callan, 1962) and that through varying its composition and density the shielding characteristics of concrete may be adapted to a wide range of uses (Kaplan, 1989). Even though concrete has some disadvantages such as low thermal conductivity which might result in high thermal stresses and high decommissioning costs, it still remains the widely used material for radiation shielding purposes because of its proven performance throughout the years.

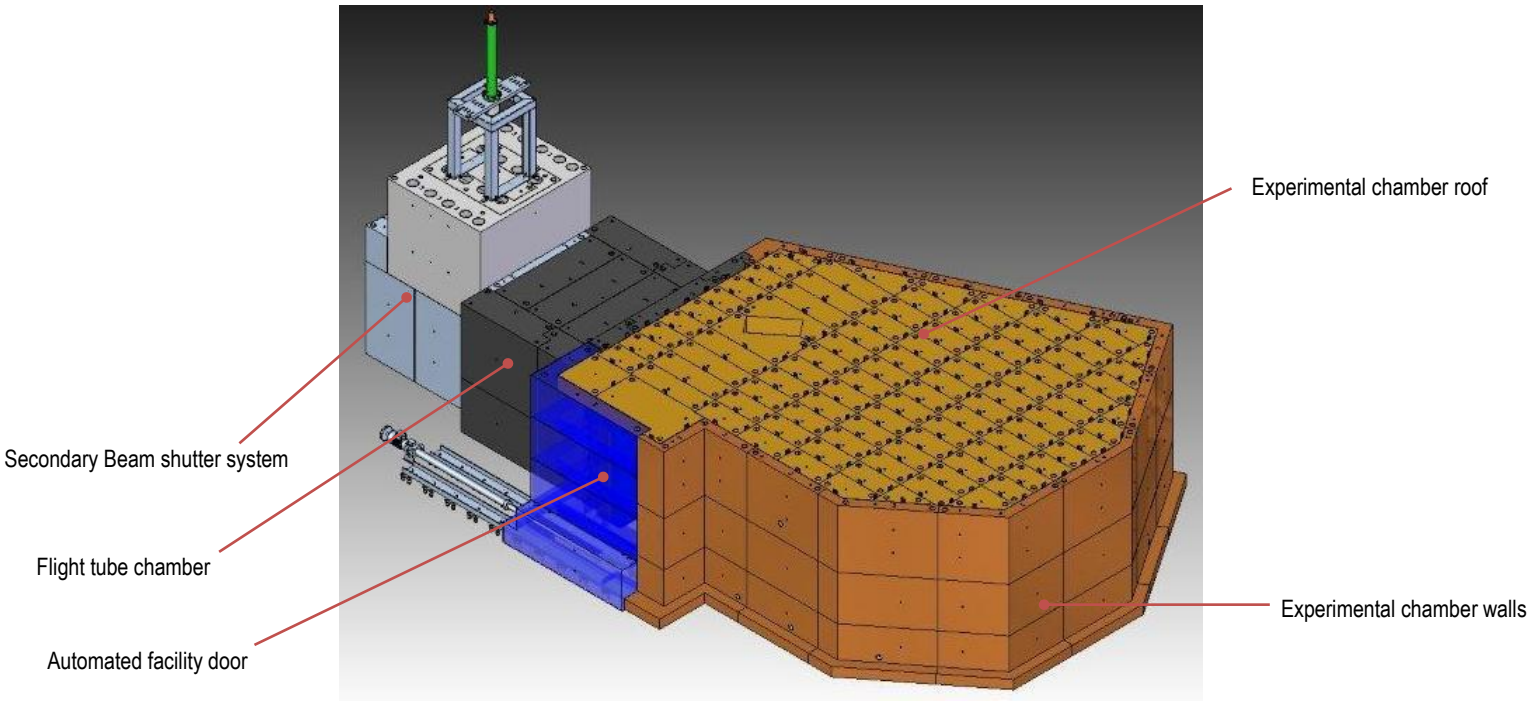

Figure 1.1: The upgraded SANRAD facility made of HDSC interlocking blocks (Masitise & Mhlanga, 2012)

1.2 The South African Neutron Radiography facility

The Southern African Neutron Radiography (SANRAD) which was formerly known as the Neutron Radiography (NRAD) is situated at beam port number 2 of the 20 megawatt SAFARI-1 nuclear research reactor in Pelindaba in the North West province of South Africa. The facility has been in operation since 1975 where it has been using a film technique. It was later upgraded to an electronic CCD system in 1995 and in 2003 it was also equipped with tomography capabilities in collaboration with the Paul Scherrer Institute (PSI) in Switzerland (De Beer, 2005). SANRAD is a product of a South African governmental initiative to upgrade national research equipment and is a part of the South African national system of innovation. The facility is utilised by researchers and post graduate students in South Africa as an analytical tool and together with the micro-focus x-ray system at NECSA they form the South African National Centre for Radiography and Tomography (Hoffman, 2012).

The current SANRAD facility as shown in Figure 1.2 consist of the containment and experimental control areas. The containment area is where the sample is exposed to neutron radiation and shields the surrounding areas from penetrating radiation. The imaging system for radiography is located inside this containment area. An experimental control area is where stage rotations and image acquisitions are controlled (Radebe and De Beer, 2008). The facility is 2 m in length, width and height. The biological shield of the reactor forms one of the vertical sides, while the other three sides and the roof are made of 450 mm thick concrete with density of 3300 kg/m^3. The concrete is covered on the inside by a 40 mm layer made of 20 mm thick wax tiles containing 5% boron by mass and 20 mm thick polyethylene sheet (Radebe and De Beer, 2008). Part of the concrete roofing directly above the sample is removable to accommodate samples longer than 2 m. To improve the shielding performance of the facility, the outer walls of the containment is covered by 50 mm lead (Pb) bricks for shielding against secondary gamma rays emerging from neutron interaction with the sample and concrete shielding. The fourth side of the facility directly opposite to the biological shield is used as an entrance and a beam stopper. It is 1500 mm in thickness and is made of 3300 kg/m^3 concrete contained in 5 mm thick steel plates. To open and close, the block is driven

backward and forward by a motor. The front surface of the beam stopper block is covered with 40 mm layer comprised of 20 mm of wax containing 5% boron and 20 mm polyethylene (Radebe and De Beer, 2008).

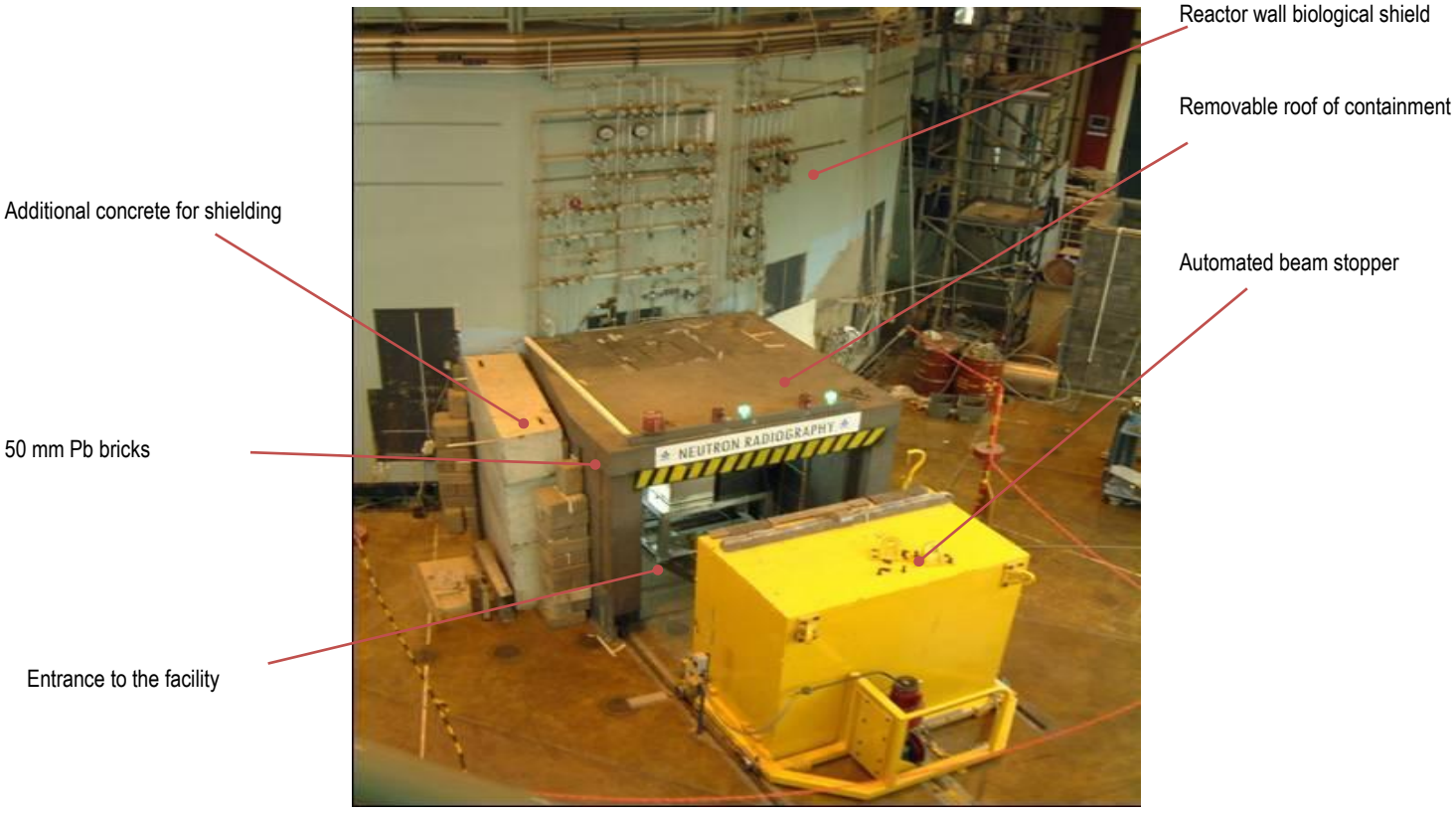

Figure 1.2: The current set up of the SANRAD facility at beam port 2 of SAFARI-1 research reactor (Radebe and De Beer, 2008)

The need for upgrading the facility to European standard was as a result of the deficiencies present at the current facility. These deficiencies include inadequate radiation shielding that shower neighbouring instruments with stray neutrons, corrosion of the collimator system, inhomogeneous beam profile and low flux (Radebe and De Beer, 2008). Besides the deficiencies, the upgrade was also necessary because of the need to improve the minimum functional scientific and experimental capabilities of the facility by incorporation multifunctional systems that offers fast neutron, thermal neutron, gamma ray, phase contrast and dynamic radiography (Radebe and De Beer, 2008). The objective of the upgrade of the facility was therefore to achieve: (a) the highest

possible neutron flux in the detector plane, (b) a homogenous neutron illumination in the detector plane within an area of 35 cm x 35 cm, (c) low background of scattered neutron and gamma ray radiation around the detector system, (d) low background radiation levels outside the facility for neighbouring instruments and compliance with radiation protection requirements and (e) low cost high density radiation shielding concrete. The facility upgrade was solely funded and supported by the Department of Science and Technology (DST) through the National Research Foundation (NRF). The proposed design of the upgrade is as shown in Figure 1.1.

1.3 Motivation

In radiation shielding, before any material can be chosen for shielding purposes, it is very important to have knowledge of the following:

- What type of radiation is to be shielded?
- What amount of radiation is to be shielded?
- What energy of radiation is to be shielded?

The answers to the above questions are obtained by determining the source of radiation. This implies that, since sources of radiations are never the same, every source will have its own specific shield requirements. This was the main motivation in this research, to develop a special concrete shield that will be used to contain the radiation source coming from beam port two of SAFARI-1 reactor.

The other motivation came from the lack of local availability of information regarding previous practical experiences in using concrete for radiation shielding in South Africa. One main source of information which was used as reference in this research was that of the installation of the Advanced Neutron Tomography and Radiography Experimental System (ANTARES) facility installed at Forschungsreaktor München Two (FRM-II) reactor in Germany. The only useful information that could be extracted from the installation of this facility was the types of aggregates that could potentially be used for developing high density concrete for radiation shielding (Gruenauer, 2005). The mixture proportion of the concrete, mechanical properties and shielding properties of the concrete were still undefined as they were all a function of the source to be shielded.

The study and construction of the facility did however provide an insight on how to go about developing the high density concrete for shielding.

The ANTARES facility's research on the concrete was mainly focused on neutron particle models and simulations. No focus was placed on the mechanical properties of the concrete, and as a result, the concrete was of undesirable quality as the compositions were only based on the outputs from the Monte Carlo N-Particles (MCNP) simulations. There were segregation and cohesion problems experienced with the final product. The consistence achieved was also not completely suitable for the application. This is because during pouring and placing of concrete into the permanent interlocking steel boxes, the concrete could not properly fill in the corners of the boxes. Consequently, the facility was demolished and a different shielding material has been used. To avoid the mistakes encountered in the ANTARES facility, it was decided to divide the development of the shielding concrete research into four areas of concerns which were: chemical analyses of raw aggregates, MCNP simulations, mechanical testing and evaluation of shielding properties. This was to ensure that all aspects that could negatively affect the performance of the shielding material were addressed.

1.4 Objectives

The main objective in this research was to produce a verified and validated design of a concrete shield to be utilised to contain the radiation emerging from a core of SAFARI-1 nuclear reactor and being transported by the port into the neutron radiography experimental chamber as schematically presented in Figure 1.2. In order to achieve this objective, the following needed to be conducted:

- Identifying and sourcing of raw materials to be used in development of the special concrete.
- Testing of the identified materials for chemical compositions.
- Performing MCNP simulations using the identified aggregates for selection of the most effective mixture for shielding purposes.
- Performing trial concrete mixtures using the identified aggregates and outputs from the MCNP simulations.

- Testing of the concrete's mechanical properties.
- Validating the shielding capabilities of the developed concrete using foil activation method and verifying against the MCNP simulations.

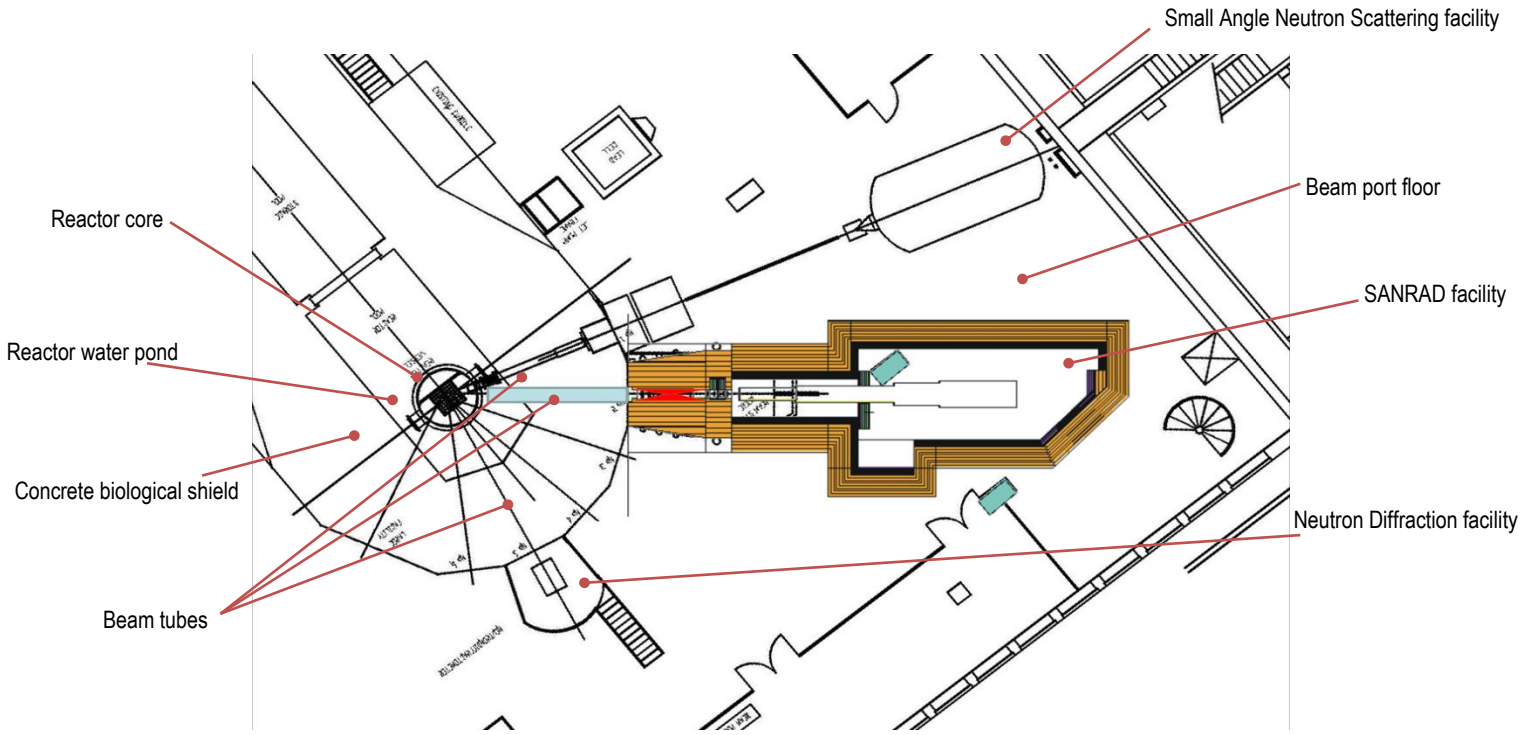

Figure 1.3: The top view of SAFARI-1 building beam port floor showing the beam ports and location of the SANRAD facility (De Beer, 2005).

1.5 Scope and limitations of the study

The scope of this investigation was to develop a high density shielding concrete that will be used in the construction of the upgrade of the SANRAD facility. The development of the product was guided by the As Low As Reasonably Achievable (ALARA) principle which entailed that the product to be produced was should be economical and still be capable to shield the strong radiation emerging from the facility to the lowest dose rates as possible without compromising the required mechanical properties of the concrete. The product was also required to be composed of mostly locally sourced ingredients. The materials used to produce the product were required not to contain chemical elements that when irradiated will take long time to decay. This was to enable the facility to be decommissioned within a reasonable period of time at the end of its design life

and that during decommissioning there should not be elements that are still active and emitting radiation which will be harmful to workers. The product was also required to be theoretically designed through the use of simulation packages so that the output could be used as the basis for the physical development process. Furthermore the final developed product was required to be verified using the available Neutron Radiography facility at NECSA.

The limitations of the above defined scope were from the fact that the resulting product was required to be practical for implementation as it would be used for the installation of the real operating facility. One of the main limitations was time given for the research as the product was required at a specific date. Cost of the product was also a major limitation. The product was required to be cost effective with the optimisation of the cost required in the selection of raw materials. The project required 90% of the material to be sourced locally. Therefore only known and accessible materials could be used in the investigation. The materials selected were also required to be used in the form obtained from the suppliers as converting them was expected to be uneconomical. The space availability where the facility was to be erected was one of the limitations that contributed a great deal to this investigation. Normally if space is available in abundance, the thickness of the shielding walls of the facility can be increased so that the density of the concrete does not have to be very high. In the case of SANRAD facility, the space was limited and therefore the shielding walls were required to be 600 mm which implied that the density was required to be higher. In order to comply with scheduled date for the construction date of the facility; the physical development of the product was limited to the following mechanical properties: consistence, workability, cohesion, density and strength.

1.6 Research Outline

This research was divided into four main sections which were materials investigation, theoretical modelling, concrete development and radiation shielding performance evaluation. The purpose of these consecutive sections was to ensure that an adequate and cost effective shielding concrete was developed.

The raw materials investigation section analysed the chemical compositions and characteristics of the identified aggregates with the purpose of selecting raw materials with better compositions and eliminating those with undesired compositions. The outcome of this section was optimisation of the final product by ensuring that raw materials selected contained high quality of desired chemical elements required for shielding and that these were cost effective and obtainable for mass concrete casting. The theoretical analysis section of this research modelled the radiation shielding performance of the concrete based on the selected aggregates from the raw materials investigation section. This was necessary as a guideline and basis for the subsequent concrete development section. The section provided an indication of the required properties of concrete for shielding of radioactive energies emerging from the facility to be shielded. The physical shielding concrete development section used the outcome of the previous sections to design trial concrete mixtures which were cast and tested until all necessary desired mechanical and physical properties of the product were achieved. The final section of the research was the physical testing of the shielding performance of the adopted shielding concrete which satisfied the mechanical and physical properties in the previous section. The purpose of this exercise was to confirm the capability of the final developed concrete in shielding SANRAD facility's radiation.

Chapter 2 Theoretical rumination and literature review

2.1 Radiation Theory and units of measure

Radiation refers to energy emerging from a source and travels through space and may be able to penetrate various materials (Health physics society, 2013). The phenomenon of radioactivity was discovered by Henri Becquerel in France in 1986 following the discovery of x-rays by Wilhelm Roentgen in 1985 (Kaplan, 1989). Becquerel found that certain minerals which contained elements such as uranium, thorium and radium were capable of emitting invisible penetrating energy spontaneously and because of their ability to give off this extraordinary energy, he described these minerals as being radioactive (Kaplan, 1989).These discoveries were later followed by the development of artificial sources of radiation in the twentieth century with the discovery of the neutron in 1932, the discovery of nuclear fission in 1938, the construction of the first nuclear reactor in 1942 and the development of the nuclear explosives in 1945 (Kaplan, 1989).

The kind of radiation that required shielding is known as ionising radiation because it can produce charge particles in the matter it interacts with. This radiation is produced by unstable atoms. Unstable atoms are created by means of disturbing nuclei of stable atoms. In order to reach stability, unstable atoms emit radiation. This emission of radiation is called decaying and the time it takes for atoms to fully decay different from atom to atom. The most used indication of the decaying of atoms is given by the half-life measure which is the period it takes for an unstable atom to lose half of its radiation to reach stability. An example of disturbing a nucleus of a stable atom into unstable atom is given in Figure 2.1 (Bishop, 2013). Cobalt-60 is not a naturally occurring isotope. It is therefore formed from the neutron activation of a stable isotope cobalt-59. When a cobalt-59 nucleus is bombarded by a neutron, the added neutron changes the cobalt-59 to unstable cobalt-60. To reach a more stable state, cobalt-60 undergoes a beta emission decay process whereby a neutron becomes a proton and an electron. The proton stays in the nucleus and the electron which is called a beta particle is ejected from the atom. The beta and energy (gamma rays) emission of the Cobalt-60 therefore results in a stable Nickel-60.The decay half-life of Cobalt-60 is 5.27 years.

Cobalt-59 converted to cobalt-60

$$^{59}_{27}\mathrm{Co} + {}^{1}_{0}\mathrm{n} \rightarrow {}^{60}_{27}\mathrm{Co}$$

A neutron collides with a Co-59 nucleus and forms Co-60.

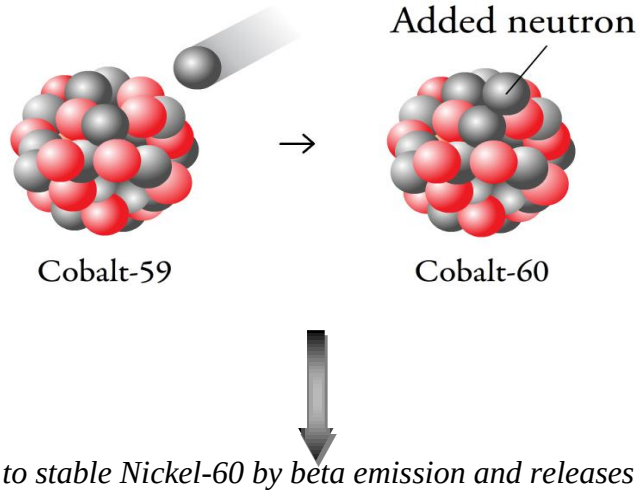

Cobalt-60 decays to stable Nickel-60 by beta emission and releases gamma radiation

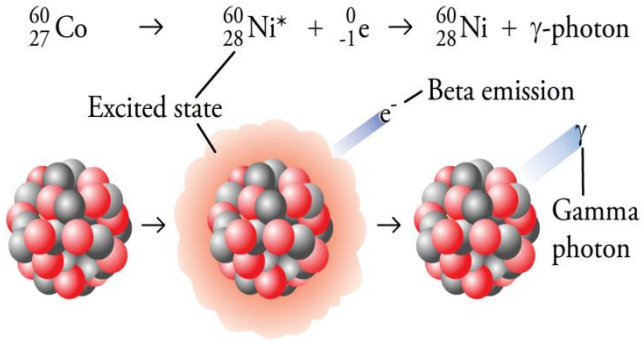

Figure 2.1: Changing of stable cobalt isotope to an unstable cobalt isotope (Bishop, 2013).

Unlike other types of radiations such as heat and light, ionising radiation produced by decaying of atoms is invisible to human senses. It cannot be seen, heard, tasted or smelled and this is what makes it dangerous to human beings. It can however be detected and measured with quite simple radiation measurement instruments such as personal dosimeters and full body count devices (NNR, 2013). The exposure to ionising radiation is measured in Sieverts [Sv]. The main types of ionising radiation are alpha particles, beta particles, gamma rays and neutrons. All these types of radiation can

cause physical damage to living cells which may result to cancers and cause genetic damage to present and future generation (NNR, 2013). The materials effective for shielding these types of ionising radiation are given in Figure 2.2 (NNR, 2013). Alpha particles are barely able to penetrate skin and can be stopped completely by a sheet of paper. Beta radiation consists of fast moving electrons ejected from the nucleus of an atom. More penetrating than alpha radiation, beta radiation is stopped by a book or human tissue. Gamma radiation is a very penetrating type of radiation. It is usually emitted immediately after the ejection of an alpha or beta particle from the nucleus of an atom. It can pass through the human body, but is almost completely absorbed by denser materials such lead (NNR, 2013). Neutron radiation is produced when neutrons are ejected from the nucleus by processes such as nuclear fission (Equation 1). Neutrons are the most difficult to shield as they penetrate through almost every material. Lighter material such as the atoms of boron and hydrogen are very effective in slowing down fast neutron to thermal neutrons. This slowing down process then generates secondary gamma rays which also need to be shielded. Heavy atoms such as iron are effective in stopping thermal or slow neutrons. Therefore to effectively shield neutron radiation, a composite material with all these atoms is necessary.

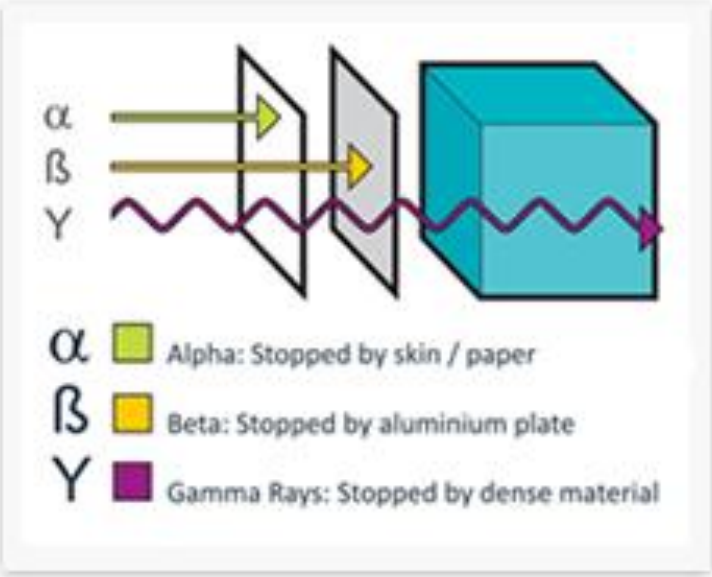

Figure 2.2: Shielding material for different types of ionising radiation (NNR, 2013)

2.2 Neutron Radiography

The term “radiography” refers to the creation of images on film or digital data media by the irradiation of objects. Usually the purpose is to see and evaluate the inside of the objects without destroying them in the process. The most familiar and widely used form of radiography is x-ray radiography. Less well known, but not less valid, is Neutron Radiography (NR) which instead of x-rays uses neutrons. In contrast to x-rays, neutrons are able to penetrate heavy metals such as lead and uranium and can also be used for analyses of delicate organic materials and water. As such, NR is becoming increasingly established as a method of Non-Destructive Testing (NDT) as a supplementary to x-ray radiography or as the only option under consideration. It is increasingly used in the nuclear research and development field to analyse objects by transmitting a neutron beam through an object and recording it by a plane positioned sensitive detector. The detector records a two-dimensional image that is a projection of the object on the detector plane and by combining images from measurements at different angles tomographic re-construction may be carried out (Scherrer, 2007).This technique is based on the application of the universal law of attenuation of radiation passing through matter. Because different materials have different attenuation behaviours, the neutron beam passing through a sample can be interpreted as a signal carrying information about the composition and structure of the sample (Scherrer, 2007).

In principle, NR works in the same way as x-ray radiography but with a few important physical differences. NR can provide certain information that would be impossible with x-ray radiation. Neutron and x-ray radiography of the same object often produces different but complementary information, as can be seen from the illustration on Figure 2.3. In this figure, a sample of reinforced concrete was subjected to the two methods of radiation imaging and the results show the different effects of the methods (Scherrer, 2007). The green image shows a tomogram (3D) generated by neutrons. It is possible to recognise the hydrogen-containing components, though nothing can be seen of the steel fibres. In the blue image, an x-ray tomogram, the structure of the steel fibres is

practically all that can be recognised. The two images on the far left are radiographs (2D) of the same object (Scherrer, 2007).

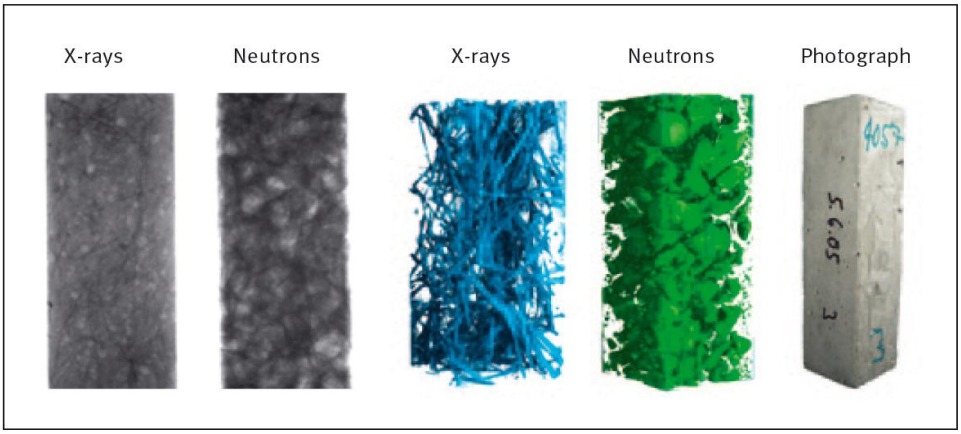

Figure 2.3: Concrete Neutron and X-rays radiography images (Scherrer, 2007)

The principle of a radiography system is illustrated as shown in Figure 2.4.

- A beam of neutrons is extracted from the source by means of a beam tube. This source of neutrons is generated by either a reaction that splits the nucleus apart, or by a spalling reaction. These options for generating neutrons are known as fission (from a reactor core) and spallation (from an accelerator).
- At the end of the beam tube there is a beam shutter which is used to close /block the beam line when the facility is not in operation.
- The evacuated collimators after the shutter are used to propel neutrons before they hit the test object.
- The filters serve to select the required type of neutrons for different experiments.
- The flight tube serves to further direct the beam onto the sample to be examined.
- Beam limiters restrict the beam from the flight tube only onto the sample.
- The detector behind the sample captures a two-dimensional image of the radiation, which will have been weakened to a greater or lesser degree by the sample.
- The catcher behind the detector absorbs any strong radiation that may be present after it has penetrated and passed the sample.

- The shield around the facility is to protect persons from the inside radiation at any particular time when conducting the experiment. Radiation protection requirements must therefore be taken into account to accommodate the facility in a room that is specially secured and shielded against the type of radiation being used.

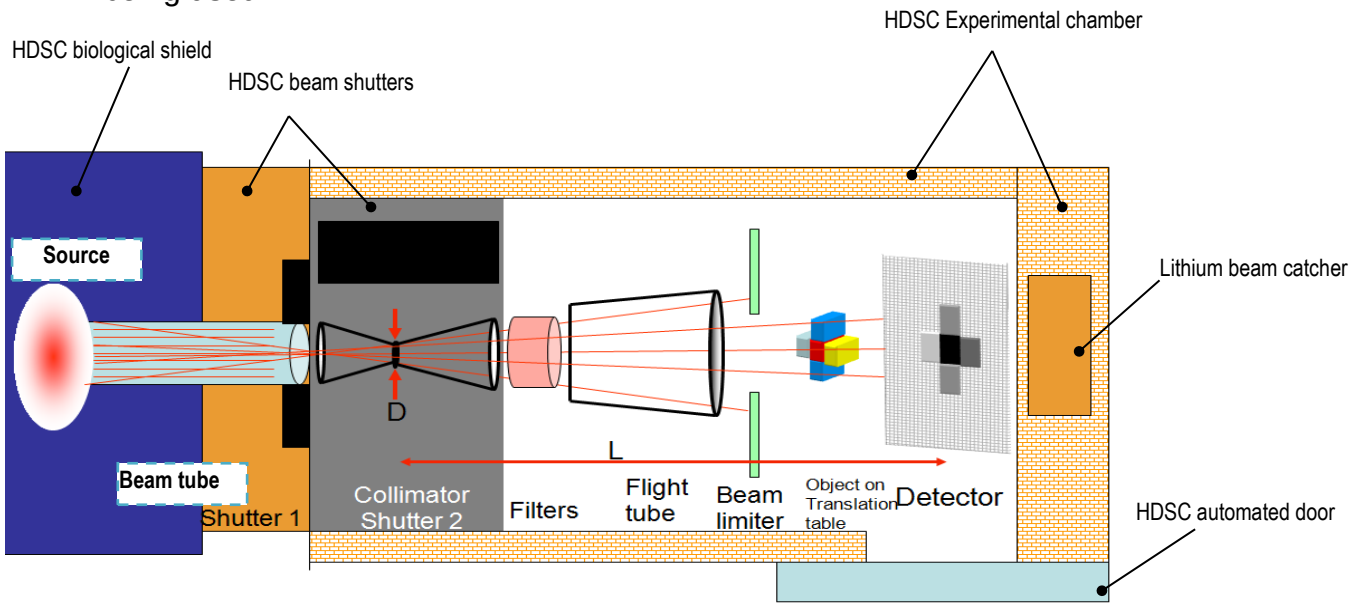

Figure 2.4: Conventional Principle of Neutron Radiography (De Beer, 2005).

2.3 Theory of radiation shielding

In radiation shielding, before any material can be decided on for shielding purposes, it is crucial to have knowledge of the source of radiation. This source is fundamentally defined by the type, amount and energies of radiation levels to be protected. The three parameters defining the source are addressed in the subsequent subsections.

2.3.1 Types of radiation to be shielded

This depends on the method used to generate the source. Fission process is the method of radiation source generation used in this study. As a result of the fission process taking place in the reactor core, the extracted beam includes photons (i.e. gamma rays) and unstable radioactive fission products which will also need to be shielded. The radiations of interest to be shielded in this case are therefore neutrons and photon and these are further discussed below. In the nuclear reactor, the nucleus of the heavy uranium-235 atoms [^{235}U] absorbs a thermal neutron [n] to initiate the fission

process where it splits into two nuclei called fission products [*Sr* and Xe]. For each fission reaction that occurs, between two or three neutrons are also emitted. These neutrons therefore cause further fission of the enriched nuclei of uranium atom and hence the release of more energy, formation of more fission products, emission of more neutrons and consequent chain reaction (Kaplan, 1989). The typical initial reaction in the reactor core can simply be presented by Equation 1.

$$^{235}_{92}U + ^{1}_{0}n = \ ^{94}_{38}Sr + \ ^{140}_{54}Xe + \ 2\ ^{1}_{0}n - (1)$$

To provide the best shielding for the above identified radiations, it is crucial to understand how they interact with matter and their respective reactions with matter are discussed below.

2.3.1.1 Interaction of photons (gammas) with matter

The gamma radiations [γ] to be considered for shielding are only those which have energy greater than 0.1 MeV. These are:

- Prompt–Fission gamma photons.
- Fission product gamma photons.
- Capture gamma photons.
- Activation gamma photons.

In radiation shielding, three types of photon interaction with matter are generally considered to be of importance (Callan, 1962) and these are called:

- Photoelectric effect [σ_{pe}]
- Pair production [σ_{pp}]
- Compton scattering [σ_{cs}]

Photoelectric effect

This process gets its name from somewhat similar process by which light produces current in a photoelectric cell (Kaplan, 1989). This is the interaction process in which an orbital electron is ejected from an atom by a photon. As shown in Figure 2.3, this occurs when a photon possess a higher energy than the binding energy of the orbital electron with which it collides (Kaplan, 1989). All of the energy of the incident photon in excess

of the electron binding energy is transformed into kinetic energy of the ejected photoelectron. The effectiveness of a shield in attenuating a beam of photons by this process therefore depends upon the relation between the energies of the incident photon and the energy required to eject the various electron (Kaplan, 1989). The probability of absorption through removal is greater for a photon whose energy is approximately equal to the binding energy of that electron. If however the incident photon energy is less than the binding energy, no interaction whatsoever can take place. From radiation shielding perspective, the photoelectric effect is considered to be a genuine absorption process (Kaplan, 1989).

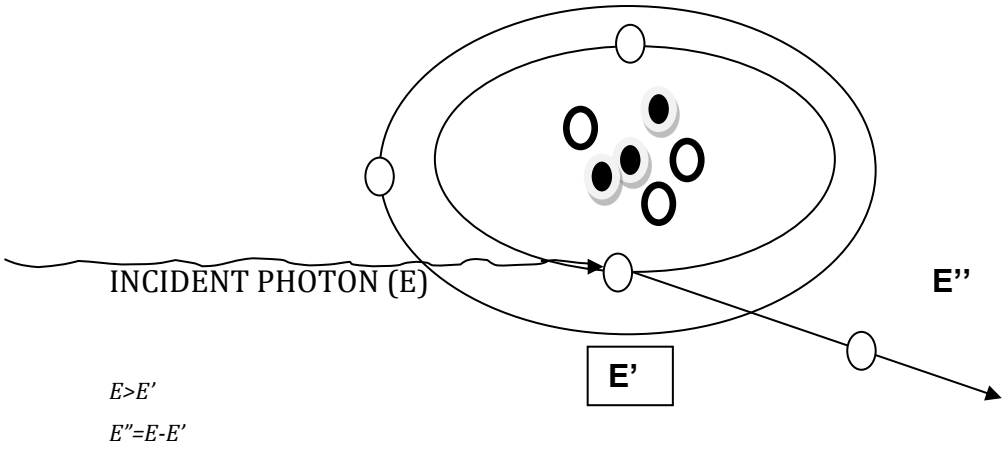

Figure 2.5: The photoelectric effect (derived from Kaplan, 1989)

Pair production

As shown in Figure 2.4, this is the process in which a photon is converted into a pair of electrons, one positron and one negatron in the Coulomb field of an atomic nucleus. Pair production, just like the photoelectric effect, is considered to be a true absorption process (Kaplan, 1989).

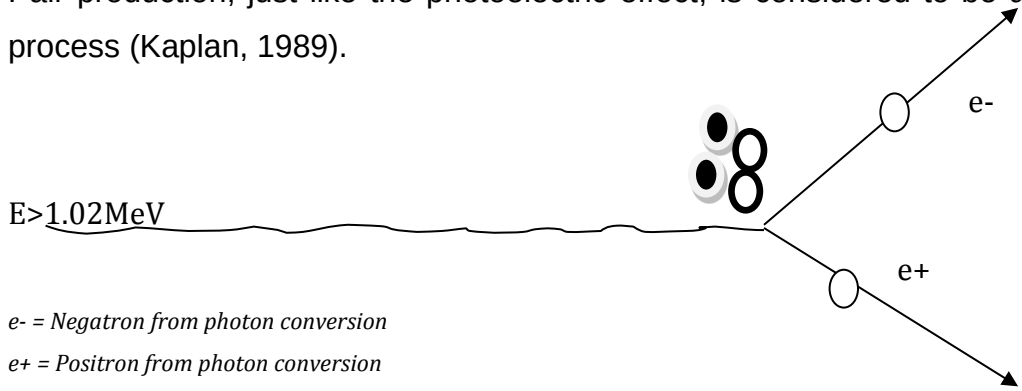

Figure 2.6: Pair production (derived from Kaplan, 1989)

Compton scattering

In this process, a photon collides elastically with an electron of an atom and transfers part of its energy to the electron being deflected from its original path (Figure 2.5). However, since the photons are only scattered and not destroyed, the total intensity of the radiation passing through a shield may be much greater than the intensity of the unscattered radiation component passing the shield. Successive collisions due to several compton scatterings may lead to the energy of the photon being reduced to a level where it is absorbed by the photoelectric effect process.

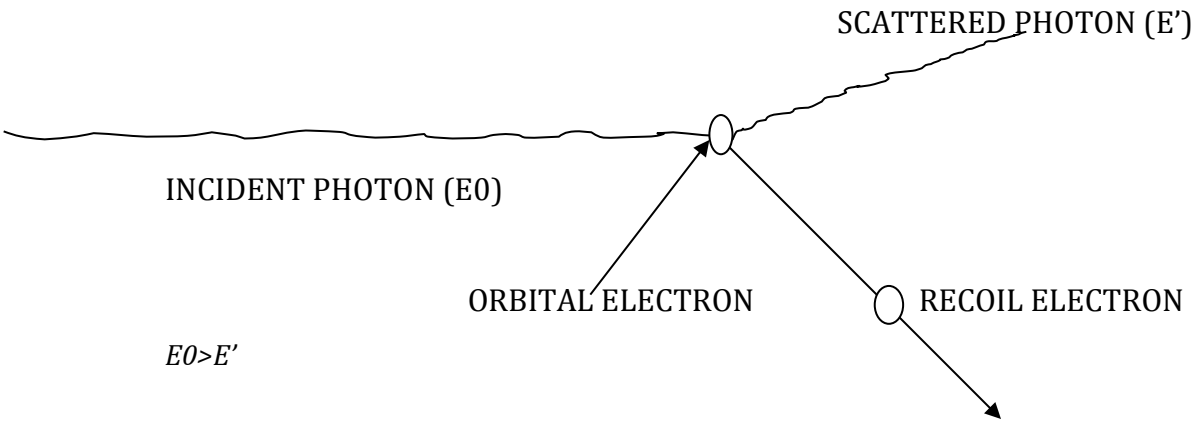

Figure 2.7: Compton scattering (derived from Kaplan, 1989)

From the above, the absorption of the gamma radiation is accomplished by three processes. The total photon interaction cross-section which is the measure of a probability of occurrence of the photon absorption process is given by Equation 2.

$$\sigma_{total} = \sigma_{pe} + \sigma_{pp} + \sigma_{cs} \quad (2)$$

2.3.1.2 Interaction of neutrons with matter

Unlike photons which interact with electrons in the atom, the neutrons interact with the nucleus of the atom and their interaction is dependent on the kinetic energy of the neutrons themselves (Callan, 1962). The attenuation of neutrons is accomplished chiefly by:

- Causing them to lose energy or
- Causing them to be slowed down in collision with the nuclei, followed by capture of slowed down neutrons in nuclei, with emission of gamma rays by the target nuclei.

In transmission of neutrons through matter, many types of reactions or interaction with the nuclei of atoms are possible. In shielding of neutrons, the most significant of these interactions are:

- Elastic scattering.
- Inelastic scattering, and
- Neutron capture.

Elastic scattering

In this process, a neutron collides with a nucleus and re-bounds with a transfer of energy to the target nucleus. The more nearly the target nucleus has the same mass as the neutron, the greater the possible energy loss in a collision. For an example, hydrogen nuclei have approximately the same mass as neutrons and so are most efficient in slowing the neutrons. This collision-reaction can be written as in Equation 3.

$$n + nucleus = n' + \gamma \quad (3)$$

Inelastic scattering

This process also leads to loss of energy by neutrons. It involves the loss of energy in exciting the target nucleus, without loss of identity of the neutron. The excitation energy of the residual nucleus is subsequently emitted in the form of photons. Inelastic scattering is dependent on the energy of the neutron and the target material, occurring only for certain energy bands within which the inelastic scattering cross-section increases markedly. This process is important for high energy neutrons but is normally not a major factor for neutrons near the thermal energies with respect to elements present in concrete.

Neutron Capture

In this process, the incident neutron is captured or absorbed by nucleons leading initially to the formation of an intermediate nucleus in highly excited state. Fast neutrons which have slowed down may however have large radioactive capture cross-section area. This gives rise to the emission of one or more photons per capture and these are of much concern in radiation shielding analysis.

The source of radiation for the SANRAD facility is generated by fission process taking place in the core of SAFARI-1 research reactor. The photons produced will therefore experience photo electric effect, pair production and compton scattering when colliding with the concrete shield. The produced neutrons will also experience elastic scattering, inelastic scattering and neutron capture when interacting with the high density concrete shield. The wall thicknesses of the concrete shield developed in this study should therefore be able to accommodate all the interaction processes discussed above.

2.3.2 Amount and energies of radiation to be shielded

These are obtained from a theoretical calculation method based on the theory of transportation of radiation through matter. The method that was used in this project was the Monte Carlo N-Particles (MCNP) simulation method as explained in section 3.3 of this report. This technique has a statistical basis which has been developed by making use of the physics of the transportation equation. The low enriched uranium (LEU) core of SAFARI-1 was modelled using the MCNP simulations to determine flux intensities in the beam port and the facility.

2.4 Use of concrete as a radiation shield

As mentioned above, concrete is versatile and economical for shielding purposes and that was the reason it was chosen to be used as a shielding material in this study. The difficulty in radiation shielding especially from sources generated by the fission process in the nuclear reactors is the presence of different types of radiation in the source. This implies that different elements need to be combined to be able to shield a single source.

Concrete is therefore important because of its composite nature. This allows different materials of different chemical compositions to be combined to provide adequate shielding. The composition of concrete has an important effect on its shielding properties. For shielding of gamma rays, the density of concrete is of most importance. Density can be increased by incorporating heavy aggregates in the concrete mixture. The greater the density, the smaller the thickness of concrete required (Kaplan, 1989). For protection from neutron radiation the most desirable composition of materials in a concrete shield is more complicated (Kaplan, 1989). Materials of low atomic weight such as hydrogen usually in the form of water are required to reduce fast neutrons to slow neutrons of thermal energy. Materials such as boron are required to absorb thermal neutrons without producing high-energy secondary gamma radiation in the process (Kaplan, 1989). Concrete for radiation shielding must therefore in most cases be effective against both gamma and neutron radiation. This implies that heavy as well as light materials are required for shielding purpose and a compromise must therefore be made in the composition of concrete for radiation shielding. In addition to these shielding requirements, a concrete radiation shield also serve a structural function. This means that mechanical properties that are important structurally should also be satisfied.

The important properties of concrete which need to be established during any radiation shielding concrete development include:

- Ingredients
- Density
- Mechanical properties
- Shielding properties and
- Thickness of the shield

Determining the above parameters is a challenge because the published literature on the use of concrete for radiation shielding is not extensive. In most cases when there is literature on this topic, most of it is presented primarily from the standpoint of the shielding properties, with mechanical characteristics of the concrete mixtures which are normally of concern being subordinated or completely omitted (Callan, 1962). Many of

the studies, some which will be extensively discussed in this section, were found to be concerned primarily with heavy concrete, most of which contained iron ore as aggregate. No emphasis was placed on mechanical properties of concrete and as a result many problems arose with regard to cohesion, workability, segregation and strength. The other challenge presented by previously studied heavy density concretes was that most of the aggregates used were neither available nor well-graded materials because they were sourced directly from the mines and their primary used was not for concrete casting. The aggregates therefore contained particle sizes which were not standardised and not suitable for concrete casting. Callan (1962) in his research also found that the effects of the above omitted factors have not been sufficiently discussed.

Just like any other radiation shielding concrete design and development, the major difficulty in this research has been the lack of experimental data for various conditions of radiation energies and concrete types. The reason for this is that most of the work in the nuclear field is classified for security purposes. As a result of this sensitive information classification, it is found that technical problems involved in the development of HDSC mixtures are not extensively studied. There are therefore areas that still require attention in developing and designing HDSC. These include (Callan, 1962):

- The question of segregation and workability to provide a sound homogenous mixture.
- The use of high water content that is desirable for neutron shielding.
- Methods for placing in fairly massive structures.
- Special cementing media.
- Effects of different additives such as boron containing aggregates.
- Effect of high temperatures for indefinite periods.

The above items can be better achieved when knowledge from different domains such as concrete technology, nuclear physics and chemistry are integrated in developing the concrete shielding medium. This is the approach that was adopted in this research after realisation of the above mentioned difficulties.

2.4.1 Previously studied high density shielding concretes

This section discusses some of the studies that informed the selection of materials in this investigation. As previously mentioned, the data presented by these researches were limited in terms of the mechanical properties as most of them focused on shielding properties. The useful information extracted from these studies was mainly the types of aggregates that could potentially be incorporated into the concrete mixture to produce the required density for shielding the radiation fluxes of the SANRAD facility. The studies reviewed in this section were those that contain aggregates which were in accordance with ASTM C637 and ASTM C638.

ASTM C637 and C638 are the two standard specifications prepared by the American Society for Testing and Materials (ASTM) sub-committee specifically for aggregates for radiation shielding. ASTM C637 deals with the standard specifications for aggregates for radiation shielding concrete and ASTM C638 is the descriptive nomenclature of constituents of aggregates for radiation shielding concrete. The 2009 revisions of these standards were used in this investigation. Special aggregates which are used in concrete for radiation shielding and in which composition and high specific gravity of the aggregates are of primarily concern are covered in ASTM C637. Both fine and coarse aggregates derived from natural sources, as well as manufactured artificial synthetic aggregates are covered by ASTM C637. ASTM C638 nomenclature provides detail description of common and important constituent of naturally occurring and artificial aggregates which are used for radiation shielding concrete but which are not generally used for conventional concrete. The descriptions include heavy aggregates such as iron minerals and ores, barium minerals and ferrophosphorus, as well as boron-containing materials such as paigeite, tourmaline, and boron-frit glasses.

2.4.1.1 Galena based mixtures

In the study conducted by Mortazavi et al. (2007), where the focus was on production of an economic high-density concrete for shielding megavoltage radiotherapy room and nuclear reactors, galena was used as the only heavy-weight aggregate in the mixture. The main objective of this study was to develop a cost effective high-density concrete

with appropriate properties and galena was meant to fulfil this objective. In this undertaking, two types of concrete mixtures were produced. These were the control and galena mixtures of w/c of 0.53 and 0.25 respectively. The galena used in this study had a density of 7400 kg/m^3 and was obtained from a mine in Firouzabad in Iran. The reference mixture is given in the study to have been composed of sand (945 kg/m^3), filler (214 kg/m^3), cement (920 kg/m^3), and water (180 kg/m^3). The mixture is reported to have yielded a density of 2350 kg/m^3.The composition of the galena mixture is not given in the publication of the work. What was mentioned about the mixture is that it had a density of 4800 kg/m^3 and showed good shielding properties (Mortazavi et al.,2007).

The findings of this particular study claimed that the galena concrete samples showed significantly better performance in radiation shielding and compressive strength in comparison to the reference mixture. The obtained strength of the galena mixture was reported to be 50 MPa compared to only 30 MPa obtained for the reference mixture. The problem with these results in both radiation and mechanical aspects is that, even though the study claimed that the mixture can be used for nuclear reactors, it will not be able to shield the most complex radioactive particles which are neutrons. It is well known from nuclear physics that only lighter elements such as hydrogen and boron are capable of shielding neutrons. Neutrons penetrate through lead easily, and since lead was the only special aggregate used in the mixture, the concrete will not be able to stop them. The reason for the good shielding properties obtained is that a gamma ray source in the form of a narrow beam emitted from a cobalt-60 therapy unit was used for the measurements. The results were therefore positive because lead is good at shielding gamma rays but ineffective for neutrons.

Furthermore, even if good strength was reported in this study, from the high density obtained, it can be deduced that other properties such as homogeneity, workability, place-ability, segregation and cohesion were most likely compromised. It is therefore suspected that the concrete was of too poor a quality to be used for construction of any structure. The reported strengths are also suspicious as exact whole numbers were achieved. The 50 MPa strength obtained for the galena mixture also seem to be low for

the 0.25 w/c used. The insight provided by this study was that, it is possible to use galena as a potential aggregate for concrete casting. This is what informed the inclusion of galena in the aggregates of the mixtures in my current investigation into development of the shielding concrete. The galena was mainly included for its capability to shield the gamma rays.

2.3.1.2 Colemanite based mixtures

Gencel et al. (2010) conducted a study on the impact of colemanite on the mechanical properties of concrete. Colemanite as discussed in section 4.15 is a useful aggregate in radiation shielding as it contains boron and hydrogen in its fixed water of crystallisation which are desirable for slowing down of fast neutrons. The main intention of this study was to investigate the effect of colemanite on physical and mechanical properties of concrete when used as a replacement aggregate. Concretes containing different ratios of colemanite were therefore cast and investigated. The properties investigated included slump, air content, compressive strength, splitting tensile strength, modulus of elasticity and freeze-thaw durability.

The colemanite used in this study was obtained from a mine in Turkey and was prepared as an aggregate by sorting it with sieves into coarse (C_c) and fine (C_f). The other aggregates used in the study were: crushed sand of up to 3 mm (CSt-I), natural river sand of up to 7 mm (NRS), crushed stones ranging between 7-16 mm (CSt-II) . The physical properties of all aggregates used are presented in Table 2.1 while the chemical composition of the colemanite used is given in Table 2.2 (Gencel et al., 2010).

Table 2.1: Physical properties of aggregates used (Gencel et al., 2010).

Aggregate Code	Specific gravity (g/cm^3)	Water absorption (%)	Loose unit weight (kg/m^3)
CSt-I	2.61	2.91	1913
NRS	2.63	3.13	1830
CSt-II	2.7	0.83	1676
Cf	2.41	3.28	1455
Cc	2.42	1.35	1315

Table 2.2: Chemical properties of colemanite used (Gencel et al., 2010).

	C_C	C_f
B_2O_3	41.24	39.48
CaO	24.35	24.42
MgO	1.42	1.59
Fe_2O_3	0.44	0.76
SiO_2	5.07	6.38
LOI	24.28	24.83

Concrete mixtures containing different volumes of colemanite were designed and cast into moulds. A control mixture of plain or normal concrete was also designed and samples were prepared as reference. In all the mixtures, the cement content was kept at 400 kg/m^3 with w/c at 0.42. The effects of colemanite on the physical and mechanical properties of concrete were evaluated by comparing the cast control mixture with 10, 20, 30, 40 and 50 percentage mixtures of colemanite aggregates in volume. These mixtures are given in Table 2.3.

Table 2.3: Investigates mixture designs (Gencel et al., 2010).

Material	PC	CC10	CC20	CC30	CC40	CC50
Cement (kg)	400	400	400	400	400	400
Water (kg)	168	168	168	168	168	168
W/C	0.42	0.42	0.42	0.42	0.42	0.42
Air content (%)	1.5	1.5	1.5	1.5	1.5	1.5
CSt-I (kg)	447.3	402.57	357.84	313.11	238.38	223.65
NRS (kg)	443.44	399.1	354.75	310.41	266.06	221.72
CSt-II (kg)	926.83	834.14	741.46	648.78	556.10	463.41
Cf (kg)	-	79.40	158.8	238.19	317.59	396.99
Cc (kg)	-	82.43	164.86	247.28	329.71	412.14

The results obtained in this study were as follows:

- The slump of the concrete decreased with more addition of colemanite as shown in Figure 2.6. It was observed that the water in the concrete was absorbed into the fine aggregates and the concrete formed small lumpy masses (flocculated) immediately when colemanite was added into the mixtures. It was therefore suspected that the reduction of slump was a result of this flocculation which was due to the reaction of colemanite with the cement paste.

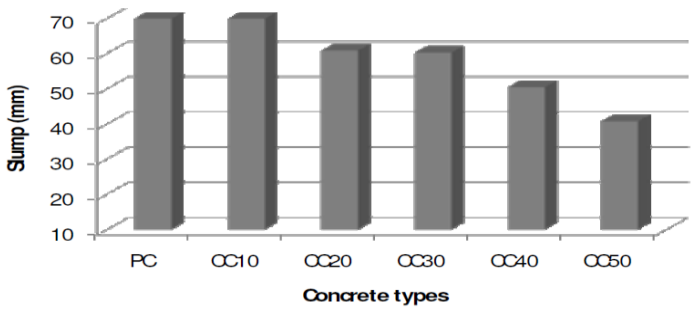

Figure 2.8: Slump results of the cast mixtures (Gencel et al., 2010).

- The air content as shown in Figure 2.7 was observed to have increased with more addition of colemanite.

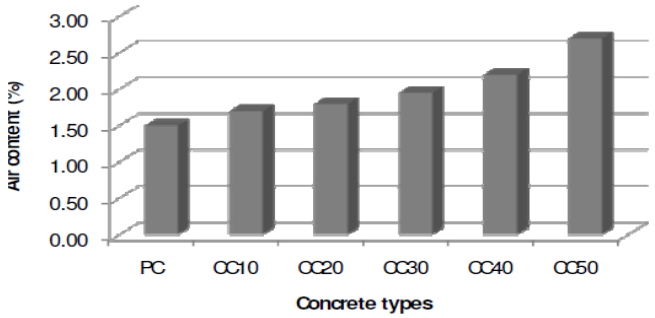

Figure 2.9: Air content of the mixtures (Gencel et al., 2010).

- The 28-day compressive strength decreased as more colemanite was added into the mixture. It was also observed that these reduction in strength as shown in Figure 2.8 were parallel to the reduction of densities.

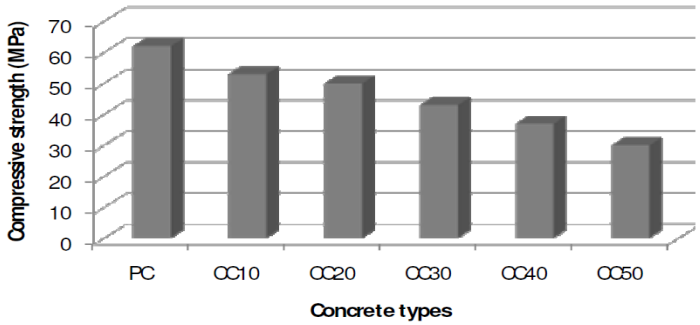

Figure 2.10: 28-day strengths of the mixtures (Gencel et al., 2010).

- The tensile strength also as shown in Figure 2.9 decreased as a result of addition of colemanite.

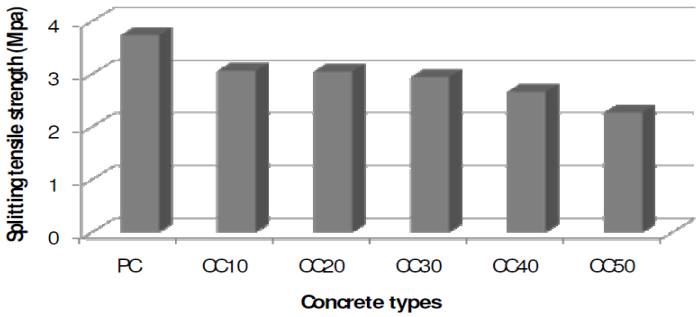

Figure 2.11: Splitting tensile results test of the mixtures at 28 days (Gencel et al., 2010).

- As shown in Figure 2.10, it was found that the density of the concrete dropped with increasing addition of colemanite. This was due to the low density of the colemanite material itself and increasing air content.

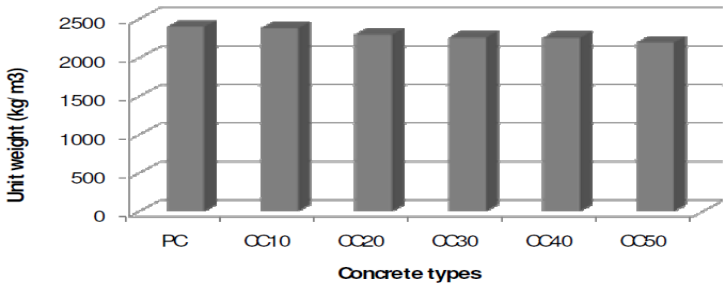

Figure 2.12: Densities of the mixtures (Gencel et al., 2010).

Besides the above obtained results, it was further observed that the addition of colemanite delayed the setting time of the concrete. All the concrete mixtures with colemanite were reported to have taken more than two days before they could be properly removed from the cast moulds. The reason for this long retardation was not known but it was suspected that it was related to the flocculation problem mentioned earlier. The overall conclusion of their study was that using colemanite ranging from 10 to 50 % as aggregates in concrete negatively affects the concrete in respect to both physical and mechanical properties. The recommendation that emerged from this research was that further investigations on the subject were still required but that an addition of up to 30 % of colemanite into the concrete mixture should be considered an acceptable level in order to achieve the suitable workability and strength.

The problem with the conclusion and recommendation from this study was that the dosage of the colemanite seemed to be too high. This is because colemanite is a water soluble boron material, which according to Kaplan (1989) is known to delay the setting

of concrete even when added in small quantity. Furthermore, the study does not provide information on how the flocculation difficulties experienced in the colemanite mixtures were resolved. The key information that was extracted from their study and informed the approach of the study presented in this report was that colemanite can be used as an aggregate. Due to its reduction in strength and delay in setting time of concrete, the intention was therefore to use it in the mixture developments but in small quantities sufficient to attenuate neutrons. These quantities would have to be determined by shielding simulations which would provide effective quantities required for neutron attenuation.

2.4.1.1 Iron ore and steel shot based mixtures

Iron ore and steel shot are primarily included in concrete for radiation shielding to obtain the desired high density which helps in attenuation of photons and slowing down of fast neutrons. Several studies and developments have been carried out using these aggregates where magnetite and hematite have been used as the main sources of natural iron. Some of these studies are discussed in this section.

In the study carried out by Dubrovskii et al. (1970), hematite was used as the natural source of iron where it was applied both as fine and coarse aggregates. The purpose of the study was to investigate the properties of high density hematite concrete for shielding against high neutron fluxes. The concrete mixture produced was of cement, coarse hematite, fine hematite and water. The mixture design was as given in Table 2.4 with the obtained density of 3030 kg/m^3 (Dubrovskii et al., 1970). The results of this study showed good shielding properties for the high density hematite aggregate concrete. However, due the low w/c used, the strengths obtained were very low.

Table 2.4: Hematite concrete mixture design (Dubrovskii, et al., 1970)

Material	Quantity (kg/m^3)
Cement	298
Coarse hematite	2134
Fine hematite	298
Water	300
Obtained Density	**3030**

In a study conducted by Kharita et al. (2007), hematite was used to produce special shielding concrete that was tested using two different gamma sources and a neutron source. At the conclusion of the study hematite samples were considered the best for shielding gamma rays as compared to those which contained no hematite. It was also found that the samples showed good results for shielding neutrons and this was suspected to be from the high iron content of hematite and the presence of iron hydroxide (Kharita et al., 2007).

Mahdy, Speare and Abdel-Reheem (2002) conducted a study to investigate the effect of transient high temperature on magnetite aggregate heavy-weight and high strength concrete. In their study, twelve mixtures with slump values of over 100 mm and strength of 140 MPa at 180 days were investigated. The study used a constant w/c ratio of 0.24 and superplasticiser dosage of 3.5 % while the control mixtures had a w/c of 0.5 and no superplasticiser. The mixtures contained combinations of cement, silica fume, and coarse magnetite with maximum size of 16 mm, fine magnetite and natural fine sand (Mahdy, Speare & Abdel-Reheem, 2002). The mixture proportions of the concrete tested are given in Table 2.5.

Table 2.5: Tested mixture proportions (Mahdy, Speare & Abdel-Reheem, 2002).

Mixture No.	C	Sf/C	W/(C+Sf)	C/(F+C)	Slump	Density
	kg/m³	%	Ratio	Ratio	mm	kg/m³
MMO	350	0	0.5	0.65	117	4050
MMC	500	0	0.24	0.65	108	3970
MM1	500	10	0.24	0.48	120	4000
MM11	500	20	0.24	0.48	125	3870
MM3	500	10	0.24	0.65	115	4010
MM33	500	20	0.24	0.65	125	3990
MSO	350	0	0.5	0.65	112	3400
MSC	500	0	0.24	0.65	102	3380
MS1	500	10	0.24	0.48	100	3260
MS11	500	20	0.24	0.48	120	3280
MS3	500	10	0.24	0.65	119	3560
MS33	500	20	0.24	0.65	128	3560

Figures 2.11 and 2.12 shows the results of tests conducted on the effect of high temperature on compressive strength of concrete. The strength decreased when temperatures were raised to 100 °C. With further increase in temperature, the loss in strength recovered and reached peak strength of 10 % to 30% above the room temperature strength. At temperatures of 500 and 700 °C, the strength dropped sharply (Mahdy, Speare & Abdel-Reheem, 2002). The results also indicated that silicafume is effective in enhancing concrete strength after exposure to high temperatures, particularly when using magnetite as a fine aggregate. The study suggests that raising temperature from normal room temperature to about 100 °C would decrease the strength of concrete. According to this study, best performance of concrete under raised temperatures is obtained between 100 °C and 300 °C. Temperatures above 300 °C have negative impact on iron ore based high density concrete as the strength was observed to be on a constant decrease. It is therefore concluded that operating temperatures between room temperature and 100 °C as well as temperatures above 300 °C be avoided in iron ore based high density concretes as they have negative impact on the strength of the concrete. In the case of the SANRAD facility, raised temperatures are not a concern as operations will always be at room temperature of ± 25°C.

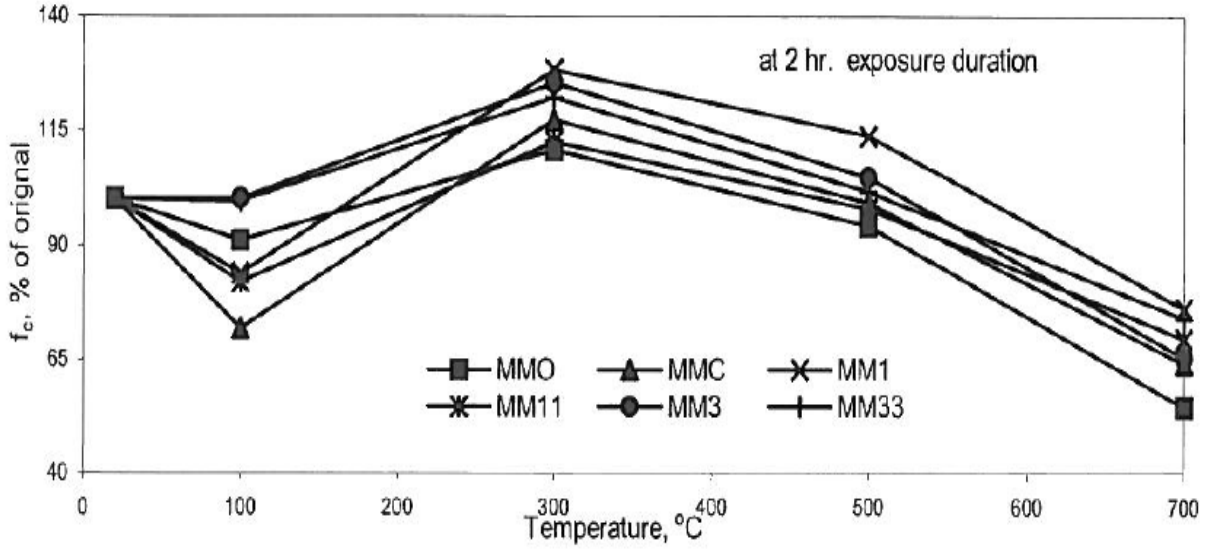

Figure 2.13: Effect of temperature on concrete strength in concretes containing magnetite fines (Mahdy, Speare & Abdel-Reheem, 2002).

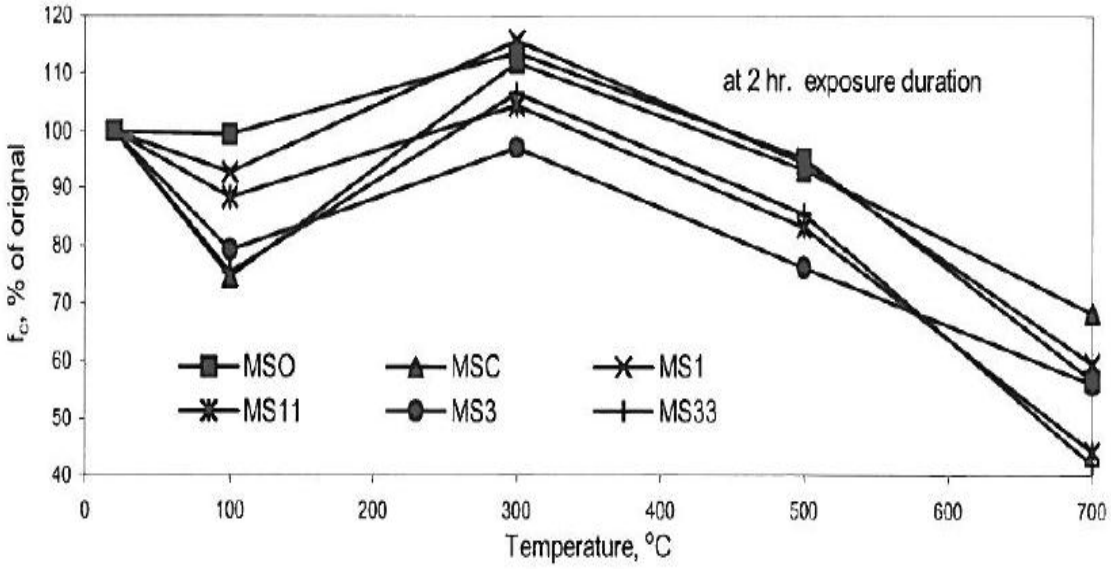

Figure 2.14: Effect of temperature on strength in concretes of normal sand fines (Mahdy, Speare & Abdel-Reheem, 2002).

Warnke et al. (2001) developed a new concrete shielding material for transportation and storage casks containing low radioactive waste using steel granules. The granules were produced from a melting plant that recycled low radioactive scrap from nuclear installations. Instead of using iron ore such as hematite or magnetite, iron granules were used to achieve the required density. The portion of the iron granules used in the concrete mixture was reported to be approximately 50 % by weight of the aggregates. The development also reported that densities were raised from normal 2400 kg/m^3 to 4000 kg/m^3 and that the compressive strength reached up to 65 MPa (Warnke et al. 2001). The mixture design of this concrete was not reported and only referred to as a "*special recipe"*.

2.5 Conclusion from literature review

Even though there seem to be shortfalls in the above discussed literature studies, they all showed that it is possible to use the different aggregates to produce high density concrete for radiation shielding. In the hematite based studies carried out by Dubrovskii et al. (1970) and Kharita et al. (2007), the densities obtained seemed not to be adequate for shielding of a neutron radiography facility. The study carried out by Mahdy, Speare & Abdel-Reheem (2002) showed good results under normal room temperature conditions but the problem was the low w/c ratios used. The iron granule study of Warnke et al. (2001) did not give much detail about the mixture and its performance in the fresh state. It is suspected that the mixture which had iron granules forming part of 50 % of the aggregates may not have been homogenous and could have suffered segregation problems. Furthermore, the mixture can be expected to be costly because of the amount of iron granules used.

In terms of mechanical properties reported, all the studies were successful in obtaining the densities and strength required as a result of using special aggregates for radiation shielding. Table 2.6 presents a summary and comparison of all mechanical properties obtained in the surveyed studies.

Table 2.6: Comparison of mechanical properties from literature review

Study		Strength		Density	Slump
Authors	*Material investigated*	*Age(days)*	*MPa*	*kg/m³*	*mm*
Mortazavi et al.(2007)	Galena	28	50	4800	-
Gencel et al. (2010)	Colemanite (Cc 10-mixture)	28	50	2400	70
Dubrovskii et al. (1970)	Hematite	28	-	3030	-
Mahdy, Speare and Abdel-Reheem (2002)	Magnetite	180	±100	±3500	>100
Warnke et al. (2001)	Iron granules	28	-	4000	-

In most of these studies the consistence and workability of the concrete produced were not of primary concern. In the two studies were the consistence was reported a plasticiser was used. In the study by Gencel et al. (2010) this was not reported but the flocculation problems experienced could have only been resolved by an introduction of an additive or chemical admixture. Formation of concrete into smaller masses would

definitely results in no slump because all the water would have been absorbed for this to occur. The achievement of the 70 mm slump is an indication that some sort of an admixture which was not reported was employed. The obtained slumps in both studies were adequate for the objectives of the investigations. The densities obtained for all high density material studies were adequate and satisfactory for the purposes of the investigations with the galena based mixture resulting in the highest density of 4800 kg/m^3 followed by iron granules mixture with a density of 4000 kg/m^3. This is because the galena used had a density of 7800 kg/m^3 and the iron granule mixture contained 50% of iron granules. For the other mixtures the densities were reasonable for the amount of the high density materials used. The compressive strengths obtained in the studies were also satisfactory for structural application. There is however a concern about the galena mixture where the strength is expected to be higher than the one reported as low w/c has been used. The 50 MPa reported for the colemanite mixture on the 28th day is also suspicious given the retardation effect of the material on concrete.

The researches provided much valuable insight on how to go about producing the high density concrete required in this study. Since it was found that it is possible to use the different aggregates for radiation shielding purposes, it was decide to investigate all the identified aggregates by preparing different aggregate combinations that would yield a mechanically sound and cost effective concrete mixture that would suitably shield the complex radiation source of the SANRAD facility.

Chapter 3 Theoretical calculation of radiation shielding by simulation techniques

Simulations are conducted as the initial step of theoretical modelling the shield and evaluating its performance in protecting the radiation emerging from any source. These theoretical calculations are then supported by empirical observation and experimentation in order to obtain complete designs. There are several simulation methods that could be used for theoretical calculation of radiation shielding. These methods might be different in terms of functionality but they are all based on the theory of transportation of radiation through matter as defined by the equation of radiative transfer (Kaplan, 1989). The equation is derived by considering the inflow and outflow of radiation particles. Mathematically, the equation is complex and its precise analytical solution is known only for simple cases which are often not directly applicable to practical shielding situations (Kaplan, 1989). The complexity of this equation led to development of a number of approximations of the equation and methods of its solutions.

Together with the MCNP method used in this research, brief backgrounds of two other deterministic methods are discussed. These are the moments method and the discrete-ordinate method of radiation particle transport. Deterministic methods solve the radiation transport equation in a numerically approximated approximate manner everywhere throughout a modelled system. Monte Carlo methods model the nuclear system with high accuracy and then solve the model statistically (approximately) anywhere in the modelled system. Although deterministic methods are fast for one-dimensional models, both methods are said to be slow for realistic three-dimensional problems.

3.1 Moments method

The method of moments was developed by Spencer and Fano (Kaplan, 1989). It is a powerful method for computing the spatial and energy distribution radiation particles from a point, plane or line source in an infinite medium (Kaplan, 1989). In the moment method, the transportation equation is approximated by an equation of moments. The unique equation over the specific intensity is then replaced by two equations over the radiative energy and flux. To solve the problem, a closure relation is then needed which relates the different moments. The advantage of the moments method closure is that it is analytical and correct both in the diffusive and the transport limit (García-Fernandez, Gonzalez & Velarde, 2008). The main drawbacks of the moment method and hence the reason it was not used as a method of choice for computation in this study is that, it solves the moment equations which are just an approximation of the radiative transfer equation. The method is simplistic in nature and suitable for less complicated geometries and fails in the case of more complex geometries such as the one for the SANRAD facility.

3.2 Discrete-ordinates method

Also referred to as the S_N method, the discrete-ordinate method is a straightforward and well-known deterministic solution, which is a procedure for approximating the solution of the energy dependent linear transport equation with anisotropic scattering (Kaplan, 1989). In this method, a set of discrete directions (or ordinates) is chosen and directional fluxes are evaluated for these directions. The derivatives and integrals appearing in the transport equation must be replaced by a corresponding discrete representation by using finite difference techniques and numerical schemes (Saglam, 2003). Although this method has some advantages and capabilities to solve the transportation equation, there are also some deleterious numerical problems associated with it. One of these problems is the ray effect. The ray effect distortions are anomalous ripples that appear in the scalar flux for problems with isolated sources and scattering ratio in two or three dimensional geometries (Saglam, 2003). Besides the ray effect, the other disadvantage of the discrete-ordinate method is that, it is computationally expensive as it requires an employment of an acceleration technique to achieve a good

convergence. The method is also fast for one-dimensional models but slow for realistic three-dimensional problems. For these reasons this method was not suitable for the modelling of the SANRAD facility problem.

3.3 Background of the Monte Carlo simulation method

This is a method which has a statistical basis and which has been developed by making use of the physics of the transport equation. It can be loosely described as statistical simulation method, where statistical simulation is defined in quite general terms and utilizes sequences of random numbers to perform the simulation (Ivanov, 2012). The Monte Carlo method, in all its forms therefore involves some sort of a random sampling process to mathematical or physical problems. It is quite different from deterministic transport methods in that deterministic methods solve the transport equation for the average particle behaviour while the Monte Carlo method does not solve an explicit equation, but rather obtains results by simulating individual particles and calculating some aspects of their average behaviour (Wagner, 1994). In contrast with the other two methods discussed above, the Monte Carlo simulation does not impose any restrictions on problem geometry nor on the detail which may be used to describe physical event (Brown and William, 1984).

In this technique, the histories of the behaviour of a randomly chosen number of particles are determined as they pass through a shielding medium. Random sampling is used because the entire life of a radiation particle from its birth to its death is governed in nature by many random processes (Wagner, 1994). For instance, the birth of a particle in the source during a given time interval is itself a random process that has associated probability. The same applies to the initial direction of travel, the particle's initial energy, and the position at which the particle originates (Wagner, 1994). The name is therefore derived from the fact that random numbers are used in the statistical analogy to the physical problem (Kaplan, 1986). In many applications of this method, the physical process is simulated directly, and there is no need to write down the differential equations that describe the behaviour of the system (Ivanov, 2012).The only requirement is that the physical system be described by probability density functions.

Once the probability density functions are known, the simulation can proceed by random sampling. Many simulations are then performed and the desired result is taken as an average over the number of observations which may be a single observation or perhaps millions of observations (Ivanov, 2012). This method therefore becomes necessary and useful when it is difficult to describe physical systems using deterministic methods.

As already mentioned above, the important feature of this method is that the histories of a large number of particles, each of which is random in nature, are used to ascertain average particle behaviour (Kaplan, 1989). Particle histories can be followed on a computer in a way which is similar to the actual physical process which occurs when a particle is transported through a medium (Kaplan, 1989). The steps followed in simulating an actual particle history are as follows (Wagner 1994):

- Initially a particle will be born at a particular position, with a particular energy, as well as a particular direction of travel. All three variables are chosen through random sampling of the probability distributions that describe the source's energy and angular dependence.
- Then the distance to collision, which is the distance the particle travels before its first interaction, is determined.
- From the distance to collision, the starting point coordinates, the direction of particle point and the site of the subsequent interaction are determined.
- At the interaction site, the atom of the material with which the particle interacts and the type of interaction are selected. If the interaction does not lead to absorption, new energy and direction are determined and the particle proceeds. If the interaction is an elastic scattering event, for example, the new direction is selected form the distribution of scattering angles and the subsequent new energy is determined by conservation of energy and momentum. In events that can result in the creation of new particles, the initial parameters (i.e. energy and angle of direction) are selected and, along with the position, are temporarily stored. The transports of these secondary particles are then performed after the primary particles are terminated.

- The above steps are then repeated until one of the following occurs: (a) the particle is absorbed or (b) the particle exits the shield.

This method is an important method of analysis, especially for shields which have complex geometries and this is the reason it was used in this study. Although calculations by this method are expensive and time consuming, it is probably the method of choice in situations where scattering or source geometry is important. Currently, this method constitutes the only feasible means of solving many problems with complicated geometry and/or interaction probabilities and is valuable in providing calculation standards for validating approximate methods (Brown and William, 1984). Because of its long computer execution time, the method was mainly used for complex shielding problems and for benchmarking of deterministic calculations in the past. Today, however, because of the advent of faster computers and parallel computing, the technique is being used more extensively for routine calculations (Ivanov, 2012).

3.3.1 Modelling in Monte Carlo

Before developing any calculation model, the objective of the calculation as well as the information desired from the calculation must be clearly defined. These are entered in the code through the *domain of interest* and *objective* fields (Wagner, 1994). Thereafter the geometry of the shield must be defined. After the geometry has been defined, the next step is to specify the materials used in the shield. These are entered as atoms making up the shielding material. The other cell entry in the simulation is the combined density made by these different atoms (e.g. the density of concrete made by different aggregates containing different atoms). The defined shielding medium under study is then subjected to radiation particles from the modelled source by interacting individual particles with the medium. The particles are then followed, one by one and the various events in which they participate (collision, absorption, fission, escape, scattering etc.) are recorded. All the events associated with one particle constitute the history of that particle (Ivanov, 2012).

3.4 Monte Carlo N-Particles eXtended Modelling

3.4.1 Calculation approach

The objective of the radiological safety assessment conducted in this study was to model the source of radiation and determine the efficiency of the shielding material to stop or attenuate radiation as the radioactive particles travel through the shield. The computation of the model was conducted by NECSA's Radiation and Reactor Theory (RRT) section using the Monte Carlo N-Particles eXtended (MCNPX) technique. The preliminary mixture design which was already optimised by selecting materials which are less expensive, accessible and had best required chemical compositions as determined in section 4 was provided to RRT's computational analyst as an input into the model. The worst case scenario was modelled and every measure was taken to ensure conservatism. This included modelling the concrete with density lower than expected value and reducing the dose rate target to 1 μSv/h instead of the regulatory requirement of 10 μSv/h.

3.4.2 Materials modelled

To perform the simulations, a mixture design with defined proportions was required. In this case, a preliminary mixture design needed to be produced. From the chemical analysis results, economic considerations, availability and ease of access of aggregates, it was decided that hematite, colemanite and steel shot would be the main aggregates in developing the High Density Concrete (HDSC). A mixture design of 0.42 water-cement ratio HDSC was used as an input into the simulation as presented in Table 3.1. The total (neutron and gamma) dose rate used was determined based on a model which included an equilibrium Low Enriched Uranium (LEU) core, internal geometry and layout of the beam, and material composition of the experimental chamber. HDSC was modeled as per the composition given in Table 3.1 which led to the elemental composition (atoms) summarised in Table 3.2. Although the density of about 4341 kg/m^3 was expected for this composition, the heavy weight concrete was modelled conservatively as 4000 kg/m^3.

Table 3.1: Preliminary mixture-Input to MCNP simulation

Ingredient	Mass(kg)	Density(kg/m^3)
CEM I 52.5	440	3150
Water	185	1000
Coarse Hematite	1750	5200
Fine Hematite	666.1	5200
Fine Colemanite	100	2400
Steel shot	1200	7100
Estimated Density(kg/m^3)	**4341.1**	

Table 3.2: Elemental composition of heavy concrete modelled in the MCNP calculations

Element	w%
Al	0.4292
Ca	5.0126
Fe	66.8533
H	0.5296
Mg	0.1222
B-10	0.0673
B-11	0.2960
O	25.6002

The internal cover of borated polyethylene was modelled as $(CH_2)_n$ with 5 % of B_2O_3 with a density of 920 kg/m^3. The beam stopper used in these calculations was modelled with the same borated polyethylene used at the walls, and a layer of metallic lead. The existing floor of the building where the facility will be assembled was modelled as normal concrete with density of 2400 kg/m^3 and its elemental composition is presented in Table 3.3. The current thickness of the beam port floor slab of the SAFARI-1 reactor building varies between 685 mm and 830 mm and was modelled accordingly.

Table 3.3: Elemental composition of normal concrete modelled in the MCNP calculations

Element	w%	Element	w%
Al	4.3800	O	48.3400
Ca	5.7600	P	0.0100
Fe	1.0500	S	0.2200
H	0.3000	Si	33.0700
K	2.2500	He	2.9790
Mg	0.6400	Co	0.0002
Na	1.0000	Ta	0.0005

3.4.3 Modelling of the facility

All dimensions and configurations of the facility were according to the design presented in Figure 1.1. The wall thickness of the collimators and filters sections were modelled with a thickness of 1100 mm HDSC. The wall thickness of the flight chamber section was modelled as 1000 mm made out of 800 mm HDSC and 200 mm borated polyethylene. The experimental chamber section was modelled with wall thickness of 800 mm composed of 600 mm HDSC and 200 mm borated polyethylene with the exception of the back wall facing the beam (hot spot) where a total thickness of 1300 mm was modelled made up of 800 mm HDSC, 400 mm borated polyethylene and 100mm layer of metallic lead. The floor was modelled with different thicknesses of 830 mm and 685 mm as indicated on the building's beam port floor drawings. Figure 3.1 to 3.4 shows some of the modelled components and sections from MCNPX model.

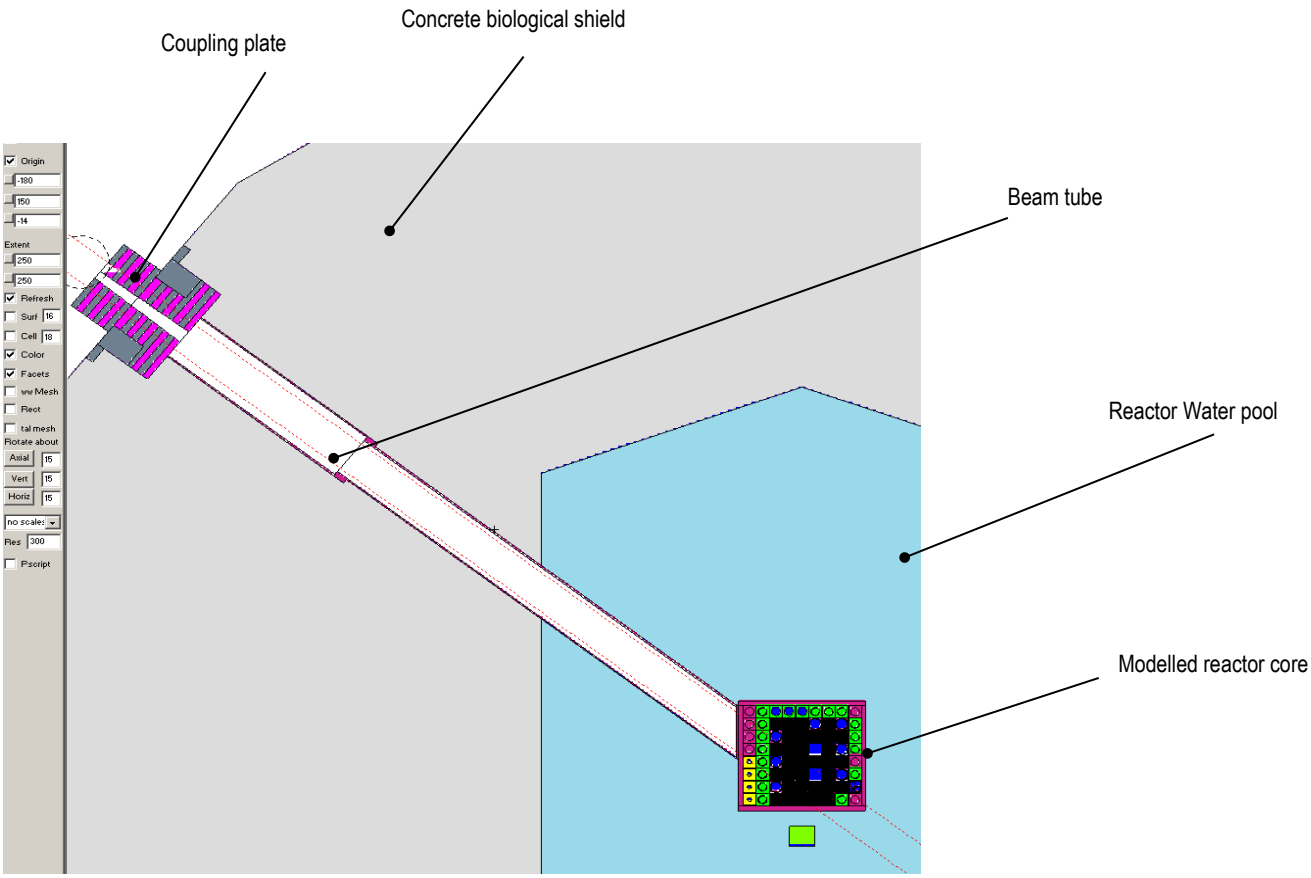

Figure 3.1: Horizontal cut at beam axis showing the position of the beam relative to the core, and the new coupling plate at the end of the beam.

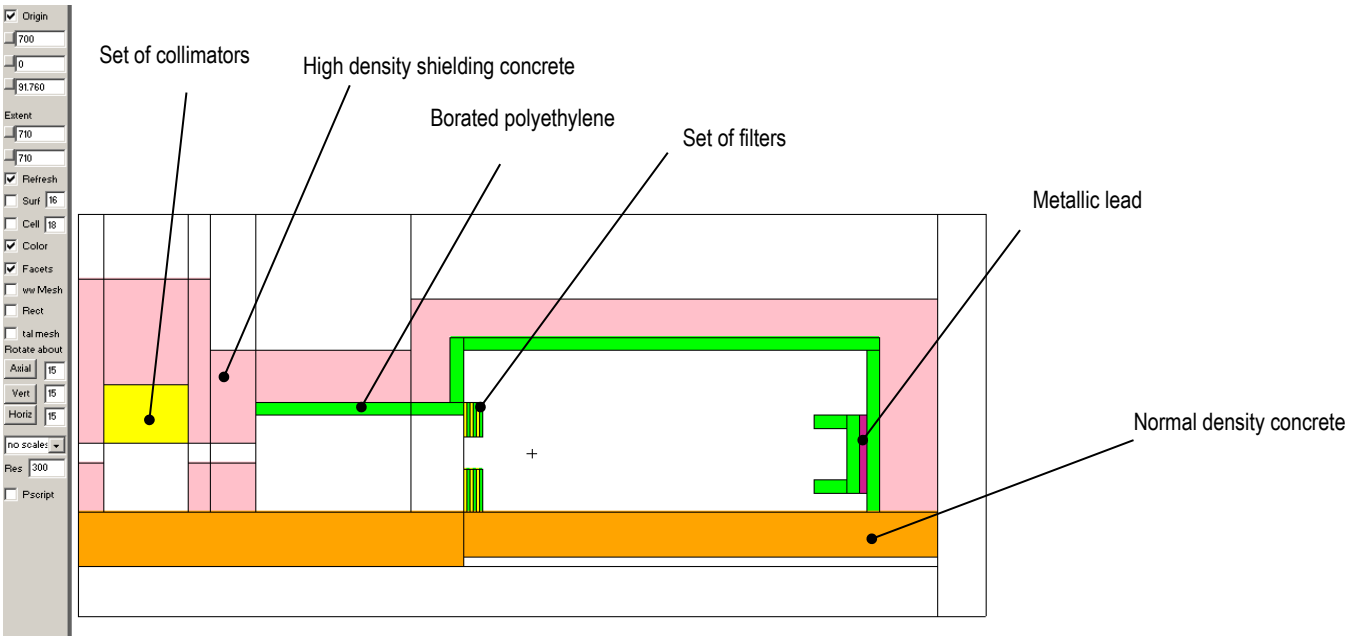

Figure 3.2: Vertical cut at beam axis showing the layout of the new SANRAD facility

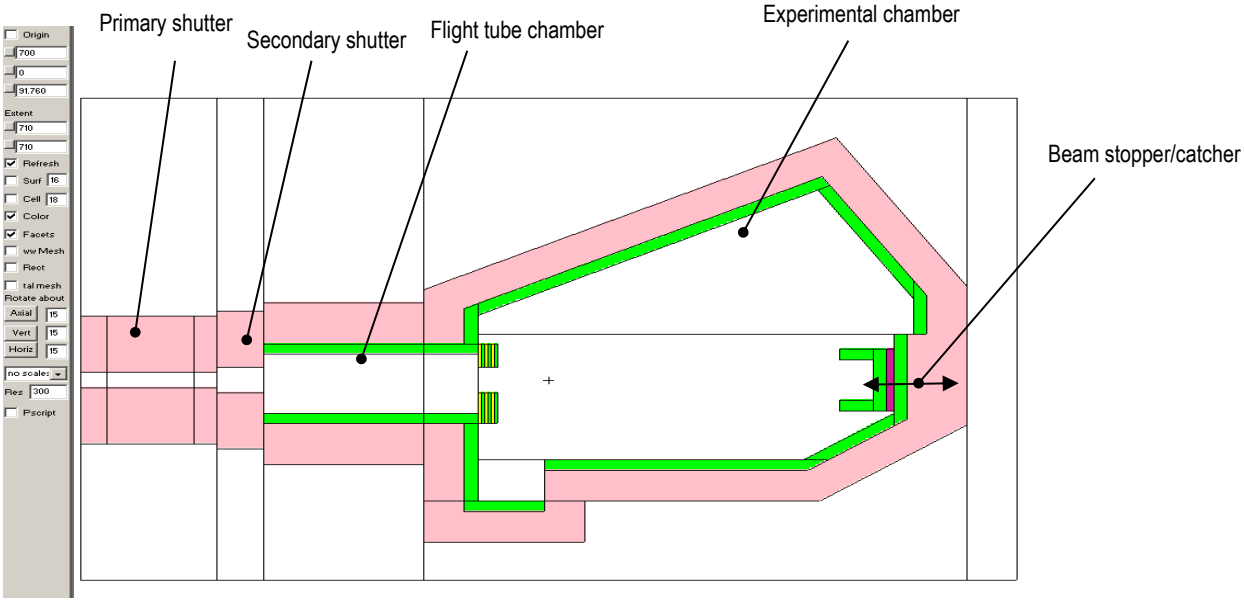

Figure 3.3: Horizontal cut at beam axis showing the layout of the new SANRAD facility

3.5 Outcomes of the MCNPX simulations

The sections below show contour level plots for neutron, primary gamma ray, and secondary gamma ray dose rates for the two situations assessed, namely dose rates around the SANRAD facility when both shutters are open and dose rates inside the experimental chamber when the secondary shutter is closed. The dose rate fields were calculated for the worst possible scenarios namely: (a) at the horizontal and vertical planes of the components that include the axis of the beam as shown in Figures 3.10 to 3.15, and (b) when the beam is completely open with no collimator and no filters of any kind as presented in Figures 3.4 to 3.9. Both the thickness of the walls as well as their material compositions were defined as to achieve the target of less than 1 μSv/h for contact dose rate, which is a requirement that is one order of magnitude more stringent than the normal radiological safety regulations.

Secondary shutter open, neutron dose rate [μSv/h]

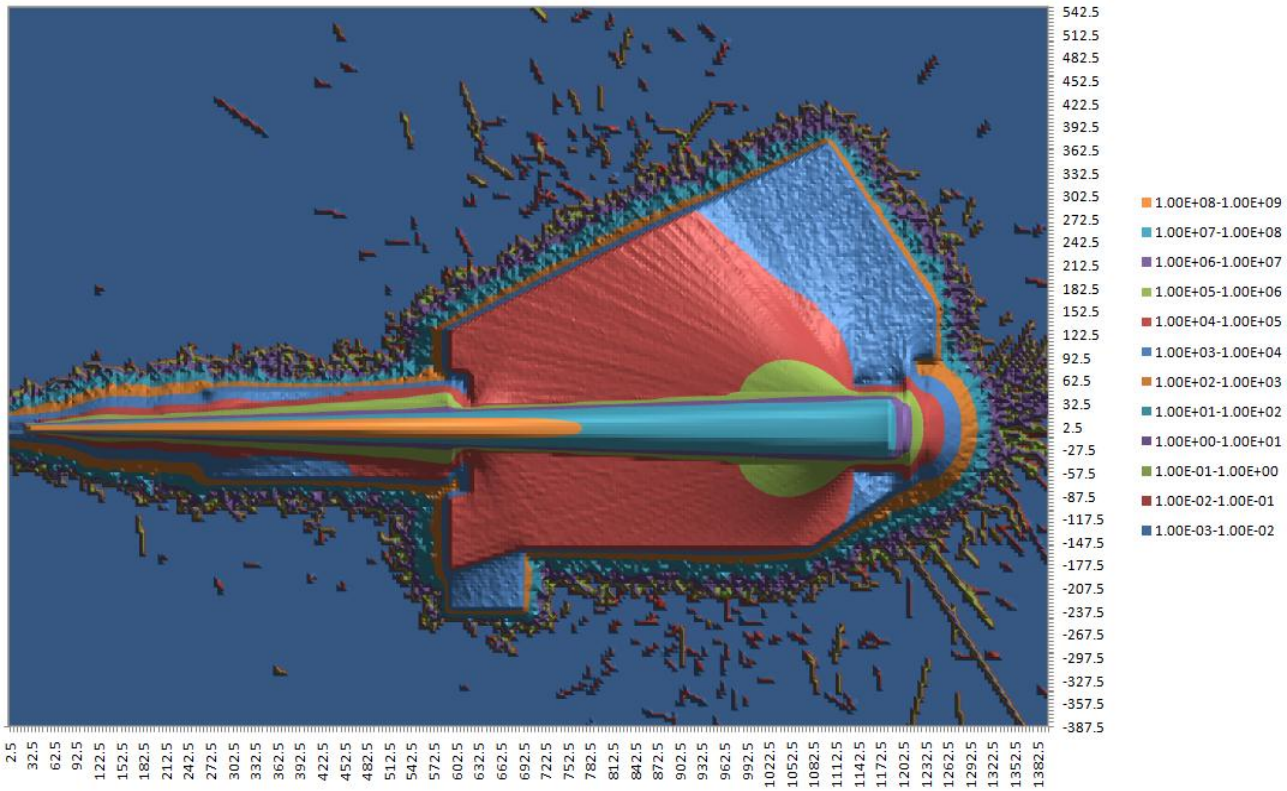

Figure 3.4: Horizontal cut at beam axis showing dose rate [μSv/h] due to neutrons from the core when secondary shutter is open (primary shutter also open).

Figure 3.4 shows results for shielding of neutrons on the horizontal cut of the facility with both primary and secondary shutter open. This implies that the beam is open and that the facility is in operation. Therefore the main concern in this case is the dose rates outside the facility to protect people working on the beam port floor of the building and to ensure that there is no noise transferred to neighbouring instruments. The dose rates obtained in most areas outside the facility were impressive with the range of 0.02 (red) to 1 μSv/h (green). It was only at the area around the beam stopper where just above 1 μSv/h (purple) were observed. This was not a concern because the actual regulatory limit is 10 μSv/h.

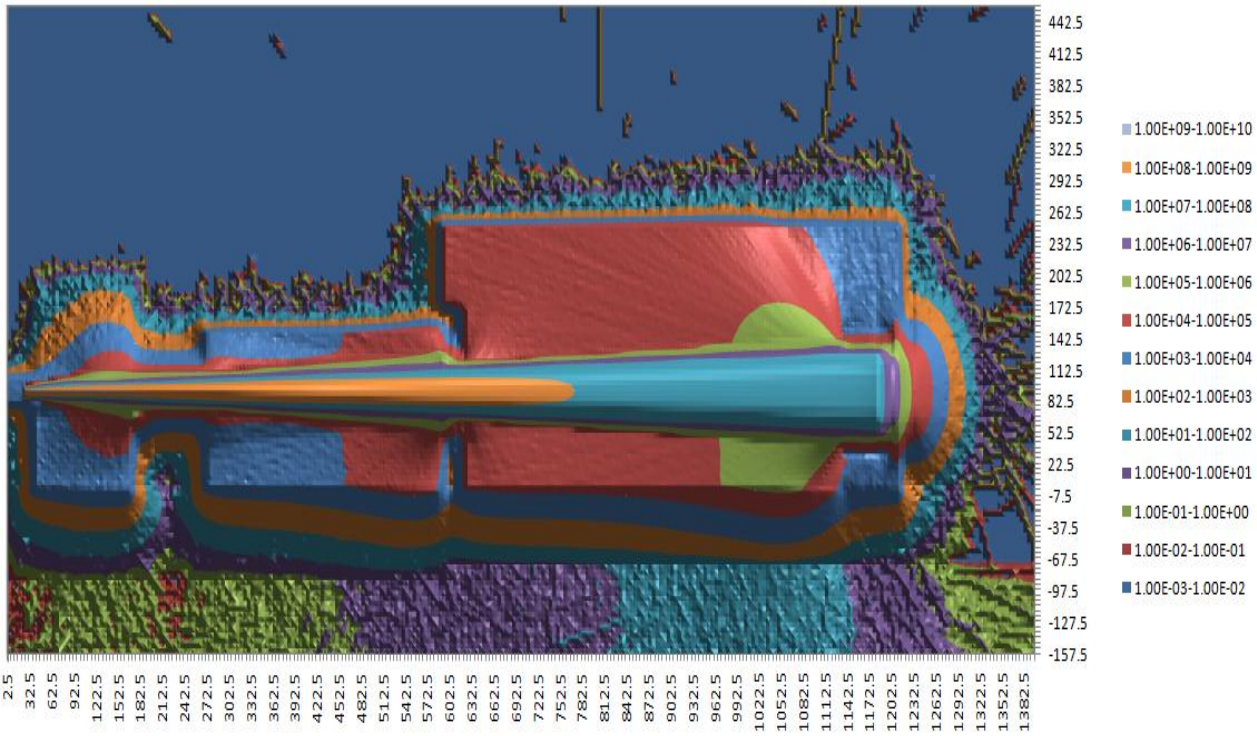

Figure 3.5: Vertical cut at beam axis showing dose rate [μSv/h] due to neutrons from the core when secondary shutter is open (primary shutter also open).

Figure 3.5 presents the shielding of neutron on the vertical cut of the facility when the beam is open and the facility is in operation. Just like the results obtained on the horizontal cut in Figure 3.4, the results were within the target except for the floors of the facility were the maximum contact dose rate in the range of 200 μSv/h was observed underneath the floor slab. This is because the floor was not part of the upgrade as it is part of the already existing reactor building made out of normal concrete. This was

however not a problem because of the occupational factor (i.e. average time workers spend at the basement) and the dose rates requirement for the basement. The basement area is classified as red and workers are not allowed in the area when any of the facilities on the beam port floor are in operation. The area is only declassified when the facilities are not in operation and the time that could be spent in the basement is limited to ensure that regulated limits are not exceeded.

Secondary shutter open, secondary gamma dose rate [µSv/h]

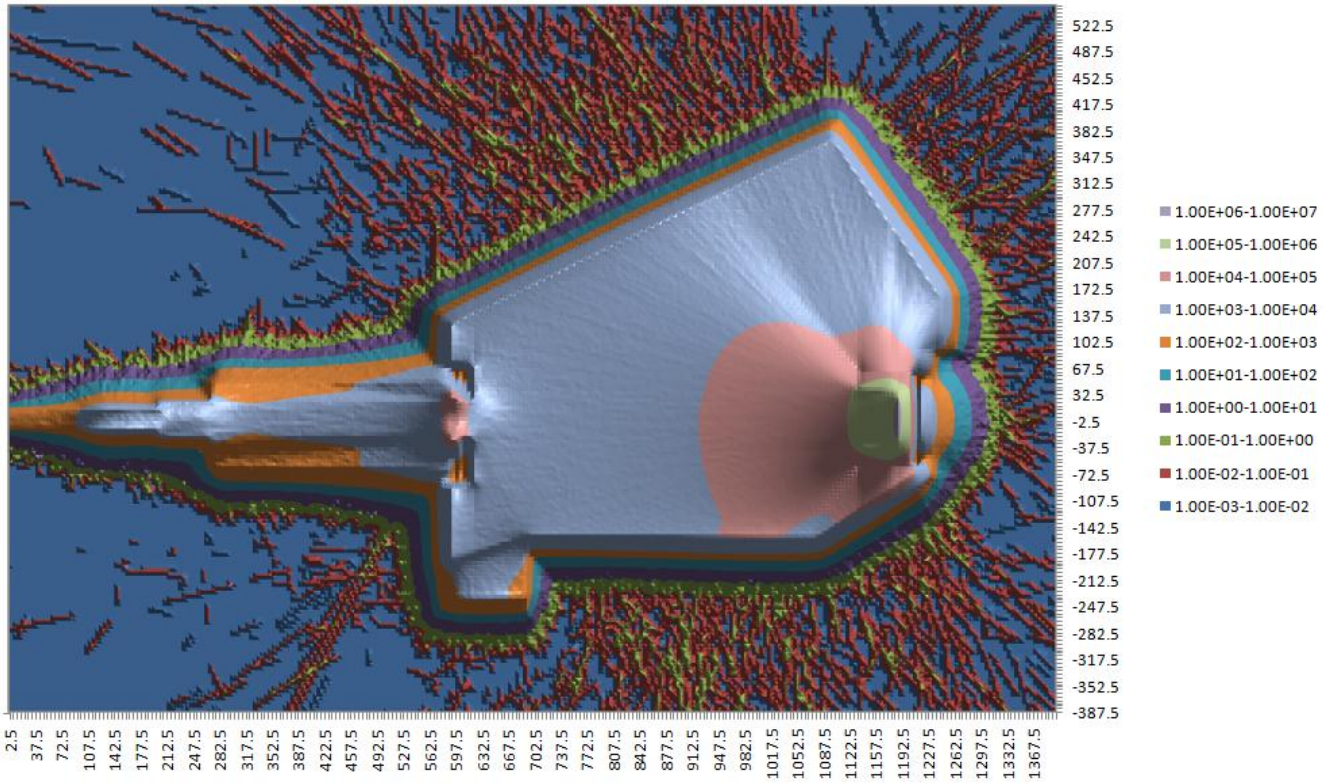

Figure 3.6: Horizontal cut at beam axis showing dose rate [µSv/h] due to secondary gammas from inelastic scattering and neutron capture when secondary shutter is open (primary shutter also open).

Figure 3.6 presents results for shielding of secondary gamma rays on a horizontal axis when the facility is in operation. Secondary gamma rays are created when the fast neutrons are slowed down from higher energies to lower energies. Again the shield was effective with only green and red ranges observed.

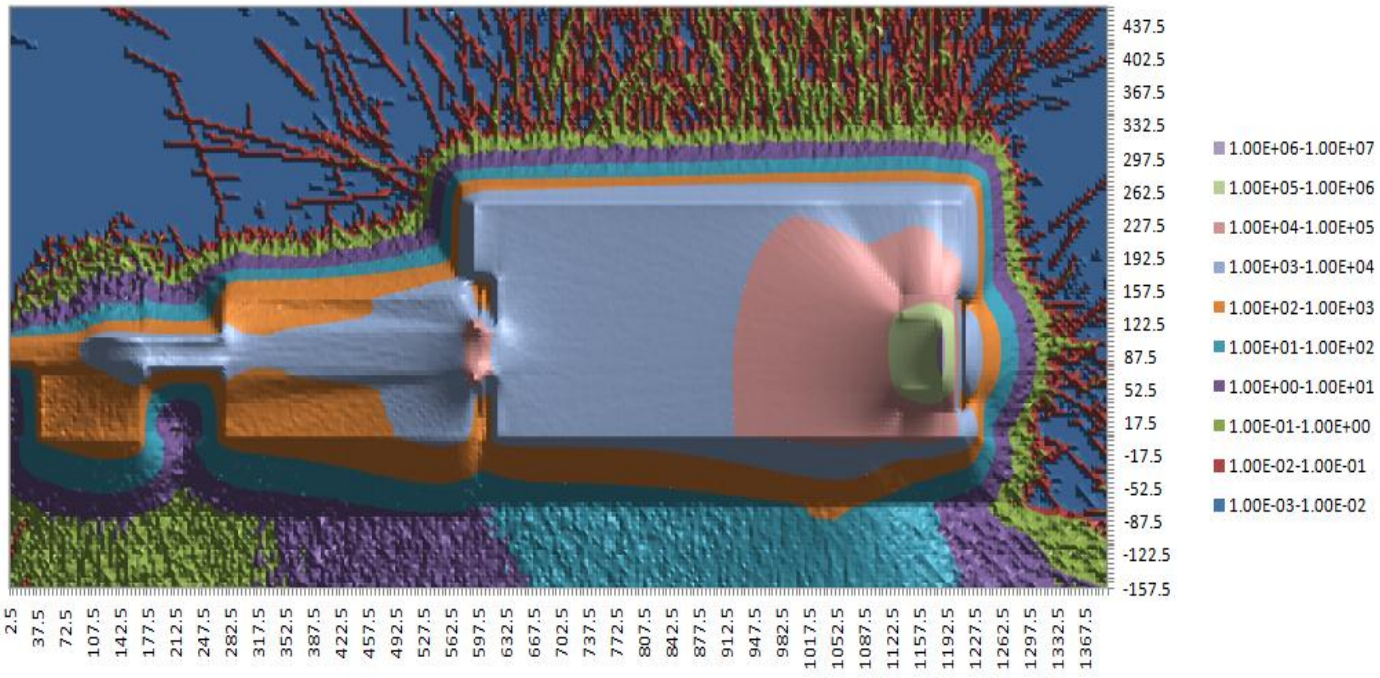

Figure 3.7:Vertical cut at beam axis showing dose rate [µSv/h] due to secondary gammas from inelastic scattering and neutron capture when secondary shutter is open (primary shutter also open).

The vertical cut section of shielding of the secondary gamma rays in Figure 3.7 indicated good performance of the shield around the facility on the beam port floor with maximum dose rates of less than 1 µSv/h noted. Dose rates at the basements were still more than the target. As discussed before this was not a problem because of the basement occupational factors and strict monitored access to the area.

Figure 3.8 and 3.9 shows performance of the concrete in shielding primary gamma rays on horizontal and vertical sections of the facility when it is in operation. The results indicated a good performance in both cases. The normal concrete floor was also able to absorb all the primary gammas rays to an acceptable level. Maximum of just below 1 µSv/h (green) was noted around the beam stopper.

Secondary shutter open, primary gamma dose rate [µSv/h]

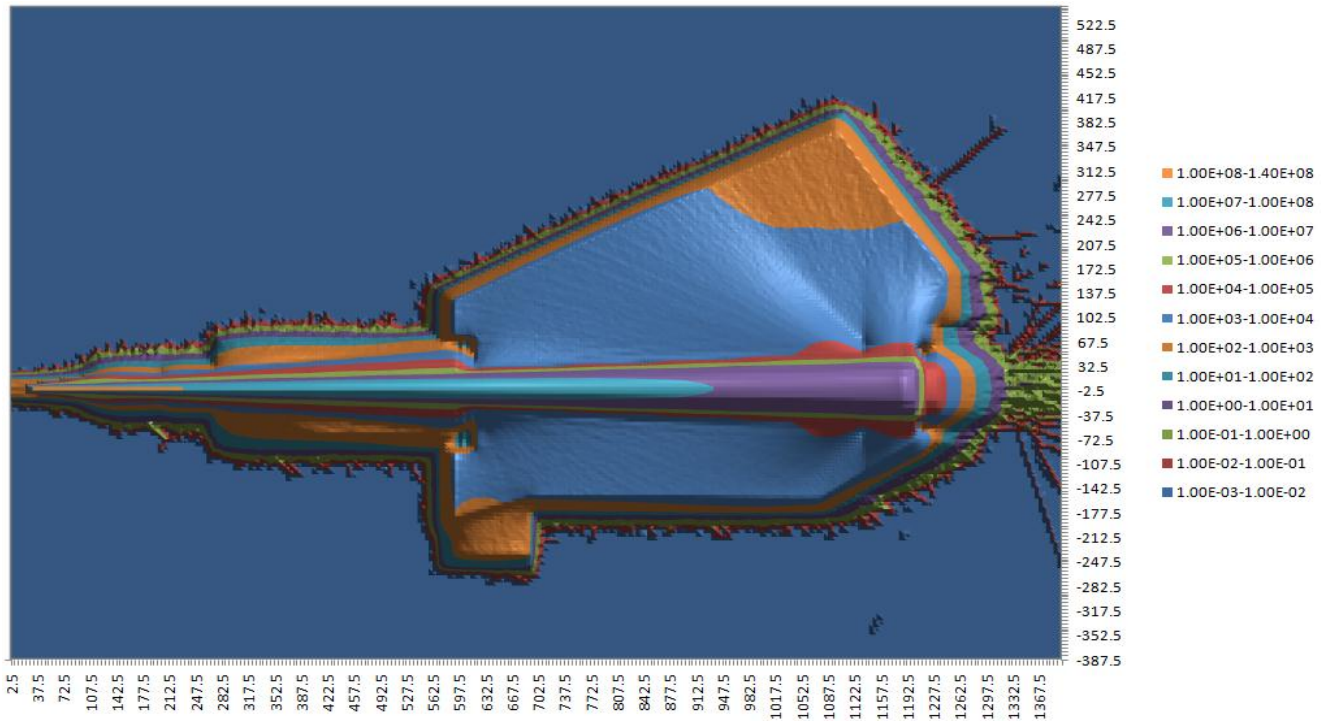

Figure 3.8: Horizontal cut at beam axis showing dose rate [µSv/h] due to primary gammas from the core when secondary shutter is open (primary shutter also open).

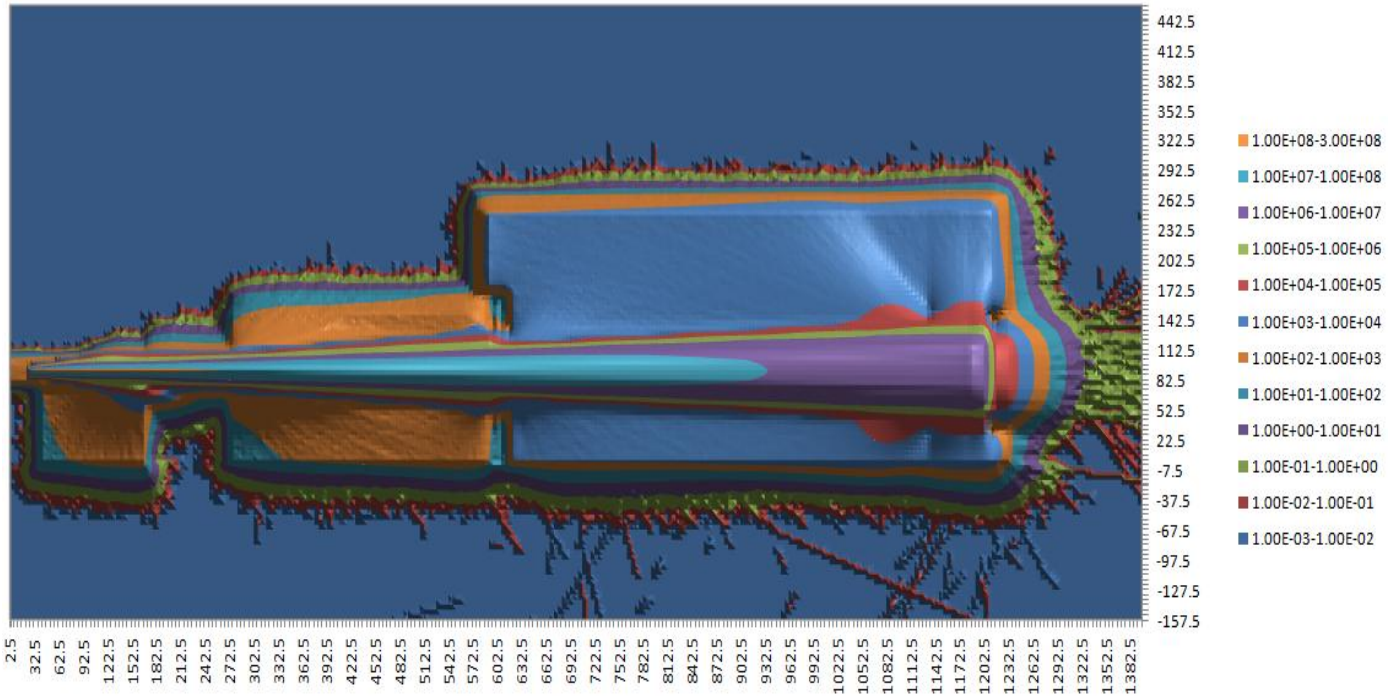

Figure 3.9: Vertical cut at beam axis showing dose rate [µSv/h] due to primary gammas from the core when secondary shutter is open (primary shutter also open).

Figure 3.10 to 3.15 presents the results of neutrons, secondary and primary gamma rays when the secondary shutter is closed and the primary shutter open. This implies that the beam has been stopped and that the facility is not in operation. In reality when the facility is not in operation both the shutters will be closed which means that the actual results are expected to be better than those obtained in this analysis. To be conservative, the analysis was performed with only one shutter closed. The performance of the concrete shield was satisfactory with less than 1 μSv/h observed inside the facility in all the simulated cases besides for the primary gamma rays (Figure 3.14 and 3.15) where just above 1 μSv/h (purple range) were noted. This was not a concern because the actual regulatory limit is 10 μSv/h and that this is expected to be less as the primary shutter will also be closed when the facility is not in operation.

Secondary shutter closed, neutron dose rate [μSv/h]

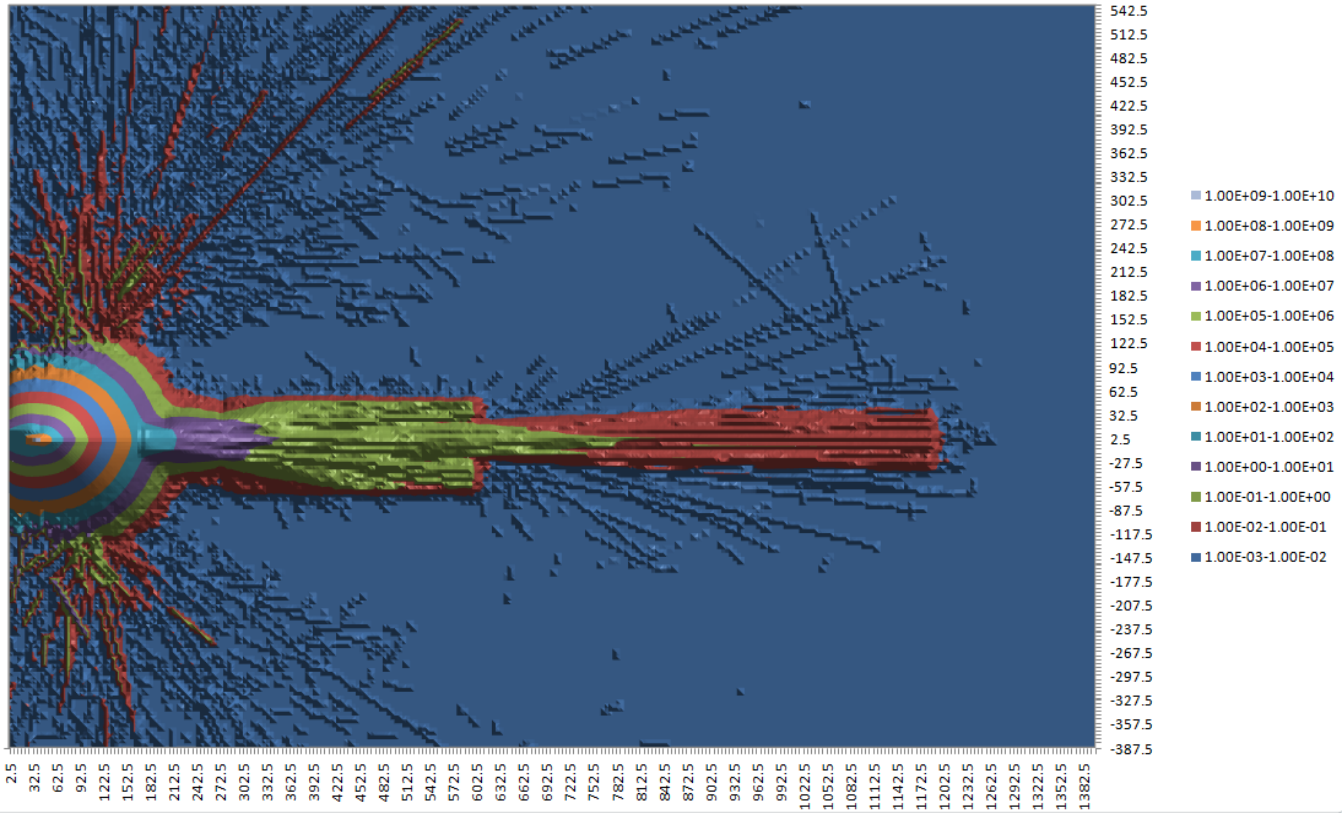

Figure 3.10: Horizontal cut at beam axis showing dose rate [μSv/h] due to neutrons from the core when secondary shutter is closed (primary shutter open).

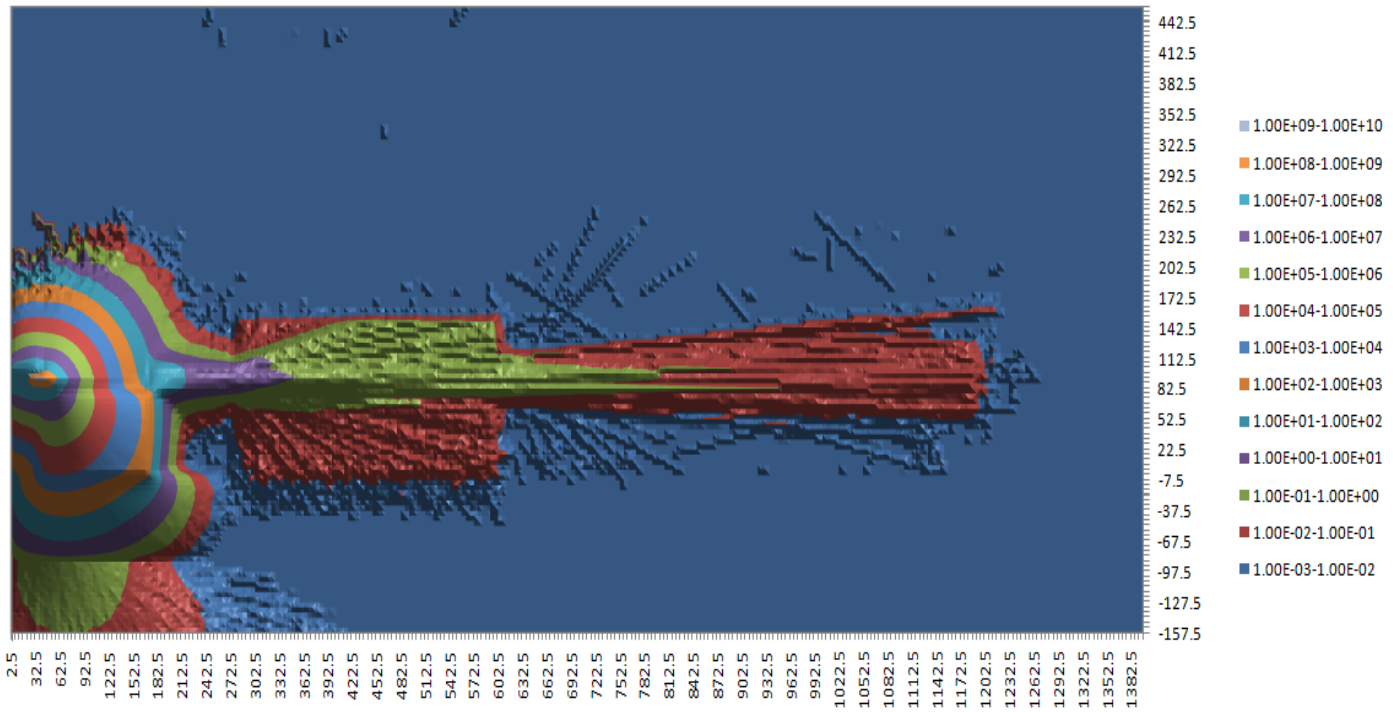

Figure 3.11: Vertical cut at beam axis showing dose rate [µSv/h] due to neutrons from the core when secondary shutter is closed (primary shutter open).

Secondary shutter closed, secondary gamma dose rate [µSv/h]

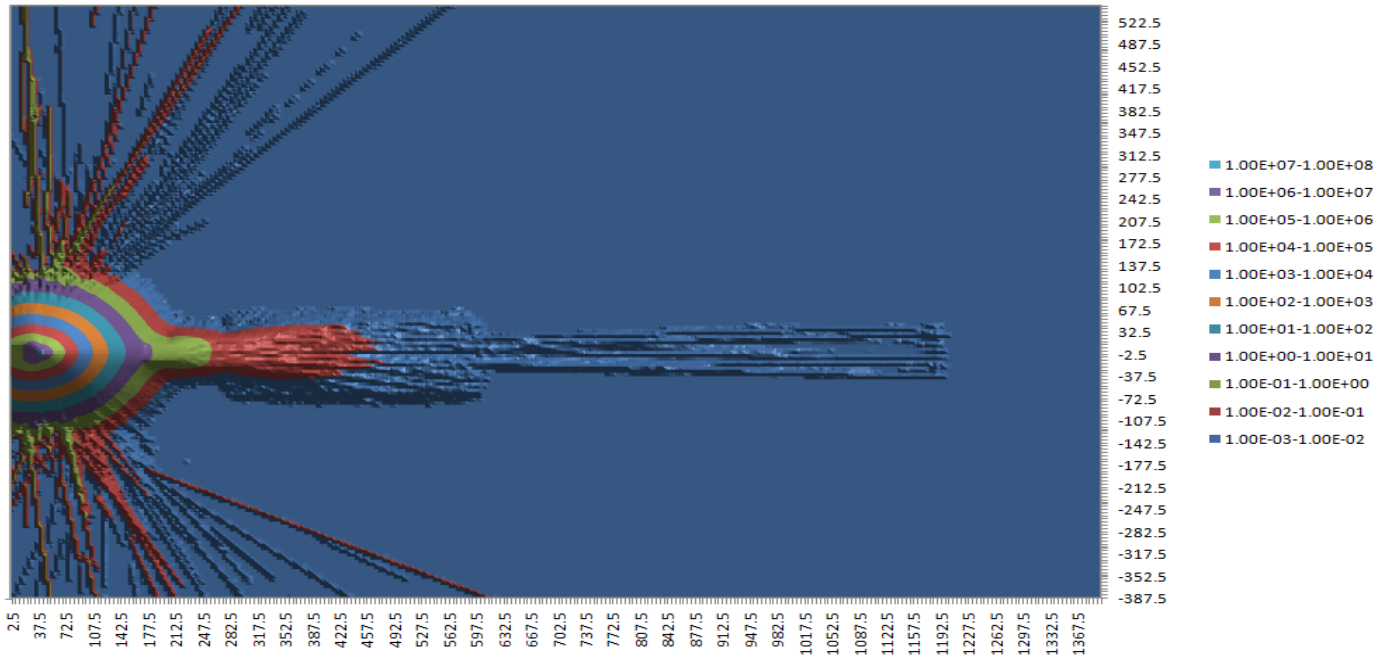

Figure 3.12: Horizontal cut at beam axis showing dose rate [µSv/h] due to secondary gammas from inelastic scattering and neutron capture when secondary shutter is closed (primary shutter open).

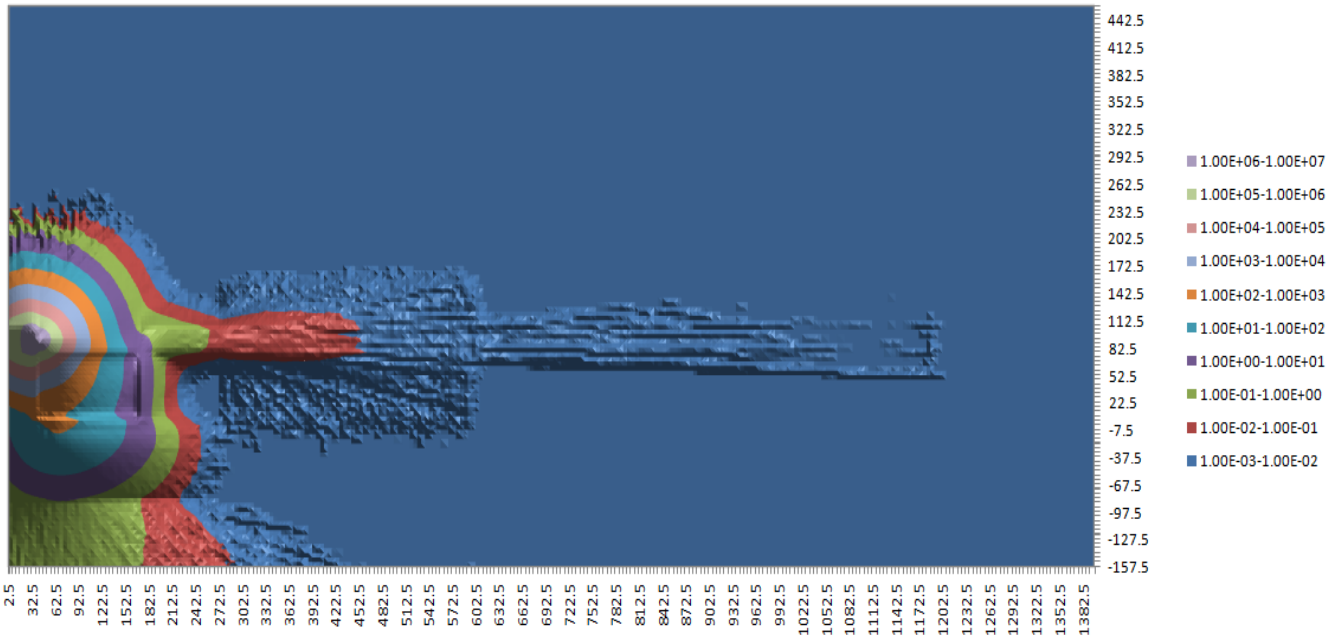

Figure 3.13: Vertical cut at beam axis showing dose rate [µSv/h] due to secondary gammas from inelastic scattering and neutron capture when secondary shutter is closed (primary shutter open).

Secondary shutter closed, primary gamma dose rate [µSv/h]

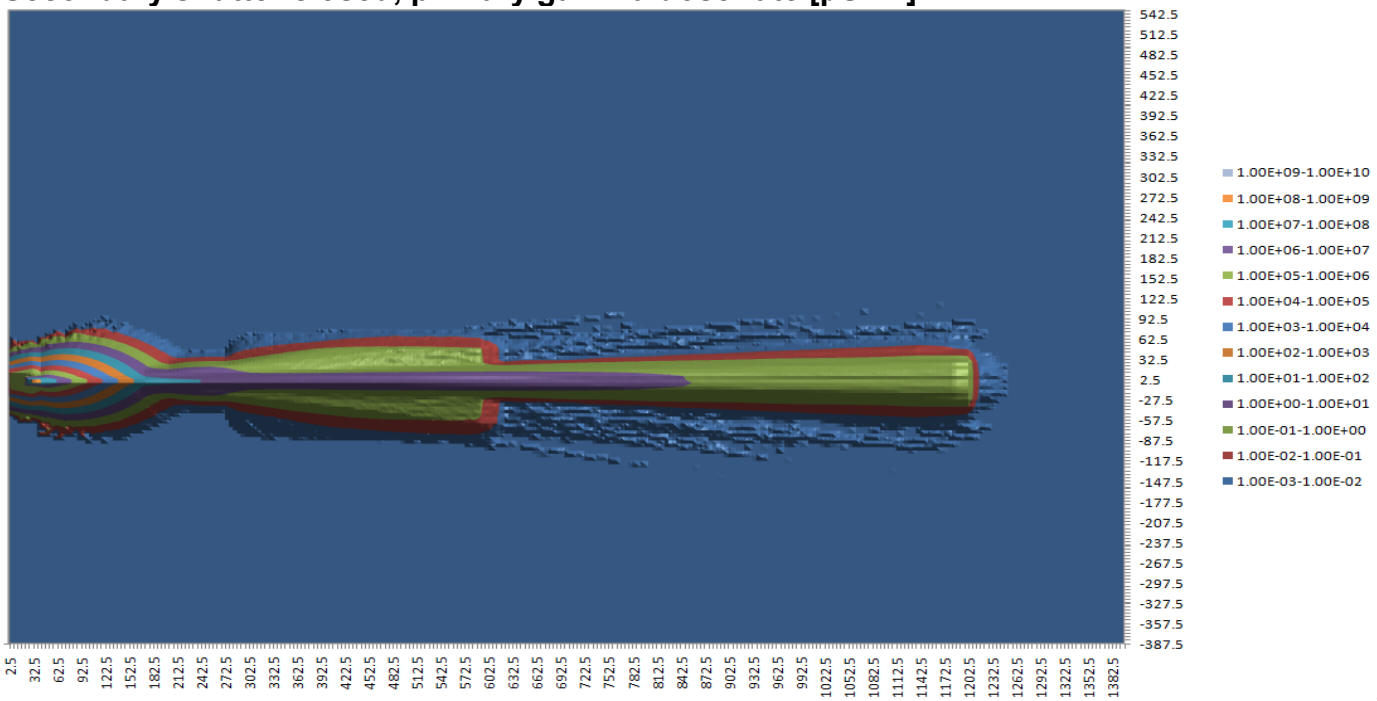

Figure 3.14: Horizontal cut at beam axis showing dose rate [µSv/h] due to primary gammas from the core when secondary shutter is closed (primary shutter open).

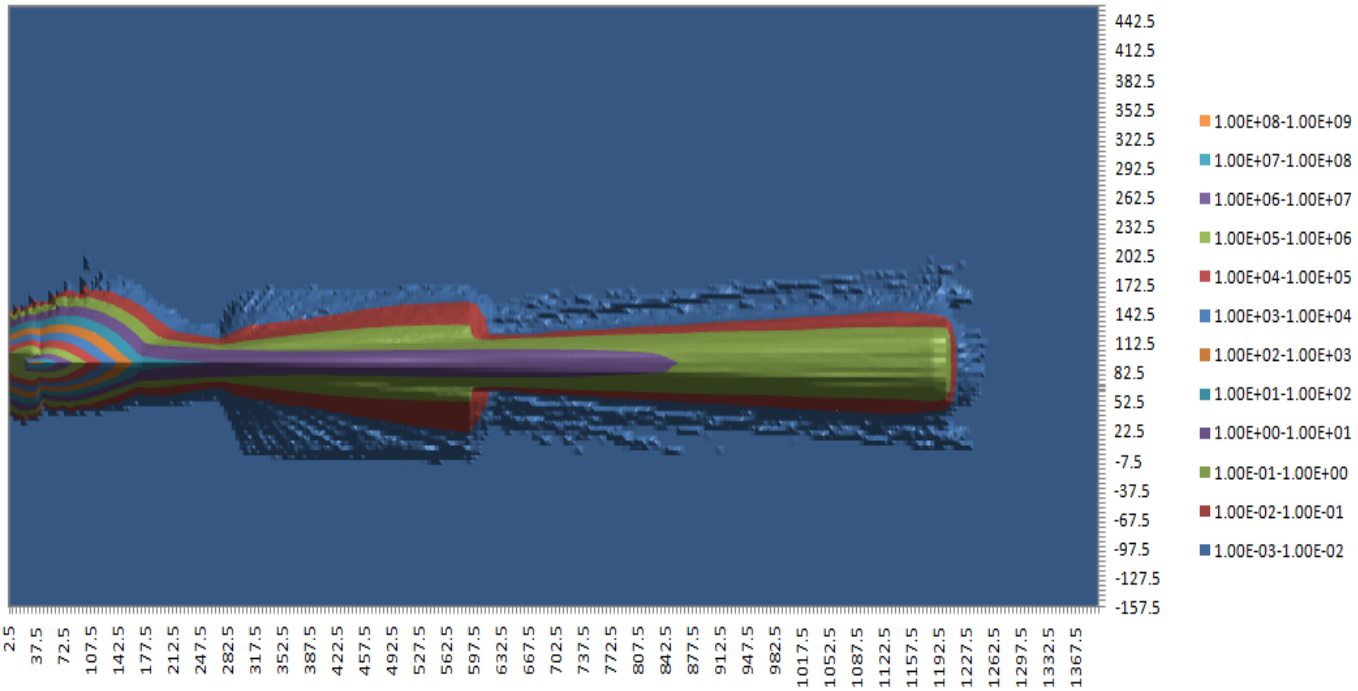

Figure 3.15: Vertical cut at beam axis showing dose rate [µSv/h] due to primary gammas from the core when secondary shutter is closed (primary shutter open).

The above results showed that the contact dose rates achieved met the requirement in all the simulated scenarios, with the only exception being the back wall directly exposed to the open beam, where the contact dose rate at the hot spot was more than 1 µSv/h but lower than10 µSv/h. To achieve this, a thicker wall as well as a radiation beam stopper were included in the model. The floor of the facility also presented a different situation where 830 mm and 685 mm thick 2400 kg/m^3 normal concrete do not offer enough shielding. As results of this a total contact dose rate of gamma rays and neutrons at the hottest point in the basement ceiling was in the order of 200 µSv/h but this was not a concern because of the occupational factor of the area (i.e. the average time workers spend at the basement) and the classification of the area when any facility is in operation. Lastly, the situation when the shutter is closed was considered to assess dose rates inside the experimental chamber. By procedure, both the primary shutter and the secondary shutter will be closed before the experimental chamber door can be opened. Nevertheless, the extremely conservative assumption of keeping the primary shutter open was used. Even in this situation, every point inside the experimental chamber had a total (neutron+gamma rays) dose rate for lower than 10 µSv/h.

The results obtained from this section were an indication that the identified materials were able to produce high density concrete with adequate shielding performance. The outcome of the simulations also provided a good indication that these material could be manipulated and altered until a good shielding concrete with desirable mechanical and physical properties was obtained. However, when these alterations of material contents were conducted in the trial mixture designs, some of the properties were required to remain unaltered or increased to more than what was obtained or used in this section. These included:

- The hardened density of concrete which was required to not be less than the 4000 kg/m^3 used in the simulation.
- The water content in the final mixture which was to be higher than 4.3 % of the total aggregates.
- The colemanite content which was to be more than the simulated amount which is 2.3 % of the total aggregates.

The high density of the concrete obtained as a result of the inclusion of iron ore and steel shot was necessary for the attenuation of primary gamma rays, slowing down of fast neutrons and absorption of secondary gamma rays. The water content was critical because of the hydrogen content which fulfils a vital function of attenuating slow neutrons. Colemanite content was also vital because of the boron and water of crystallisation contents which plays an important role in absorption of slow neutrons. If all of the above were achieved or exceeded in the physical concrete development section, the final developed shielding concrete was expected to perform as or better than the obtained theoretical results.

Chapter 4 Concrete ingredients used in the experiment

4.1 Ingredients and their compositions

The concrete developed in this research was required to be of high density (heavy weight) which meant it had to be of a special type in order to fulfil the purpose of a shielding material against neutron and gamma-rays. Normal or ordinary light-weight concrete had to be too thick if used for this purpose. This would in turn result in the shield that could exceed the space limitations and would also be uneconomical. Each of the identified ingredients used in the mixture development had a certain role to play. The materials listed below were identified for investigation in this research. All the materials identified were in line with the American Society for Testing and Materials ASTM C637 (2009) which specifies aggregates for radiation shielding. Material data sheets from the manufactures for cement and all chemical admixtures and additives material are given in appendix B of this report.

1. Portland cement (PC), CEM I 52.5 N.
2. Hematite (natural high density aggregate 1).
3. Magnetite (natural high density aggregate 2).
4. Iron/steel shot (artificial high density aggregate).
5. Municipal water.
6. Colemanite (boron containing aggregate).
7. Galena (natural high density, lead containing aggregate).

The ingredients were divided into three categories consisting of: (a) high density ingredients which produce heavy-weight concrete to attenuate (absorb) photons and scatter neutrons (change the energy from fast to thermal), (b) neutron absorption ingredients for attenuation of thermal neutrons and (c) a binder that sticks the aggregates together.

4.1.1 Portland cement

This is a substance applied as a mineral powder that, when mixed with water, hardens to make the ingredients stick together. When it is mixed with water, a chemical reaction referred to as hydration occurs and, as a result, the mixture sets and hardens to form a binder that glues the aggregates together to make concrete (Addis, 2004). PC is made

by firing a mixture of limestone and clay in a kiln, and grinding the product to a fine powder with a small amount of gypsum. The oxides used for the manufacturing of cements are as given in Table 4.1.

Table 4.1: composition of Portland cement (Addis, 2004)

Oxide	Chemical Formula	Symbol	Clinker Content%
Calcium	CaO	C	63-68
Silica	SiO_2	S	19-24
Alumina	Al_2O_3	A	4-7
Iron	Fe_2O_3	F	1-4

NB: Gypsum is calcium sulphate hydrate which is added to retard the setting of cement when it is mixed with water.

In the presence of water, the Portland cement constituents listed in Table 4.1 are involved in the hydration reaction. The most important reactions are expressed by equations 4 and 5.

$$C_3S + 6H \rightarrow C_3S_2H_3 + 3C_a(OH)_2 \quad (4)$$

$$C_2S + 4H \rightarrow C_3S_2H_3 + C_a(OH)_2 \quad (5)$$

$C_3S_2H_3$ (calcium silicate hydrate) grows outwards from the surface of particles of unhydrated cement in the form of a rigid structure of extremely small rods and platelets joined at the points of contact. Ca $(OH)_2$ (calcium hydroxide) on the other hand is mainly in the form of relatively large crystals, some of which can be embedded in the hydrated cement gel. Some Ca $(OH)_2$ is in the solution in the water within the pores in the cement paste (Addis, 2004).The hydrogen content present in all forms of water of hardened cement paste is of importance in that it provides a large proportion of the hydrogen which may be required for radiation shielding.

The Portland cement used in the final mixture of this study was obtained from Lafarge industries South Africa and its chemical compositions and specification are given in appendix B.4.

4.1.2 Hematite (Natural high density aggregate 1)

Hematite (also known as haematite) is a naturally mined iron oxide and has Mohr hardness between 5.5 and 6.5 with specific gravity between 4.9 and 5.3. The hematite used which was crushed from the mined ore by the mine was obtained from Beeshoek mine in the Northern Cape which is red in colour (see Figure 4.1). It was used both as fine and coarse aggregate.

Figure 4.1: Coarse and superfine Beeshoek hematite

4.1.3 Magnetite (Natural high density aggregate 2)

Magnetite (Figure 4. 2) is a naturally mined oxide of an iron which is strongly magnetic. Mohr hardness in the pure mineral is reported to be between 5.5 and 6.5, with a specific gravity of about 5.2. Magnetite ore is black in colour and are structurally granular and of massive texture. The magnetite investigated in this research was sourced from Evraz-Mapoch mine in the Limpopo province.

Figure 4.2: Evraz-Mapoch mine magnetite

4.1.4 Steel shot

These are used as artificial aggregates in concrete for radiation shielding. They have a specific gravity of between 7.5 and 7.8. The shape, size and grading of these aggregates are of importance and they should possibly be of a cubical to spherical shape , with only a small proportion of flat or elongated pieces, as shown in Figure 4.3. The metal aggregates should be free from grease or oil and by washing it with hot water or steam. Thomas Abrasives Pty (Ltd) supplied the steel shot used in this study.

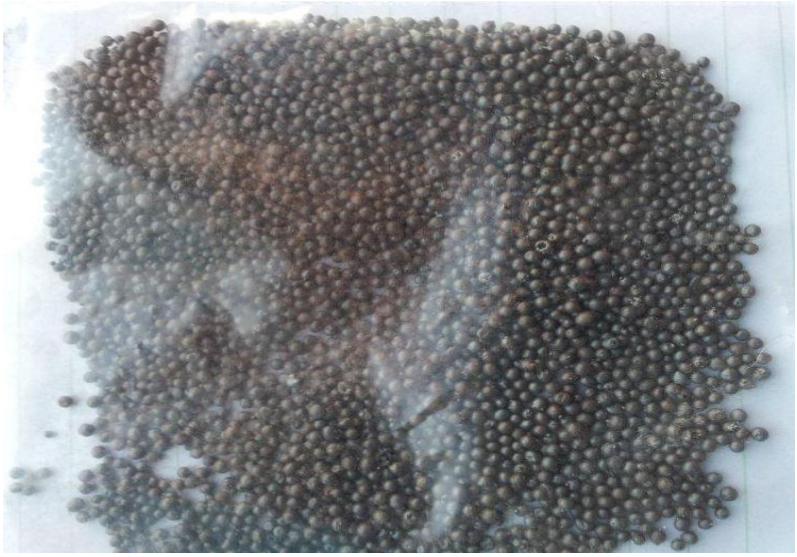

Figure 4.3: Steel shot from Thomas abrasives

4.1.5 Colemanite (boron containing aggregate)

It is a common practice to add boron to concrete in order to try enhance the neutron attenuation properties and to suppress secondary gamma-ray generation. Since boron is difficult to obtain by common extraction methods, the use of boron bearing minerals is more economical and practical (Gencel, et al. 2010). Colemanite ($2CaO.3B_2O_3.5H_2O$) shown in Figure 4.4 is a calcium borate mineral with Mohr hardness between 4 and 4.5, and specific gravity of about 2.4. It is one of the least soluble of the natural borates. As discussed in section 2.3.1.2, it has deleterious effects on the setting of Portland cement and it has been stated that the behaviour of concrete containing colemanite is somewhat unpredictable (Kaplan, 1989). Compared with other boron-containing additives such as boron carbide, boron calcite and boron frit; colemanite has the advantages of being more economical and has high fixed water content in the form water of crystallization which increases its usefulness in the fast neutron shielding. The colemanite utilised in this research was obtained from Florida in the USA.

Figure 4.4: Sample and bulk colemanite material obtained from Florida

4.1.6 Galena (natural high density lead containing aggregate)

Galena (Figure 4.5) is a high density, high lead content, lead sulphide (PbS) ore. It has about 86 % of lead and 14% sulphur. It is primarily included in a concrete mixture for gamma ray attenuation (Hammer and McCarthy, 1975).The galena investigated in this research was obtained from Markudi in Nigeria.

Figure 4.5: Galena sample from Nigeria

4.2 Chemical analyses of aggregates

Samples of the aggregates were obtained from the identified suppliers and tested for chemical composition. The purpose of this testing was to ensure that ingredients that will become radioactive due to elements that have long decaying half-lives (i.e. Cobalt, Copper, Nickel, Zinc etc.) are not significantly present in the aggregates.

The tests for chemical compositions were also used to confirm the guarantees presented on the suppliers' product data sheets. The chemical composition analyses of aggregates were conducted using ICP (Inductively Coupled Plasma) and XRF (X-Ray Fluorescence) methods. All aggregates used in the concrete mixture were found to not contain significant quantities of long half-life elements.

4.2.1 Chemical requirements of the aggregates

Requirements of the aggregates to be used in the mixture were as follows:

- Long half-life elements must not be significant in all the aggregates.
- Colemanite needed to have a minimum of 9% Boron content.
- Minimum content of Fe in the iron ore (hematite/magnetite) was required to be above 60%.
- Minimum content of Fe in the steel shot was required to be above 95%.
- Lead content in galena was required to be above 80%.

Results of the chemical analyses are presented in Tables 4.2. From the chemical analysis results, economic considerations, availability and ease of access of aggregates, it was decided that hematite, colemanite and steel shot would be the main aggregates in developing the concrete shield. The tests and results of the chosen aggregates are as discussed below.

Table 4.2: Chemical composition of aggregates

Determination	Units	Colemanite	Steel shot	Hematite	Magnetite	Galena
Aluminum(Al)	% m_m	4.05	0.16	1.2	0.631	0.018
Arsenic(As)	% m_m	0.12	-	-	-	-
Barium(Ba)	% m_m	0.028	-	-	-	0.018
Boron(B)*	% m_m	9.32	0.12	-	-	-
Calcium(Ca)	% m_m	25	-	0.017	1.24	-
Chloride(Cl)	% m_m	-	-	0.019	-	-
Chromium(Cr)	% m_m	-	0.095	0.009	0.016	-
Cobalt (Co)	% m_m	-	-	-	0.034	-
Copper (Cu)	% m_m	-	0.059	-	-	-
Fluoride(F)	% m_m	0.431	-		-	-
Hydrogen(H)	% m_m	NQ	NQ	NQ	NQ	NQ
Iron(Fe)	% m_m	2.1	97.9	64	63.3	0.171
Lead(Pb)	% m_m	-	-	0.012	0.047	78.4
Magnesium(Mg)	% m_m	6.87	0.019	-	2.84	-
Manganese(Mn)	% m_m	0.022	-	0.01	0.112	-
Mercury(Hg)	% m_m	-	-	-	-	0.039
Molybdenum(Mo)	% m_m	-	0.78	-	-	-
Nickel(Ni)	% m_m	0.026	0.042	-	0.01	-
Oxygen(O)#	% m_m	NQ	-	NQ	NQ	NQ
Phosphorus(P)	% m_m	0.026	-	0.028	0.155	-
Potassium(K)	% m_m	0.914	-	0.152	0.044	-
Rubidium(Rd)	% m_m	0.005	-		-	0.081
Silicon(Si)	% m_m	17.5	0.77	2.01	0.839	0.589
Sodium(Na)	% m_m	0.324	-	0.051	0.044	-
Strontium(Sr)	% m_m	0.173	-	0.012	0.013	-
Sulphur(S)	% m_m	1.66	-	0.012	0.124	9.853
Titanium(Ti)	% m_m	0.258	-	0.057	0.961	-
Vanadium(V)	% m_m	-	-	0.009	0.056	-
Yttrium(Y)	% m_m	0.002	-	-	0.021	-
Zirconium(Zr)	% m_m	-	-	-	-	0.225
Zinc (Zn)	% m_m	0.004	0.0322	-	0.222	-

NQ: Present but not quantified. **May be more than measured.*

4.2.2 Raw materials

4.2.2.1 Fine aggregates

Sieve analysis tests (Figure 4.6) were performed on the different aggregate types to aid categorisation of the ingredients. Fine aggregate (FA) acceptable for concrete casting as described in SANS 1083:2006 could not be sourced directly from the supplier. Instead two different grades of superfine and fine aggregates were obtained. It was therefore decided to blend these two grades of FA in order to obtain the suitable size distribution as shown in Figure 4.7.The 55/45, 60/40, 65/35 and 70/30 blends of superfine/fine aggregates met the requirements of the acceptable sand as described by the code. All were tried but the 70/30 blend with Fineness Modulus (FM) of 2.1 gave better results and was used in the final mixture.

Figure 4.6: Performing sieve analysis of fine aggregates

The colemanite used had FM of 4.5. Steel shot used for casting of concrete were obtained from the manufacturer in a standard or uniform size of 2 mm in diameter. Tables A.1 to A.8 in appendix A present the sieve analysis results of the fine aggregates and different blends that were tried. Figure 4.8 shows the comparison of all the FA blends to SANS 1083:2006 requirements.

Figure 4.7: Blending of the mines superfine and fine aggregates

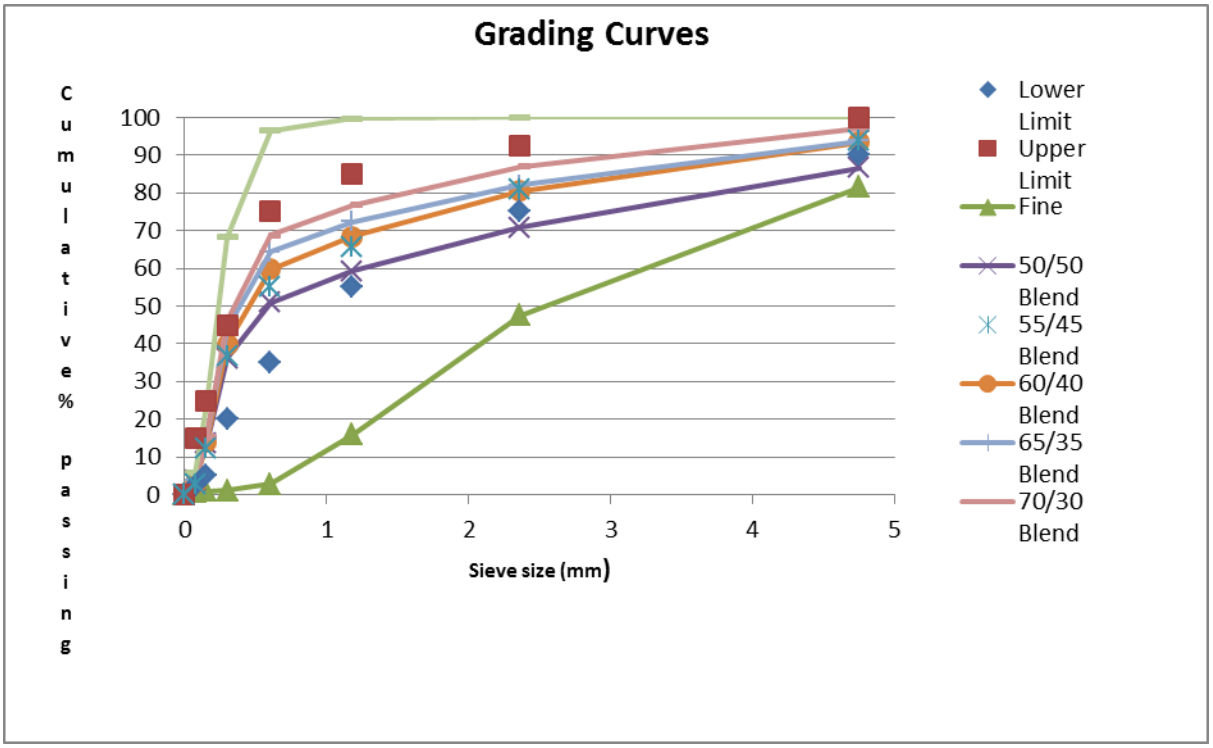

Figure 4.8: Blends grading and standard grading limits

4.2.2.2 Water and Cement

The water used was potable municipal water and the CEM I 52.5 N was obtained from Lafarge industries, South Africa.

4.2.2.3 Coarse aggregates

The mine where the coarse aggregates were sourced could only supply two grades of stone which were *DR lumpy* grade and *Lumpy* grade. The DR lumpy grade was initially not considered to be used as coarse aggregate in the mixture and the Lumpy grade comprised of stones which were too big for concrete casting. It was therefore decided to convert the big Lumpy grade into conventional 19 mm through crushing as shown in Figure 4.9. The sizes of the Lumpy grade ranged between 6.3 and 31.5 mm with the upper limit forming a majority of the stones. The crushed stones were further sieved to ensure that the aggregates used were within the 19 mm specification. Due to cost implications involved in crushing and sieving of large quantities of the stones, it was later decided to use the DR lumpy grade which had an average size of 13 mm. The DR lumpy grade improved the workability of the fresh concrete and also helped in achieving the required cohesion of the high slump concrete.

Figure 4.9: Crushing of the lumpy grade in the lab to 19 mm

4.3 Selection of materials

The results obtained from this section indicated that all identified raw materials to be used in the concrete development were of the desired chemical compositions and adequate physical properties for radiation shielding and concrete casting. The results obtained from chemical composition analysis of each material confirmed that radiation activation of any of these identified material would not result in formation of radioactive elements with long decaying lives. Some of the materials investigated were to serve the same purpose in the final shielding concrete. These were hematite, magnetite and galena. Hematite and magnetite are both ores of iron and their role was to contribute in production of the required high density of concrete. Galena which is a high density ore of lead was also to be included in the mixture for high density concrete production. Unlike hematite and magnate which are capable of attenuating primary gamma rays, slowing down fast neutron and absorbing secondary gamma rays, galena can only shield gamma rays. For this reason, excessive cost, poor grading supply and bulk accessibility difficulties of the material, galena was discarded for further investigation because it fulfilled only one function which could be achieved by either one of the investigated iron ores which has multiple functions for shielding purposes. Magnetite was also discarded for further inclusion in the research because as indicated in Table 4.2 it had a lesser content of iron as compared to hematite. It was therefore decided to use a combination of hematite and steel shot for high density concrete production in the final mixture.

Taking into consideration the results obtained from the grading analyses as given in Appendix A, the chemical composition analyses results, cost implications, accessibility and reliability of bulk supply of materials, it was decided to use hematite, steel shot and colemanite as the main ingredients to be used in the physical development of the shielding concrete.

Chapter 5 Concrete mixture development.

5.1 Concrete requirements

The mechanical and physical properties required on the fresh concrete included workability, cohesion, setting, consistence and strength in the hardened state. HDSC of high slump and a minimum 28-day cube strength of 25 MPa was specified. The strength was in line with the recommendation from SANS 10100-2 for structural elements and was deemed adequate by the design engineers since the concrete was to be cast into permanent steel boxes using 10 mm thick plates as shown in Figure 5.1. The configurations of the boxes were of different sizes and shapes depending on their position on the proposed SANRAD facility. The purpose of the steel boxes was to enhance the interlocking of the HDSC blocks to prevent potential leakage of radiation. The tallest box was designed to be about 1950 mm in height. The high slump of concrete was required to ease the casting process since only two 100 mm holes were to be employed in the casting of the concrete blocks. One hole will be used for pouring and the other for breathing and vibration purposes. To be consistent with the output of the MCNP-X simulations and to ensure that satisfactory results were obtained, the final concrete mixture was required to have a density of more than 4000 kg/m^3.

Figure 5.1: Demonstration assembly of the SANRAD facility with empty interlocking steel boxes

5.2 Developmental process

The mixture developmental process included performing the necessary tests on raw materials and casting a series of trials using the tested raw materials in order to obtain a satisfactory mixture. In developing the mixture design, the proportions of colemanite and water were required to be maintained or more than those used in the MCNP-X models.

5.2.1 Trial tests

Various trial concrete mixtures with w/c of 0.42, 0.45, 0.5 and 0.6 were prepared as presented in Table 5.1 to 5.8.Thirteen 100 x 100 x 100 mm concrete cubes were cast for every mixture assessed as shown in Figure 5.2. Adjustments were conducted in attempt to obtain suitable properties for the application. The essential properties tested consisted of workability, cohesion, density and compressive strength. These mixture modifications and their results are discussed in the subsequent developmental procedure.

Figure 5.2: Casting of 100 x100 x 100 mm concrete cubes

5.2.2 Developmental procedure

The literature review in the previous sections indicated that behaviour of mixtures with colemanite is unpredictable. The study by Gencel et al. (2010) also reported formation of small masses of concrete when colemanite was introduced into the mixtures and referred to it as flocculation. There were also reduction in strength and delay in setting time of concrete as a result of addition of colemanite into the concrete mixtures. This informed the procedure adopted in the physical development of the shielding concrete. The procedure adopted was as follows:

1. Since colemanite was an obligatory aggregate in the mixture as indicated by the MCNP-X simulation results, it was decided to first cast the control mixture with no colemanite, extenders and additives and analyse it. The basis of this mixture was the proportions used in the MCNP-X simulations.
2. Colemanite was added into the initial mixture and the effects were noted. At this stage no cement extenders and chemical additives were added into the mixture. The required properties in both fresh and hardened states of the mixture were determined.
3. Necessary cement extenders and additives were added into the mixture to counteract the effects of colemanite and improve the properties obtained in the previous mixture.
4. Stage 3 was repeated until a mixture with satisfactory mechanical properties was achieved.
5. The concrete obtained by the mixture with satisfactory mechanical properties was sent to NECSA for radiation shielding testing using a radioactive beam emerging from a core of SAFARI-1 research reactor.
6. The mixture with satisfactory mechanical and shielding properties was adopted as the final mixture to be used in the construction of the SANRAD facility.

5.2.2.1 The initial control mixture

The initial control mixture presented in Table 5.1 contained only high density aggregates, water and cement. Normal concrete behaviour was expected from this mixture as no unusual aggregates were used.

Table 5.1: Control mixture assessed

W/C: 0.5

Material	Mass(kg)	Density(kg/m^3)	Volume(m^3)
CEM I 52.5N-PPC	390.00	3140.00	0.12
Water	195.00	1000.00	0.20
Hematite stone	2050.00	5200.00	0.39
Hematite sand	970.00	5200.00	0.19
Steel shot	850.00	7100.00	0.12
Total	4455.00	-	1.02
Estimated Density(kg/m^3)		4368.97	
Results			
Density (kg/m^3)		4514	
Slump	Height (mm)	50	
	Spread (mm)	-	
Cohesion		Poor	
7 day strength (MPa)		39.4	
28 day strength (MPa)		54	

The control mixture was too stony and lacked cohesion. The slump as shown in figure 5.3 was also far from the desirable consistence requirements. Normal concrete behaviour was however noted with the concrete cubes setting within the normal time and cured under the normal laboratory condition of submerging the cubes in water.

Figure 5.3: Slump test of the control mixture

5.2.2.2 Trial mixtures

The first trial mixtures with colemanite are as given Table 5.2 and 5.3. The previous control mixture was slightly modified with the introduction of colemanite. The w/c ratio was decreased from 0.5 to 0.45 for trial mixture 1 and was maintained at 0.5 for trial mixture 2. It was decided to start with 2.3% and 4.4% proportions of colemanite for trial mixture 1 and 2 respectively, thus satisfying the requirements of the MCNP-X simulation outputs. The proportion of colemanite was measured by weight of the total aggregates.

Table 5.2: Assessed trial mixture 1 with 5% colemanite

W/C:0.45			
Material	**Mass(kg)**	**Density(kg/m³)**	**Volume(m³)**
CEM I 52.5N-PPC	390.00	3140.00	0.12
Water	175.00	1000.00	0.18
Hematite stone	1950.00	5200.00	0.38
Hematite sand	929.00	5200.00	0.18
Steel shot	809.00	7100.00	0.11
Colemanite -2.3%	100.00	2400.00	0.04
Total	4344.00	-	1.00
Estimated Density(kg/m³)		4323.60	
Results			
Density (kg/m³)		4421	
Slump	Height (mm)	No Slump	
	Spread (mm)	-	
Cohesion		Very poor	
7 day strength (MPa)		2.6	
28 day strength (MPa)		41.1	

Table 5.3: Assessed trial mixture 2 with 10% colemanite

W/C :0.5			
Aggregate	**Mass(kg)**	**Density(kg/m³)**	**Volume(m³)**
CEM I 52.5N-PPC	360.00	3140.00	0.11
Water	180.00	1000.00	0.18
Hematite stones	1850.00	5200.00	0.36
Hematite sand	890.00	5200.00	0.17
Steel shot	780.00	7100.00	0.11
Colemanite -4.4%	185.00	2400.00	0.08
Total	4245.00	-	1.01
Estimated Density(kg/m³)		4209.16	
Results			
Density (kg/m³)		4071	
Slump	Height (mm)	No Slump	
	Spread (mm)	-	
Cohesion		Very poor	
7 day strength (MPa)		12.6	
28 day strength (MPa)		33.8	

As already indicated in the literature, immediately when colemanite was added into both the mixtures, the water was absorbed and the fresh concrete flocculated as shown in Figure 5.4. A delay in setting time of mixtures was also noticed. Without being fully set the concrete cubes of trial mixture 1 were demoulded and placed under water. At 7th day strength testing it was noticed that 50% of the concrete cubes of trial mixture 1 had disintegrated during initial stages of curing as shown in Figure 5.5. The other cubes which did not disintegrate were used to determine strength at 7 and 28 days. The 12.6 MPa early strength of trial mixture 2 was 79% more than that obtained for trial mixture 1 which was 2.6 MPa. This was as result of different removal times of the concrete cubes from their casting moulds. The trial mixture 1 cubes were demoulded after 24 hours while the trial mixture 2 cubes were demoulded after 48 hours.

Figure 5.4: Flocculated concrete after the addition of colemanite

The introduction of colemanite into the mixtures was found to be responsible for the zero slumps and delay in the setting time of the concrete. This was further confirmed by performing slump tests of the same mixture with colemanite and the other without colemanite.

Figure 5.5: Disintegrated cubes after being placed under water

Given the two difficulties posed by the introduction of colemanite, it was decided to introduce two chemical admixtures to improve the results. In order to achieve a high slump, a superplasticiser was introduced. The superplasticiser had to be chemically

compatible for the purpose and capable of producing the required 180 mm slump or more. To improve the setting time of concrete, an accelerator was added into the mixture. This accelerator needed to be free from chlorides due to the high percentage of steel shot used in the mixture. If a chloride based accelerator is used, a chemical reaction could result in corrosion of the steel shot by chloride attack which could in turn affect the durability of the concrete. As recommended by the supplier, it was decided to start with 1 % dosage by cementitious weight of each admixture as given in Table 5.4.

The strength in this mixture was not determined as the primary purpose was to focus on the consistence and achieve the required slump. The 10 mm slump obtained from trial mixture 3 indicated that the combination of the water content and dosage of the superplasticiser was not effective enough. In addition to the 10 mm slump obtained, the mixture lacked finer aggregates and as a result, the cohesion was poor.

Table 5.4: Assessed trial mixture 3 with 1% superplasticiser and accelerator

W/C:0.5			
Aggregate	**Mass(kg)**	**Density(kg/m^3)**	**Volume(m^3)**
CEM I 52.5N-PPC	390.00	3140.00	0.12
Water	235.00	1000.00	0.24
Hematite stones	1800.00	5200.00	0.35
Hematite sand	950.00	5200.00	0.18
Steel shot	1350.00	7100.00	0.19
Colemanite	100.00	2400.00	0.04
Optima 100-1%	2.98	1060.00	0.00
Xel 650 -1%	7.63	1450.00	0.01
TOTAL	4835.61	-	1.13
Estimated Density(kg/m^3)		4287.15	
Results			
Density (kg/m^3)		4287	
Slump	Height (mm)	10	
	Spread (mm)	-	
Cohesion		Poor	
7 day strength (MPa)		-	
28 day strength (MPa)		-	

The setting time of concrete remained a challenge. This remained so after the cubes were left for 2 days before demoulding. It was therefore decided to modify the trial mixture 3 into trial mixture 4 as given in Table 5.5 as follows:

- Replace 55/45 blend with 60/40 blend.
- Reduce superplasticiser dosage to 0.8 % by cementitious content.
- Increase accelerator dosage to 1.5 % by cementitious content.
- Reduce the stone content by 10 % and transfer it to the sand content.
- Increase the w/c to 0.6

With the implemented modification, the slump of the mixture improved to 25 mm. The mixture was also cohesive and workable. The required high slump was however still not achieved. From trial mixture 4, it was discovered that increasing the finer granules in the fine aggregate and reducing the high content of the coarse aggregate has an influence on the consistence (slump), workability and cohesion of the mixture.

Table 5.5: Assessed trial mixture 4

W/C :0.6			
Aggregate	**Mass(kg)**	**Density(kg/m³)**	**Volume(m³)**
CEM I 52.5N-PPC	390.00	3140.00	0.12
Water	235.00	1000.00	0.24
Hematite stone	1620.00	5200.00	0.31
Hematite sand	1130.00	5200.00	0.22
Steel shot	1350.00	7100.00	0.19
Colemanite	100.00	2400.00	0.04
Optima 100-0.8%	2.32	1060.00	0.002
Xel 650 -1.5%	5.96	1450.00	0.004
TOTAL	4833.25	-	1.12
Estimated Density(kg/m³)		4291.89	
Results			
Density (kg/m³)		4292	
Slump	Height (mm)	25	
	Spread (mm)	-	
Cohesion		Good	
7 day strength (MPa)		-	
28 day strength (MPa)		-	

It was therefore decided to further modify the previous mixture in to trial mixture 5 given in Table 5.6 as follows:

- Replace 60/40 fine blend with 70/30 blend.
- Reduce the w/c ratio to 0.425.
- Reduce the stone content and balance the sand content to a 60:40 percentage of stone to sand ratio.
- Add superplasticiser until a high-slump cohesive mixture was achieved.
- Add accelerator of 3.5 % by weight of cementitious content.

The 3.5% and 3% dosages of superplasticiser and accelerator mixture shown in Table 5.6 gave better results. It was therefore decided to cast this mixture for strength testing. Due to the problem with setting of the concrete, it was decided to demould the cubes after 48 hours and cure them at ± 23 °C and ± 65 % RH for the first seven days and then under water for the rest of the 28 days.

Table 5.6: Assessed trial mixture 5 with 3.5 % superplasticiser and 3 % accelerator mixture

W/C :0.42

Material	**Mass (kg)**	**Density(kg/m^3)**	**Volume(m^3)**
CEM I 52.5N- PPC	450.00	3140.00	0.14
Water	191.00	1000.00	0.19
Hematite stones	1255.00	5200.00	0.24
Hematite sand	855.00	5200.00	0.16
Steel shot	1550.00	7100.00	0.22
Colemanite	100.00	2400.00	0.04
Optima 100-3.5%	11.69	1060.00	0.01
Xel 650 -3%	15.99	1450.00	0.01
TOTAL	4332.88	-	1.02
Estimated Density(kg/m^3)		4239.16	
Results			
Density (kg/m^3)		4372	
Slump	Height (mm)	190	
	Spread (mm)	-	
Cohesion		Good	
7 day strength (MPa)		2.6	
28 day strength (MPa)		38.9	

During demoulding of the cubes after 48 hours, it was noticed that the concrete was still not completely set. When this mixture was further analysed, it was decided that the dosages of the admixtures were too high and uneconomical. As a result of this, a different option was considered. The slump was later also preferred to be high enough to yield a suitable spread at the lower range of self-compacting concrete. This would be adequate to ensure that only minimal compaction is required during pouring of concrete into the steel boxes. From the above considerations, it was therefore decided to modify trial mixture 5 using the following alternatives as given in Table 5.7 and 5.8.

Figure 5.6: Improved fresh mixture with 3.5% and 3% dosages of superplasticiser and accelerator

The first option was as follows:

- Reduce the superplasticiser to a maximum recommended dosage of 1.5% by cementitious weight.
- Introduce a more effective superplasticiser which would compensate for the reduction of the superplasticiser dosage. The superplasticiser used was slowly added to the mixture in the pan until an acceptable mixture was reached. The dosage used was 0.92%.
- To compensate and further improve the cohesion of the mixture, 6.7% of cement was replaced by condensed silica fume.

- The CEM I cement was replaced by a similar 52.5 N cement which had 15 percentage of fly ash.
- High alumina cement (HAC) was introduced into the mixture to help resolve the retardation effect of colemanite.
- The accelerator was removed from the mixture.

Table 5.7: Assessed trial mixture 6 with no accelerator and addition of HAC

W/C :0.42			
Material	**Mass (kg)**	**Density(kg/m³)**	**Volume(m³)**
CEM I 52.5N- Lafarge	345.00	3140.00	0.11
Silica Fume	30.00	2700.00	0.01
High Alumina Cement	75.00	2500.00	0.03
Water	191.00	1000.00	0.19
Hematite stones	1255.00	5200.00	0.24
Hematite sand	855.00	5200.00	0.16
Steel shot	1550.00	7100.00	0.22
Colemanite	100.00	2400.00	0.04
Optima 100-1.5%	7.16	1060.00	0.01
Optima 203-0.92%	6.00	1450.00	0.00
TOTAL	4333.46	-	1.02
Estimated Density(kg/m³)		4254.24	
Results			
Density (kg/m³)		4220	
Slump	Height (mm)	210	
	Spread (mm)	530	
Cohesion		Very Good	
7 day strength (MPa)		20.0	
28 day strength (MPa)		48.0	

Results obtained from trial mixture 6 indicated good performance of concrete. The mixture was fully set after 24 hours, the cohesion of the mixture improved and both the early and late strength of the concrete had also improved. However, due to the uncertainties involved in using HAC in the mixture, the second alternative was necessary. HAC is known to have negative impact on the durability of concrete in terms of strength. The supplier of the product also recommended that it be avoided in this application and only be used in emergency repair works and floor constructions.

The second set of alterations to the mixture was as follows:

- Condensed silica fume was introduced in the mixture.
- The CEM I cement was replaced by a similar 52.5 N cement which had 15 percentage of fly ash according to the supplier's compositions.
- HAC was removed.
- The superplasticiser dosage was reduced to 1.3%.
- The accelerator dosage was reduced to 2%.
- The effective superplasticiser was slowly added to the mixture until a cohesive unsegregated uniform mixture was achieved.

The above modifications yielded trial mixture 7 given in Table 5.8. The test results of trial mixture 7 indicated that there were still retardation challenges experienced in the mixture. The concrete was demoulded after 3 days and kept at constant temperature of ± 23°C and relative humidity of ± 65% for the first 7 days of the curing period (hence the low strength) and later submerged under water for the remainder of the period.

Table 5.8: Assessed trial mixture 7 with addition of silica fume

W/C:0.51

Aggregates	**Mass(kg)**	**Density(kg/m³)**	**Volume(m³)**
CEM I 52.5N- Lafarge	345.00	3140.00	0.11
Silica Fume	30.00	2700.00	0.01
Water	191.00	1000.00	0.19
Hematite stones	1255.00	5200.00	0.24
Hematite sand	855.00	5200.00	0.16
Steel shot	1550.00	7100.00	0.22
Colemanite	100.00	2400.00	0.04
Optima 100-1.5%	5.17	1060.00	0.01
Optima 203-0.92%	2.18	1450.00	0.00
Xel 650-2%	8.25	1100.00	0.01
TOTAL	4378.35	-	0.99
Estimated Density(kg/m³)		4415.42	
Results			
Density (kg/m³)		4231	
Slump	Height (mm)	230	
	Spread (mm)	510	
Cohesion		Very Good	
7 day strength (MPa)		2.5	
28 day strength (MPa)		29.9	

5.2.3 Discussion and conclusion

The strength behaviour obtained from the results of all mixtures as given in Figure 5.7 indicated that addition of colemanite reduces the strength of concrete. The decrease between the control mixture and trial mixture 1(TM1) was observed to be 93% and 24% on early and late strengths respectively. The high decrease on early strength was as a result of the slow rate in setting of colemanite containing concrete. At 28 day strength the colemanite concrete was already set and this was the reason there was a reasonable strength reduction of 24%. The 12.6 MPa strength obtained in trial mixture 2 (TM2) which had about 4.4% of colemanite by the weight of total aggregates was due to the difference in demoulding times of concrete cubes employed between TM1 and TM2. TM1 concrete cubes were removed from their moulds after 24 hours while TM2 cubes were removed after 48 hours. The different demoulding times resulted in better early strength in TM2 because it had set better than the concrete from trial mixture 1 when tested. However, due to higher amount of colemanite used in TM2, the early and late strength still decreased by 68% and 37% respectively as compared to the control mixture. The high early and late strengths obtained in TM6 were mainly due to the rapid hardening effect induced by the introduction of HAC. The strength reduction effects of colemanite on both early and late strength of TM6 were 49% and 11% as compared to the control mixture. It was also noticed that in all the trial mixtures where the content of colemanite was maintained at 2.3%, the strengths remained almost constant besides for trial mixture 7 (TM7) where some percentage of the cement was replaced by condensed silica fume.

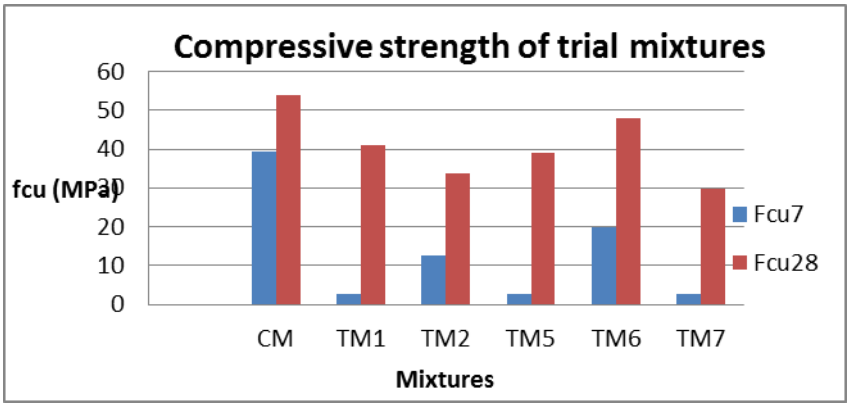

Figure 5.7: Early and late compressive strength of the assessed trial mixtures

The consistence and workability of the mixtures were poor when colemanite was introduced into the mixtures. In the control mixture, the slump obtained was only 50 mm. This was because of the high content of coarse aggregate used in the mixture. Both TM1 and TM2 produced no slump and were not workable as a result of addition of colemanite. The consistence started to improved when the chemical additives were added into the mixtures as shown in Figure 5.8 (i.e. TM 3 and TM4). The required consistence was however still not achieved using the supplier's recommended dosages. It was only when the recommended dosages were exceeded in TM5 that the required slump was achieved. Since this was not cost effective, different combinations of superplasticisers were used in TM6 and TM7 to obtain the required slumps as shown in Figure 5.9.

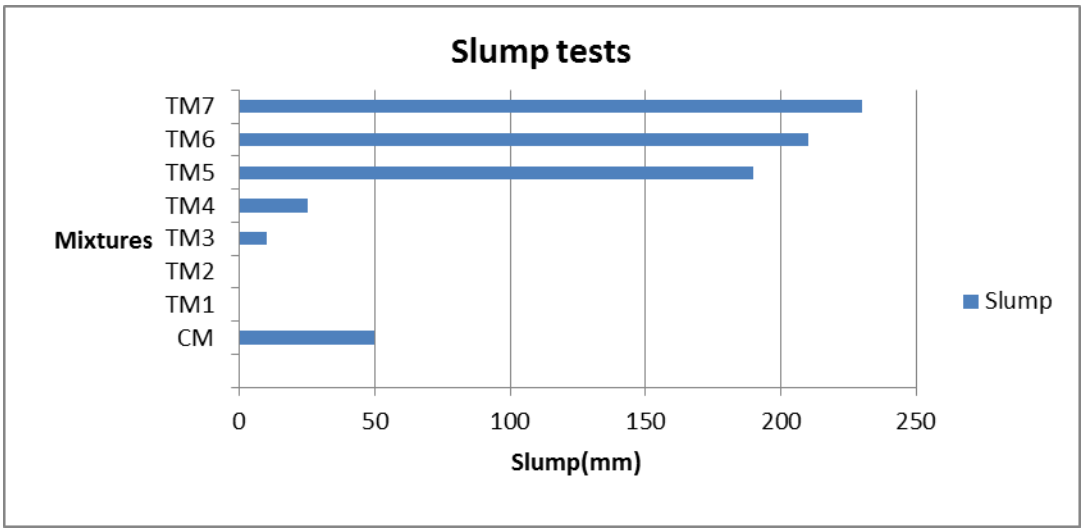

Figure 5.8: Slump results of the assessed trial mixtures

The cohesion of the mixture also improved with improving consistence and workability. It was also observed that proper proportioning of the fine and coarse aggregates contributed to improved cohesion. In this case, since the fine and coarse aggregates were from the same source and had the same density, proportioning of the coarse and fine aggregates was easy. Fine aggregate were increased in TM5, TM6 and TM7 in order to obtained better cohesive mixtures.

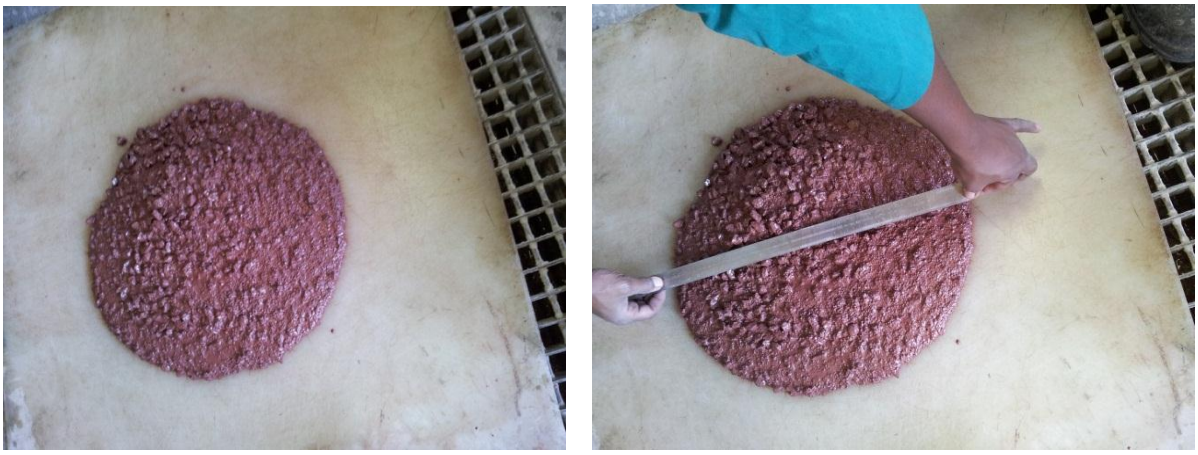

Figure 5.9: Collapsed slumps of TM6 and TM7

In all the mixtures, TM5, TM6 and TM7 produced satisfactory results with TM6 producing better results with behaviour in setting resembling that of conventional concrete. However, TM7 was adopted as the final mixture to be used despite its delay in setting time. This decision was informed by the uncertainties involved in using HAC which were previously mentioned. The use of HAC has in the past resulted in some major collapse and failure of structures. HAC may inevitably undergo a reaction called "*conversion*" where a strength loss of 50% or more is possible (Barborak, 2010). Conversion is the result of the metastable phases of the hydration products converting to more stable hydration products. Once converted, the more stable hydration products form a smaller crystalline structure and take up less space, increasing the porosity of the overall matrix and consequently reducing the strength (Barborak, 2010).Due to the nature of the application of this concrete, any uncertainty in behaviour of hardened concrete was avoided to improve the chances of obtaining the construction license from the NNR. This is the reason why TM7 was used even though it had retardation difficulties. The setting difficulty experienced in TM7 was however not much of a problem since the concrete would be permanently placed in boxes made of 10 mm thick steel plates as shown in Figure 5.1. As a result of adopting TM7, the setting period was specified as a restriction in construction. This restriction was that the cast concrete blocks cannot be moved until they have cured for 28 days.

Chapter 6 Shielding experiment

6.1 Background of the experiment

The purpose of this task was to attempt to verify and validate the above developed TM7 which will be used at the new SANRAD facility at Necsa's SAFARI-1 nuclear reactor through direct measurement of the efficiency of its absorption of neutrons in order to provide adequate shielding from a white spectrum neutron beam extracted from a reactor core. This was achieved through measuring the gamma-ray counts from the gold (Au) foils imbedded at different locations along the 800 mm thick shielding material as shown in Figure 6.1. Measurement methods applied were foil activation, gamma counting and neutron radiography. This is because neutron radiography was not sufficient as the lithium and gadolinium scintillator screens in the experimental facility to be used were optimised for cold and thermal neutrons and would poorly capture fast neutrons.

The foil activation method was adopted to be used to determine the attenuation properties of the shielding materials for thermal and fast neutrons and the methodology employed is described in this section. The foil activation method of neutron detection is based on the fact that many elements become radioactive when exposed to a neutron flux. In most studies gold and copper were used for the neutron dose measurement. However, different foils can be used depending on the neutron spectrum used for the exposure. Foil activation method can also be used to unfold an unknown neutron spectrum. Sathian et al. (2008) used the foil activation method to unfold the neutron spectrum of a cyclotron accelerator with energy of 16.5 MeV, of 60 μA and pressure of 438 psi. In the study, the sample was exposed to the neutron flux for a measured length of time and then removed for counting of induced radioactivity. The induced activity was estimated using HPGe and 4πβ-γ detector. The total number of counts were first corrected for background and then reduced accordingly to obtain activity which would have been obtained right at the end of exposure. From the specific activity, the neutron spectrum was then unfolded using the computer code (Sathian et al., 2008).

Kobayashi et al. (1988) also used multi-foil activation method to measure a neutron flux spectrum at Kinki university reactor in Japan. In their study the neutron flux spectrum

was measured using two foil activation methods where a sandwich method was applied for measurement of neutron fluxes at different energy level using gold, indium, manganese and tungsten foils. The results obtained showed good results and the spectrum was successfully unfolded using a computer code called NEUPAC (Kobayashi et al., 1988).

In this section the shielding ability for neutrons was evaluated by means of foil activation method. The setup used was the everyday operational setup which included the 15 cm thick polycrystalline bismuth filter at room temperature to filter the gamma-rays and some neutron spectrum regions. The experimental measurements conducted with gold (Au) foils and the bismuth filter indicated that the thickness of the shielding material developed in the previous section was adequate from the radiation safety point of view. Several Au foils were embedded at different locations up to 800mm within the shielding material to follow the attenuation of the neutron beam over distance within the shielding material. The Au foil was activated by the entire neutron energy spectrum expected at the SANRAD facility according to the MCNPX simulation as shown in Figure 6.1. The radiative neutron cross-sections of Au-197 shown in Figure 6.2 accommodate the entire neutron energy spectrum expected at the SANRAD facility. This made the Au foil suitable for this work.

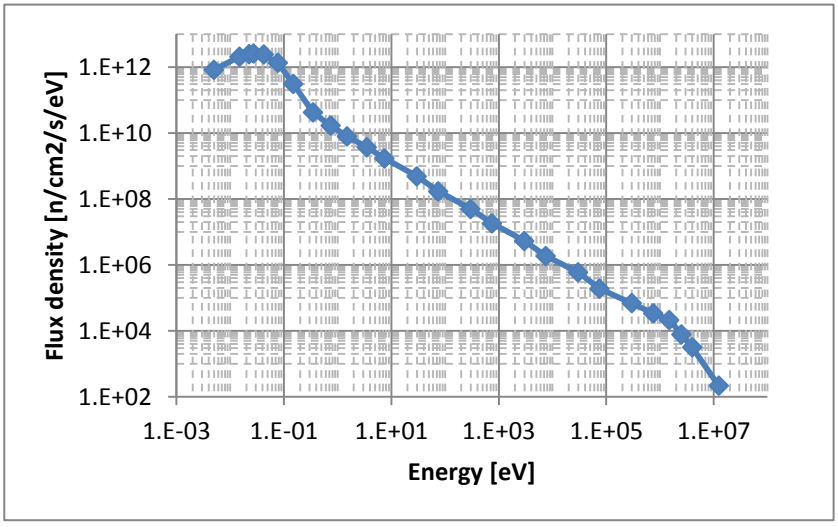

Figure 6.1: Neutron flux density as a function of energy for the new SANRAD facility (Radebe, 2012)

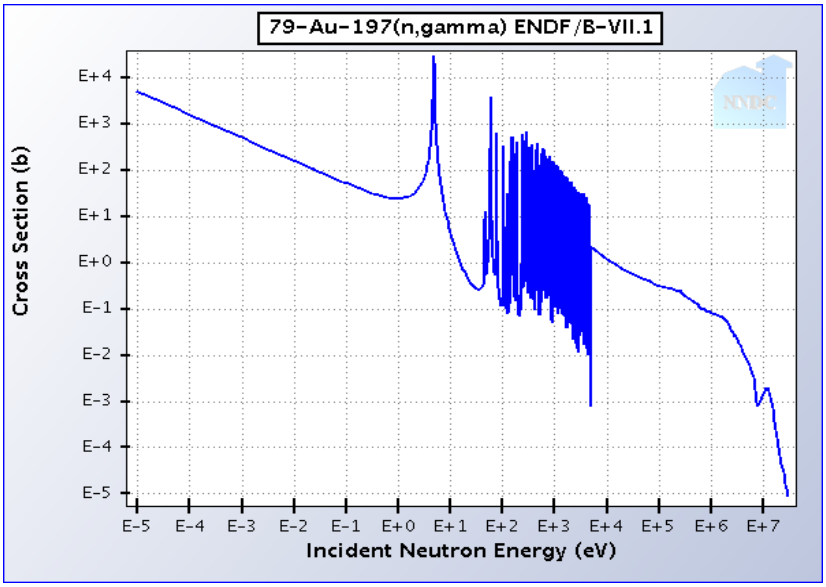

Figure 6.2: Neutron radiative capture cross-section as function of neutron energy for Au-197(Radebe, 2012)

When a gold foil is activated by a neutron beam, it emits characteristic gamma rays which can be counted and related to the neutron flux incident on the foil. By placing foils in front and between the shielding layers, the incident and transmitted neutron fluxes are obtained at each position of shielding thickness. It is known from the Lambert-Beer law that radiation attenuation character is given by:

$$\frac{I}{I_0} = e^{-\Sigma x} \quad \text{---------- (6)}$$

Where I_0 and I are the intensities of the beam before and after the transmission respectively, Σ and x are the linear attenuation coefficient (cm^{-1}) and the thickness (cm) of the sample respectively. Based on this expression, it is possible to calculate the linear attenuation coefficient which gives indication of the shielding capability of the shielding material. When corrected for electronic noise, background scattering and flux fluctuation, transmitted intensity can give a good indication of shielding ability of the shielding material. Intensities can be measured directly and indirectly through radiography and foil activation respectively. All measurements require correction for the detector efficiency in radiography and activation period, geometrical efficiency, detector efficiency, foil effective cross-section, foil storage period and material half-life in foil activation (Radebe, 2012).

6.2 Experimental procedure and set-up

6.2.1 The instruments and materials

The main apparatus used in this procedure was the current neutron radiography facility located at beam port number 2 of the 20 megawatt SAFARI-1 nuclear reactor. In addition to this, the following were required.

- Sodium Iodide (NaI) detector
- Foam to hold gold foils between the concrete samples
- Paraffin wax for limiting the beam onto the samples
- Fourteen 10 mm diameter and 0.05 mm thick gold foils
- Five 100 x 100 x 20 mm concrete slices
- Seven 100 x 100 x 100 mm concrete cubes

6.2.2 Experimental set-up

The set-up of the experiment was simplified as in Figure 6.3.The components and instruments are explained in the following sections.

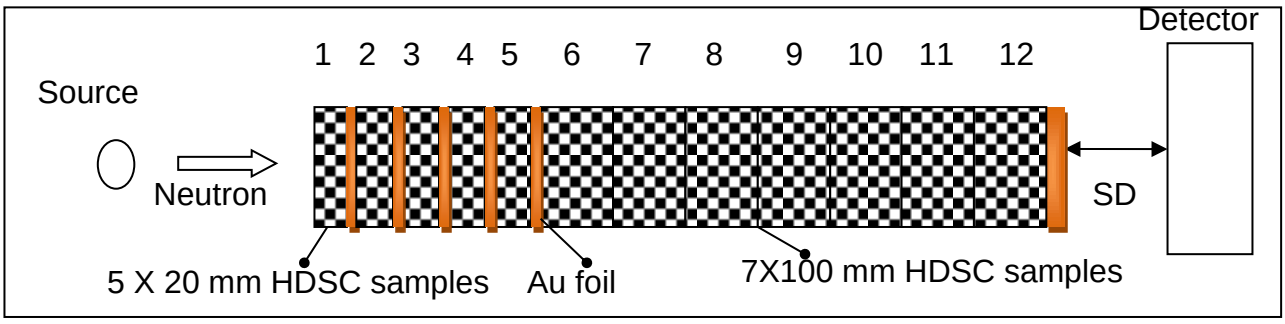

Figure 6.3: Top view experimental setup

6.2.2.1 Samples

The shielding material under evaluation was concrete with a density of 4230 kg/m^3 and surface area of 100 x 100 mm^2.The total concrete thickness tested was 800 mm which was made of 5 panels of 20 mm thickness and 7 panels of 100 mm thickness as shown in Figure 6.3. The 20 mm thick slices where obtained by cutting a 100 mm concrete cube using water jet cutting technology. This method was the only technique available

that could cut through the hard aggregates of the concrete as shown in Figure 6.4. Initially 10 mm slices were preferred but it was realised during cutting that these could not be achieved. Instead 20 mm samples were perfectly achievable and since these did not have any impact on the experiment and the set up, they were therefore used as replacement samples. The initial preferred 10 mm slices were impossible to cast directly from the fresh mixture because the average size of the coarse aggregate was 13 mm. The 20 mm slices were also not cast directly from the fresh concrete as a measure of preventing possible damage to the samples. This was because the concrete was still soft when removed from the moulds hence it needed to be cured in a room with controlled temperature and humidity for the first 7 days before it could be submerged in water for the rest of the curing period concrete.

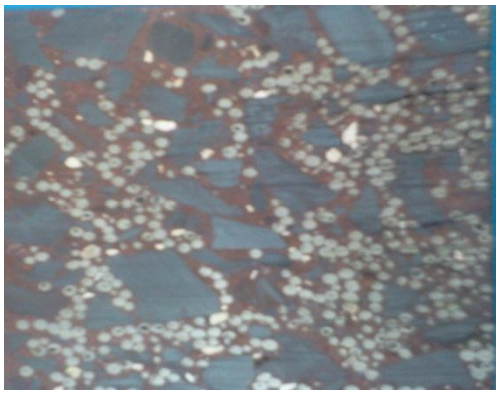

Figure 6.4: A freshly cut surface of concrete cube using water jet cutting

6.2.2.2 Beam limiting

The beam size was limited from the original size of 300 mm to 50 mm diameter circular area using wax and cadmium. This was to ensure that the neutron beam is completely focused only onto the 100 x 100 mm^2 samples so that correct readings from the foils are obtained. The wax cylinder in Figure 6.5 was prepared to fit into the protrusion of the external shutter. In this way, the set up could assist in shielding the scattered neutrons from the wax.

Figure 6.5: Prepared wax for beam limiting

The sequence of beam limiting material shown in Figure 6.6 consisted of 200 mm thick wax and cadmium sheet of 1 mm thickness. The beam limiter ensured that there was negligible neutron background from scattering neutron beam multiples.

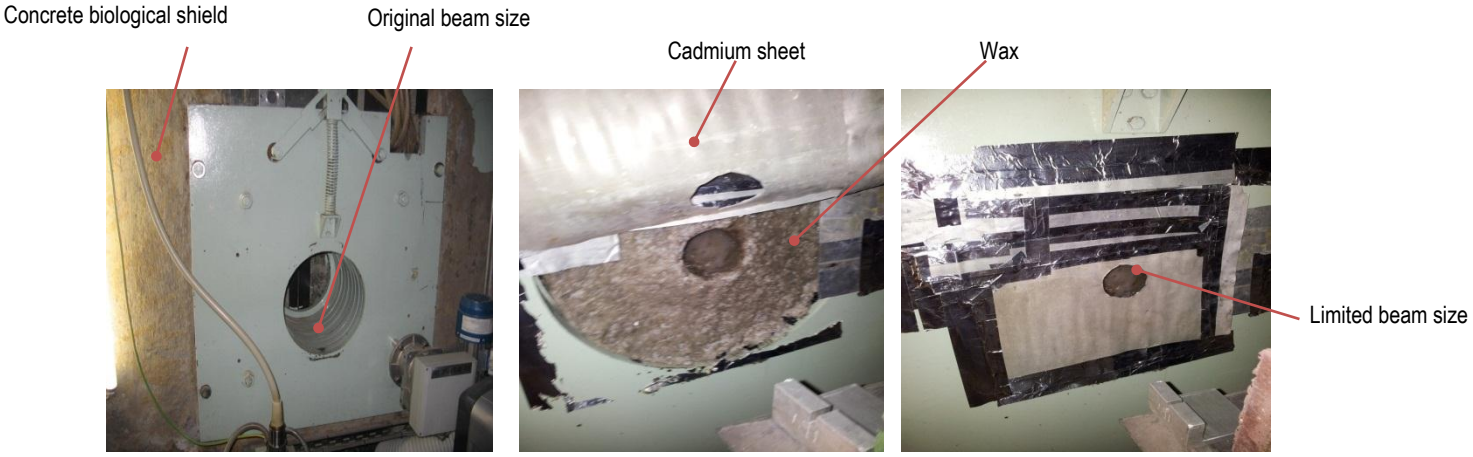

Figure 6.6: The 300 mm original size of the beam and the beam limiting mechanism used to reduce it to 50 mm.

6.2.2.3 Foil preparation and positioning

Foils were cut into 5 mm radius discs of 0.05 mm thickness. After all slices of the shielding material were placed in the beam axis ensuring that they are aligned to each other, foils were placed between the shielding material in positions F to B6 as shown in Figures 6.7 and 6.8. The 20 mm thick concrete slices were only employed in the first 100 mm thickness and the rest of the tested thicknesses were made up of 100 mm thick concrete cubes. The foils were only placed between the 20 mm slices and at the end of the 800 mm total thickness. The foils within the slices were used to determine the linear attenuation coefficient [Σ] and the last foil was used to verify the extrapolated results obtained using the experimental linear coefficient. Each foil was assigned a unique number and two foils were placed at each position on the left (L) and right (R) side with regard to the perspective of the shielding material facing the neutron beam. A total of 14 foils were used and their weights are as given in Table 6.1. Thin foam made out of formaldehyde, inorganic acid, barium sulfate and heptane was used to hold the foils in position and in line with the beam axis. The actual shielding experiment set-up is as presented in Figure 6.8.

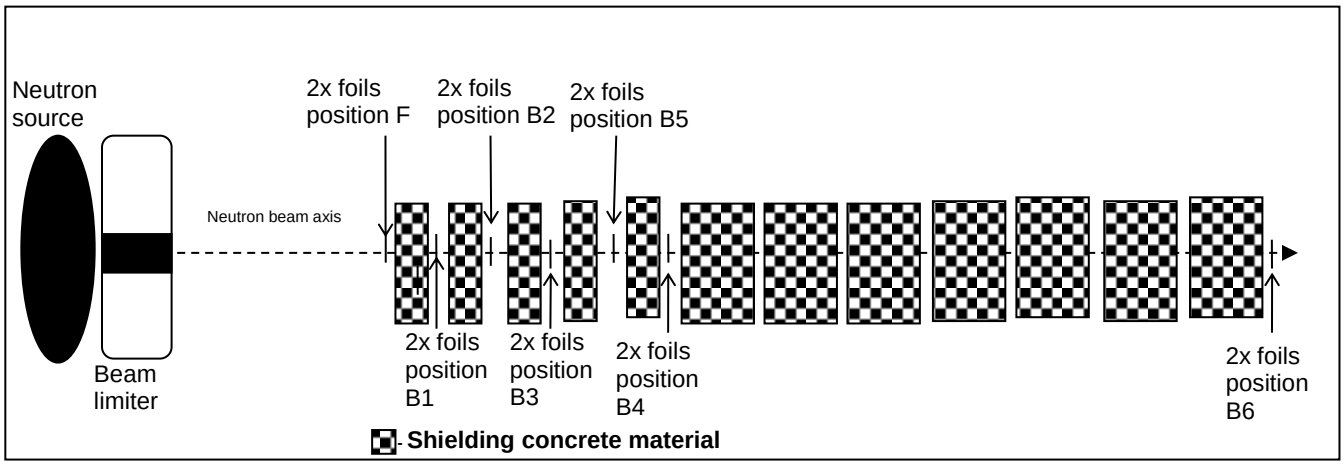

Figure 6.7: Side view of experimental setup

Figure 6.8: Experimental setup with foils

Table 6.1: Weights of the 14 foils used in the experiment

Foil ID	Weight (g)
14	0.0739
53	0.0709
49	0.0763
50	0.0766
35	0.0712
30	0.0722
36	0.0739
31	0.0715
37	0.0746
3	0.0743
12	0.0745
4	0.0715
29	0.0722
9	0.0743

6.2.3 Experimental procedure

The procedure employed in the gold foils activation by a transmitted neutron flux through the concrete shield material was as follows:

- Ensure interior and exterior shutters are closed.
- Open the facility door.
- Limit the beam tube on the wall to only 50 mm in diameter.
- Place all the layers of the shielding material in the beam axis.
- Place the gold foils inserted in the foam in front of, between and behind the shielding material layers in alignment with the beam axis.

- Close facility door.
- Open the shutters and allow the radiation from the reactor to interact with the shielding material for 5 days.
- Close the beam when activation period is over.
- Open facility door.
- Collect the foils.
- Take the foils to radiochemistry for activation analysis and calculation of the activating neutron flux from gamma rays counts.
- Determine the concrete's attenuation coefficient.
- Calculate intensities at other thicknesses where foils were not placed.

6.3 Results

The activity of the Au foils was measured with the SAFARI-1 counting facility according to the gammametry counting and correction procedure. The foils were positioned at a distance of 15 cm away from the NaI detector to ensure a reasonable count rate, and a low detector dead time. A dead time of 0% and 2% were recorded during the counting of foils and the calibration standards respectively. The 411keV (Au-198) gamma peak was used for the measurement of the Au foil activity. Measurements for flux calculation were conducted at thicknesses 0, 20, 40, 60, 80, 100 and 800 of the shielding material. The results for flux and dose rate are shown in Table 6.2. The linear attenuation coefficient was calculated to be 0.62 cm^{-1}, based on which the transmitted intensities for thickness 200, 300, 400, 600 and 700 mm were calculated. The energy deposited by the neutron beam to biological cells (i.e. dose rate) was calculated based on the effective conversion factor for the incident beam and transmitted beam behind every shielding layer where foils were activated. The conversion from neutron flux to dose rate was conducted in line with the database of the United States Nuclear Regulator Commission (USNR).The results in Figure 6.9 presents a threshold line which is the dose rate threshold below which there is adequate estimated shielding for personnel safety from neutrons as the dose rate is less than 10 µSv/h . The difference seen between the MCNP and experimental results may be related to the inclusion of the

bismuth filter in the experiment. The filter is applied in practical day-to-day setup of the facility operation.

Table 6.2: Experimental Results

Foil position		**Flux (n/cm2/s)**			**Dose rate (mSv/hr)**	
Face	Shielding thickness (mm)	Value	% difference	Average	Value	Average
F-L	0	1.10E+08	2.2	1.11E+08	4.02E+03	4.07E+03
F-R	0	1.12E+08			4.11E+03	
B1-L	20	3.98E+07	11.6	4.22E+07	1.77E+03	1.88E+03
B1-R	20	4.47E+07			1.99E+03	
B2-L	40	1.34E+07	12.5	1.43E+07	5.97E+02	6.37E+02
B2-R	40	1.52E+07			6.77E+02	
B3-L	60	4.72E+06	14.2	5.09E+06	2.10E+02	2.26E+02
B3-R	60	5.45E+06			2.42E+02	
B4-L	80	2.11E+06	19.6	2.34E+06	9.39E+01	1.04E+02
B4-R	80	2.57E+06			1.14E+02	
B5-L	100	1.22E+06	7.5	1.27E+06	5.23E+01	5.43E+01
B5-R	100	1.31E+06			5.63E+01	
Calculated[2]	200	8.64E+03	-	8.64E+03	3.70E-01	3.70E-01
Calculated[2]	300	9.60E+01	-	9.60E+01	4.11E-03	4.11E-03
Calculated[2]	350	1.01E+01	-	1.01E+01	4.33E-04	4.33E-04
Calculated[2]	400	1.07E+00	-	1.07E+00	4.57E-05	4.57E-05
Calculated[2]	500	1.18E-02	-	1.18E-02	5.08E-07	5.08E-07
Calculated[2]	600	1.32E-04	-	1.32E-04	5.64E-09	5.64E-09
Calculated[2]	700	1.46E-06	-	1.46E-06	6.26E-11	6.26E-11
L	800	2.32E-08	No signal	2.32E-08	8.52E-13	0.00E+00

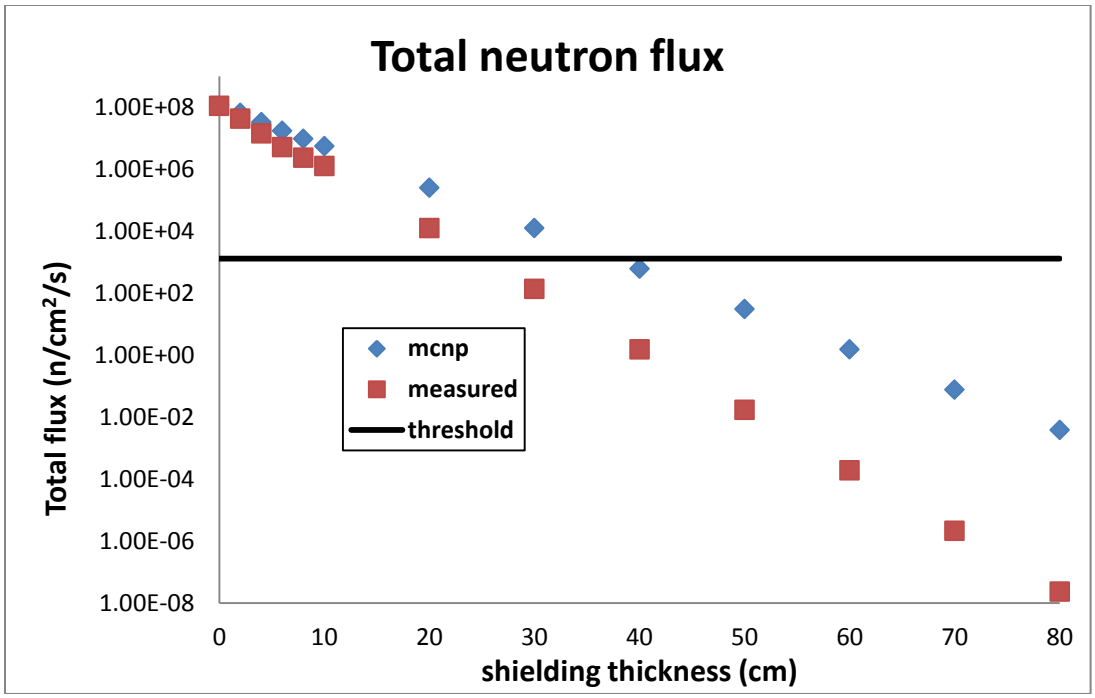

Figure 6.9: An extrapolated data of MCNP simulation and measured total flux at different thicknesses

6.4 Discussion and conclusion of results

The variation between the measured results and the MCNPX simulated data is because the measured data was conducted from a beam line with a 15 cm thick polycrystalline bismuth filter at room temperature, and the simulation considered a case where there was no filter. Satisfactory performance of the actual shield material was observed to be attained at around 250 to 300 mm thickness of the shield while that of the theoretical simulation were observed at 400 mm. Besides the effectiveness of the filter that was incorporated in the facility used for the experiment, there are also other factors that contributed for this difference. The simulation was conducted on the preliminary concrete mixture which was used as the basis for the development of the actual concrete shield. The final mixture adopted (TM7) had better properties and compositions than the preliminary mixture. The water to cement ration of the trial mixture was 0.42 and the final mixture used a water to cement ratio of 0.51. The density used in the simulation was conservatively limited to 4000 kg/m^3 while the actual concrete used in the experiment was of 4231 kg/m^3 density which is about 5.5% more than the density used in the MCNPX simulations.

The experiment has successfully demonstrated that the 600 mm thick shielding concrete of the experimental chamber of the SANRAD facility made of the developed will provide adequate shielding for personnel safety from neutrons, as the dose rates were proven to be far less than the regulatory 10μSv/hr outside the facility. The direct thermal neutron beam will be totally captured by the concrete developed in this study. The designed 600 mm thick walls of the SANRAD facility with TM7 is therefore expected to contain neutrons from the facility as required by the NNR.

The Au foil activation method successfully provided the total neutron flux and subsequently the estimated neutron dose rate through measuring gamma-rays that emerge from neutron activated Au foils by using a NaI detector. Neutron flux values obtained experimentally with gold foils are constantly lower than MCNPX simulation values which are effectively indicating the shielding requirements for the case with and without the 15 cm bismuth filter. Neighbouring facilities will be shielded by the 600 mm walls filled with the shielding concrete for scattered neutrons which will have more thermal energy distribution and less intensity than the direct neutron beam.

Chapter 7 Conclusions and recommended future studies

7.1 Conclusions

The work conducted in this study clearly indicates the procedure that should ideally be followed in developing concrete shield for any nuclear installation. Unlike other investigation conducted on the same subject, some which are reviewed in this report, this investigation did not only focus on one area of the development at the expense of the others which are also equally important in obtaining an effective shield. Firstly the study investigated the chemical compositions of the raw materials to be used in order to ensure that long half-life elements are avoided in the final mixture of the shield. Secondly the concrete was developed in such a way that critical mechanical properties of the final product important for its application are achieved. Lastly it was made sure that the developed concrete with the satisfactory mechanical properties provides the required shielding performance for the facility it was designed for.

The final developed mixture met all the requirements specified for shielding purposes. The aggregates used in the mixture contained no long half-life decaying elements. The required minimum density of 4000 kg/m^3 as simulated in the MCNP was achieved with the final mixture producing 4231 kg/m^3 and the mixture was of the desired slump and cohesion. The 28-day cube strength of 29.9 MPa achieved was well above the specified 25 MPa. The shielding capabilities of the hardened concrete were impressive with the desired dose rate being achieved at the first 250 to 300 mm thickness.

In all of these successful results, there was one challenge of the setting time of the concrete. This retardation effect was as a result of the necessary inclusion of colemanite in the mixture. The recommended concrete mixture took three days to fully set. Addition of HAC in the mixture allowed the concrete to set normally within 24 hours but this type of cement was not permitted in the concrete due to its known conversion process which resulted in failure of structure in 1970s. Even though the added HAC was in small quantities, this decision was taken because of the risk associated with not being able to obtain the construction and operation license from the NNR.

As a result of the challenging delay in setting, the gain in strength of concrete was slow during early days but increased after the concrete had fully set. To prevent damaging of the weak concrete at early days, a restriction was imposed, that the concrete blocks should be moved only after 28 days when it is known that the concrete would have gained sufficient strength. It was also recommended that the test cubes be demoulded after 3 days before being submerged under water for the rest of the remaining curing period.

The concrete mixture developed in this study was adopted for casting of the SANRAD facility at NECSA and was successfully used for the construction of the facility. The concrete was mixed at the Lafarge ready mix batching plant in Centurion in Pretoria and transported to NECSA in Pelindaba which is situated 32 km from the ready mix plant for the casting of the SANRAD facility's interlocking blocks. All the aggregates except for the accelerator were mixed at the plant. The accelerator was added at the arrival of the mixing truck on site. All the interlocking blocks of different configurations of the facility were cast successfully with ease as the concrete was workable and was of high slump. The boxes filled with concrete were left in their position covered with a curing plastic for 28 days until they could be moved.

7.2 Recommended future studies

The only recommendation in this study is with regards to the desired superior performance of the final product. In order for this type of concrete to be used in large structural elements such as reactor houses and reactor biological shields, the concrete needs to set within the normal setting time of conventional concrete. This is because in large construction, components such as columns are cast in stages. In terms of construction schedule it is not realistic for the contractor to wait for more than seven days for the next segment of the component to be cast in place. Since HAC is to be avoided in radiation shielding structural concrete, it is recommended that further studies to establish a special extender, additive, admixture or any possible aggregate that could be added to the developed SANRAD mixture to counter the retardation effect of

colemanite and achieve normal setting behaviour be conducted so that the SANRAD concrete can be applied in general construction. This modification in setting should be achieved without reducing the most important properties of the mixture such as density, strength, cohesion and high slump.

Reference List

Addis, B. (2004) *Fundamentals of concrete*. Midrand, South Africa: Cement and Concrete Institute, pp 65-77.

ASTM C637. (2009) *Standard Specification for Aggregates for Radiation Shielding Concrete*. American Society for Testing and Materials. C637-98a, pp 334 -337.

ASTM C638. (2009) *Standard Descriptive Nomenclature of Constituents of Aggregates for Radiation Shielding Concrete*. American Society for Testing and Materials. C638-92, pp 338 – 339.

Barborak, R. (2010) Calcium Aluminate Cement Concrete (Class CAC Concrete). INTERNET.http://ftp.dot.state.tx.us/pub/txdot-info/cst/tips/calcium_concrete.pdf Cited 13 December 2013.

Bishop, M. (2012) Cobalt 60. INTERNET. http://preparatorychemistry.com/Cobalt-60 Cited 16 January 2014.

Brown, FB; William, RM. (1984) *Monte Carlo methods for radiation transport analysis on vector computers*. Progress in nuclear energy Vol. 14(3), pp 269-299. Great Britain: Pregamon press Ltd.

Callan, EJ. (1962) *Concrete for radiation shielding*. 2nd edition. United States of America: American concrete institute.

Concrete Construction. (1960) High density Concretes for Radiation Shielding. INTERNET.www.concreteconstruction.net/concrete-articles/high-density-concretes-for-radiation-shielding.aspx Cited 14 July 2011.

De Beer, FC. (2005) *Neutron radiography new upgraded design- User requirements*. Pelindaba: NECSA Department of Radiation Science, pp 3-16.

Dubrovskii, V.B; Ibragimov, Sh.Sh; Korenevsii, V.V; Ladygin, A. Ya; Pergamenschik, V.K and Perevalov, V.S. (1970) *Hematite concrete for shielding against high neutron fluxes*. Atonmnaya Energiya Vol. 28(3), pp.258-260, March. New York: Consultants Bureau.

Ermichev, SG; Shapovalov, VI; Sviridov, NV; Orlov, VK; Seergeev, VM; Semyenov, AG; Visik, AM; Maslov, AA; Demin, AV; Petrov, DD; Noskov, VV; Sorokin, VI; Yuferov, OI; Dole, LR. (2005) *Optimization of composition and production technology of high-density concrete with ceramic aggregate based on depleted uranium oxide*. The 9th International Conference on Environmental Remediation and Radioactive Waste Management September 4 – 8, 2005. ICEM05-1356. Scotland: ASME.

Ferrada, JJ; Dole, LR and Ermichev, SG. (2006) *Analyses of U.S and R.F. Depleted –Uranium Concrete/Steel Transport and Storage Cask for Spent Nuclear Fuel*. IHLRWM conference April 30-May 4, 2006.Las Vegas.

García-Fernandez, C; Gonzalez, M and Velarde, P. (2008) *Study of the influence of numerical techniques of radiation in laser-matter interaction problems*. 35th EPS Conference on Plasma Physics 9 - 13 June, 2008. Hersonissos.

Gencel, O; Brostow, W; Ozel, C and Filiz, M. (2010) *An investigation on concrete properties containing colemanite*. International journal of physical science Vol 5(3), pp. 216-225.

Gruenauer, F. (2005) *Design, optimization, and implementation of the new neutron radiography facility at FRM-II*. Germany: Technische Universitat München- faculty of physics.

Hammer, EE and McCarthy, AE. (1975) *Shielding materials*. Engineering compendium on radiation shielding. Vol 2, Ch 9. Berlin Heidelberg: Springer-Verlag.

HPS. (2013) What is Radiation. INTERNET. www.hps.org/publicinformation. Cited 02 January 2014.

Hoffman, J. (2012) *Characteristics of the Micro-Focus X-ray Tomography (MIXRAD) facility at Necsa in South Africa*. WCNDT-18.

ICRP. (2007) *ICRP Publication 103— Recommendations of the International Commission on Radiological Protection*. Annals of the ICRP 37 (24).

Ivanov, K. (2013) NucE 521 Neutron Transport Theory. INTERNET. http://www.engr.psu.edu/cde/courses/nuce521/nuce521_chapter1_reading.pdf Cited 02 May 2013.

Kaplan, MF. (1989) *Concrete radiation shielding: nuclear physics, concrete properties, design and construction*. United Kingdom: Longman group.

Kharita, MH; Takeyeddin; Alnassar, M. and Yousef, S. (2007) *Development of special radiation shielding concrete using natural local materials and evaluation of their shielding characteristics*. Progress in nuclear energy 50, pp.33-36, Elsevier.

Kubayashi, K; Yamamoto, S; Kimura, I; Miki, R and Itoh, T. (1988) *Multi-foil activation at the central graphite cavity of UTR-KINKI.* Kinki University academic resource reposity.

Mahdy, M; Speare, PRS and Abdel-Reheem, AH. (2002) *Effect of transient high temperature on heavyweight, high strength concrete*. 15th ASCE engineering mechanics conference, June 2-5, 2002.New York: University of Columbia.

Masitise, NM; Mhlanga LL. (2012) *Basic Design Package for the NRAD facility*. Pelindaba: NECSA Mechanical Engineering Services, pp 2-5.

Mortazavi, SMJ; Mosleh-Shiraz, MA; Maheri, MR; Yousefnia, H; Zolghadri, S and Haji-poue,A. (2007) *Production of economic high-density concrete for shielding megavoltage radiography rooms and nuclear reactors*. Iran.J.Radiat.Res Vol 5(3), pp. 143-146.

National Nuclear Regulator. (2013) Understanding Radiation. INTERNET. www.nnr.co.za Cited 14 January 2014.

Osman, G; Witold, B; Cengiz, O; Mumin, F. (2001) *Concretes Containing Hematite for Use as Shielding Barriers*. Materials science (MEDŽIAGOTYRA). Vol. 16, No. 3.

Quapp, WJ. (1999) *Ducrete^{TM} shielding application in the Yucca mountain repository*. WM'99 Conference February 28 - March 4, 1999. Waste Management Symposia.

Radebe, MJ. (2012) *Measurement of shielding ability of the new concrete using Gold foils*. Pelindaba: NECSA Department of Radiation Science, pp 5-9.

Radebe, MJ; De beer, FC. (2008) *Current radiography and tomography application at NECSA and an envisaged upgrade towards a proposed South African National Centre for radiography and tomography (SANCRT)*. IYNC conference 20-26 September, 2008. Interlaken. Switzerland

Saglam, S. (2003) *Discrete ordinate method and examination of some benchmark problems*. Journal of Istanbul Kultur University 2003/3, pp. 99-106.

Scherrer, P. Institut,(2007) Neutron imaging. INTERNET. www.psi.ch/industry/MediaBoard/neutron_imaging_e_07.pdf Cited 12 December 2012.

Sathian, V; Deepa, S; Phadnis, UV; Soni, PS and Sharma, DN. (2008) *Neutron Spectrum Measurement in a Medical Cyclotron*. 12th International congress of the international radiation protection association October 19 – 24, 2008. Buenos Aires-Argentina.

Wagner, JC. (1994) *Monte Carlo transport calculations and analysis for reactor pressure vessel neutron influence*. Pennsylvania: Pennsylvania State University.

Warnke, EP; Wienert, R; Kramm, K and Bounin, D. (2001) *A new concrete shielding material for waste management*. SMiRT 16, August. Washington DC

A. Appendix

Sieve analysis results of fine aggregates.

Table A.1: Superfine grading results (A)

SANS Sieve size(mm)	Mass of Sieve(g)(A)	Mass of sieve After Shaking(B)	Mass retained on Sieve (B-A)	Retained as % of total mass	Cumulative % Retained on Sieve	Cumulative % Passing sieve
4.75	451.5	451.5	0	0	0	100
2.36	559	559	0	0	0	100
1.18	556.8	557.8	1	0.2	0.2	99.8
0.6	343.3	363.3	20	3.3	3.5	96.5
0.3	295.5	465.3	169.8	28.3	31.8	68.2
0.15	456.6	722.1	265.5	44.3	76.1	23.9
0.075	265.3	374.6	109.3	18.2	94.3	5.7
Pan	449.6	483.7	34.1	5.7	100	0
Total	-	-	599.7	100	111.6	-
FM			**1.1**			

Table A.2 : Fines Grading Results

SANS sieve size(mm)	Mass of Sieve(g)(A)	Mass of sieve After Shaking(B)	Mass retained on Sieve (B-A)	Retained as % of total mass	Cumulative % Retained on Sieve	Cumulative % Passing sieve
4.75	451.4	561.7	110.3	18.4	18.4	81.6
2.36	558.9	762.4	203.5	34.0	52.4	47.6
1.18	556.7	746.5	189.8	31.7	84.1	15.9
0.6	343.3	422.1	78.8	13.2	97.2	2.8
0.3	295.5	305.5	10	1.7	98.9	1.1
0.15	456.6	457.3	0.7	0.1	99.0	1.0
0.075	265.3	266.1	0.8	0.1	99.2	0.8
Pan	449.7	454.7	5	0.8	100.0	0.0
Total	-	-	598.9	100	450.1	-
FM			**4.5**			

Table A.3: 50/50 blend (A/B)

SANS SIEVE SIZE(mm)	Mass of Sieve(g)(A)	Mass of sieve After Shaking(B)	Mass retained on Sieve (B-A)	Retained as % of total mass	Cumulative % Retained on Sieve	Cumulative % Passing sieve
4.75	451.5	530.8	79.3	13.3	13.3	86.7
2.36	559	653.8	94.8	15.8	29.1	70.9
1.18	556.8	626.3	69.5	11.6	40.7	59.3
0.6	343.3	393.5	50.2	8.4	49.1	50.9
0.3	295.5	384.2	88.7	14.8	63.9	36.1
0.15	457.1	592.3	135.2	22.6	86.5	13.5
0.075	265.4	322.8	57.4	9.6	96.1	3.9
Pan	449.7	473	23.3	3.9	100.0	0.0
Total	-	-	598.4	100	282.6	-
FM				2.8		

Table A.4: 55/45 blend (A/B)

SANS SIEVE SIZE(mm)	Mass of Sieve(g)(A)	Mass of sieve After Shaking(B)	Mass retained on Sieve (B-A)	Retained as % of total mass	Cumulative % Retained on Sieve	Cumulative % Passing sieve
4.75	451.5	488.9	37.4	6.2	6.2	93.8
2.36	559	634.6	75.6	12.6	18.9	81.1
1.18	556.8	649.9	93.1	15.5	34.4	65.6
0.6	343.3	406.1	62.8	10.5	44.9	55.1
0.3	295.5	406.2	110.7	18.5	63.4	36.6
0.15	456.7	602.2	145.5	24.3	87.7	12.3
0.075	265.3	321.7	56.4	9.4	97.1	2.9
Pan	449.6	467	17.4	2.9	100.0	0.0
Total	-	-	598.9	100	255.5	-
FM			**2.6**			

Table A.5: 60/40 blend (A/B)

SANS SIEVE SIZE(mm)	Mass of Sieve(g)(A)	Mass of sieve After Shaking(B)	Mass retained on Sieve (B-A)	Retained as % of total mass	Cumulative % Retained on Sieve	Cumulative % Passing sieve
4.75	451.5	491.1	39.6	6.6	6.6	93.4
2.36	559	635.6	76.6	12.8	19.4	80.6
1.18	556.8	630	73.2	12.2	31.6	68.4
0.6	343.3	396	52.7	8.8	40.3	59.7
0.3	295.5	414	118.5	19.7	60.1	39.9
0.15	456.7	613.3	156.6	26.1	86.2	13.8
0.075	265.3	329.8	64.5	10.7	96.9	3.1
Pan	449.6	468	18.4	3.1	100.0	0.0
Total	-		600.1	100	244.1	-
FM			**2.4**			

Table A.6: 65/35 blend (A/B)

SANS SIEVE SIZE(mm)	Mass of Sieve(g)(A)	Mass of sieve After Shaking(B)	Mass retained on Sieve (B-A)	Retained as % of total mass	Cumulative % Retained on Sieve	Cumulative % Passing sieve
4.75	451.5	489.2	37.7	6.3	6.3	93.7
2.36	559	628.7	69.7	11.6	17.9	82.1
1.18	556.8	615.9	59.1	9.8	27.7	72.3
0.6	343.3	391.1	47.8	8.0	35.7	64.3
0.3	295.5	416	120.5	20.1	55.8	44.2
0.15	456.7	630.1	173.4	28.9	84.7	15.3
0.075	265.3	335.8	70.5	11.7	96.4	3.6
Pan	449.6	471.1	21.5	3.6	100.0	0.0
Total	-	-	600.2	100	228.1	-
FM			**2.3**			

Table A.7: 70/30 blend (A/B)

SANS SIEVE SIZE(mm)	Mass of Sieve(g)(A)	Mass of sieve After Shaking(B)	Mass retained on Sieve (B-A)	Retained as % of total mass	Cumulative % Retained on Sieve	Cumulative % Passing sieve
4.75	451.5	469.4	17.9	3.0	3.0	97.1
2.36	559.0	619.4	60.4	10.1	13.1	87.0
1.18	556.8	617.2	60.4	10.1	23.2	76.9
0.6	343.3	392.0	48.7	8.2	31.4	68.7
0.3	295.5	430.6	135.1	22.6	54.0	46.1
0.15	456.7	640.0	183.3	30.7	84.6	15.5
0.075	265.3	338.6	73.3	12.3	96.9	3.2
Pan	449.6	468.7	19.1	3.2	100.1	0.0
Total	-	-	598.0	100.0	209.2	-
FM			**2.1**			

Table A.8: Colemanite grading results

SANS sieve size(mm)	Mass of Sieve(g)(A)	Mass of sieve After Shaking(B)	Mass retained on Sieve (B-A)	Retained as % of total mass	Cumulative % Retained on Sieve	Cumulative % Passing sieve
4.75	451.5	460.2	8.7	1.5	1.5	98.5
2.36	559	914	355	59.2	60.7	39.3
1.18	556.8	775.6	218.8	36.5	97.1	2.9
0.6	343.3	348.5	5.2	0.9	98.0	2.0
0.3	295.5	296.2	0.7	0.1	98.1	1.9
0.15	456.7	457.6	0.9	0.2	98.3	1.7
0.075	265.3	267	1.7	0.3	98.6	1.4
Pan	449.6	458.2	8.6	1.4	100.0	0.0
Total	-	-	599.6	100	453.7	-
FM			**4.5**			

B. Appendix

Material Data Sheets

B.1 Superplasticiser 1: Optima 100

CHRYSO

LA CHIMIE AU SERVICE DES MATERIAUX DE CONSTRUCTION

CHRYSO®Fluid Optima 100

Plasticizer – Water reducer

CE NF

Description

CHRYSO®Fluid Optima 10 is a plasticizer – water reducer which works as a new generation superplasticizer based on modified phosphonate. Its specifically designed molecular structure gives it exceptional properties as a concrete additive.

Using **CHRYSO®Fluid Optima 100** results extensive workability at all levels of consistency, compared to standard additives.

In this respect, **CHRYSO®Fluid Optima 100** is particularly adapted to the pumping of concrete over long distances.

CHRYSO®Fluid Optima 100 is compatible with most types of cement. In most cases, it is the solution to cement / admixture incompatibility.

On account of all these characteristics, **CHRYSO®Fluid Optima 100** is a superplasticizer which is particularly adapted for use on construction sites and in the ready mix concrete industry.

Characteristics

- Nature: liquid
- Colour: white / yellow, slightly milky
- Density (20 °C): 1.06 ± 0.01
- pH: 4.0 ± 0.5
- Freezing point: about – 3 °C
- Cl^- ions content: ≤ 0.10%
- Na_2O equivalent: ≤ 0.3%
- Dry extract (halogen): 30.0% ± 1.5%
- Dry extract (EN 480-8): 31.0% ± 1.5%

Packaging

- Bulk
- Drums 60 L
- Plastic barrels of 215 L

Conformity

CHRYSO®Fluid Optima 100 is a plasticizer – water reducer which conforms to CE marking. The appropriate declaration can be found on our internet site.

CHRYSO®Fluid Optima 100 also conforms to NF 085 certification, which technical specifications are those applied in the non harmonised part of the **NF EN 934-2**.

AFNOR – 11 avenue F. de Pressensé – 93571 Saint Denis La Plaine cedex - France

Application

Domains of application

- All types of cement
- High performance and very high performance concrete
- Extended workability concrete
- Pumped concrete
- Prestressed concrete
- Highly reinforced concrete

Method of use

Dosage: from 0.3 to 5 kg per 100 kg of cement.
A 1% dosage of the product of the weight of cement is commonly used.

CHRYSO®Fluid Optima 100 is completely miscible in water and must be added to the mixing water in order to take advantage of the concrete workability to the best. However, it can also be added later.

The optimum dosage of **CHRYSO®Fluid Optima 100** can only be established after trial tests, taking into account local conditions affecting the workability of the mix and the mechanical properties required for concrete.

Depending on the application, it is possible to use **CHRYSO®Fluid Optima 100** at the same time as other **CHRYSO®** additives.

Precautions

- Avoid prolonged exposure to high temperatures.
- Store away from frost.
- Should the product freeze, it will recover its properties after thawing and agitating.
- Shelf life: 9 months.

CHRYSO : 19, place de la Résistance - 92446 Issy les Moulineaux cedex France - Tél. : 01 41 17 18 19 - Fax : 01 41 17 18 80

Entreprise certifiée AFAQ ISO 9001

B.2 Superplasticiser 2: Optima 203

CHRYSO
LA CHIMIE AU SERVICE DES MATERIAUX DE CONSTRUCTION

CHRYSO®Fluid Optima 203

Plasticizer – Water reducer

CE NF ASTM

Description

CHRYSO®Fluid Optima 203 is a new generation plasticizer – water reducer based on modified polycarboxylate, which works as a superplasticizer.

CHRYSO®Fluid Optima 203 is particularly formulated to maintain high workability with cement for which this specificity is difficult to obtain.

CHRYSO®Fluid Optima 203 is especially recommended for use in ready-mix concrete.

CHRYSO®Fluid Optima 203 is suitable for use in homogeneous self-compacting concrete.

Characteristics

- Nature: liquid
- Colour: green-brown
- Density (20 °C): 1.04 ± 0.01
- pH: 7.0 ± 2.0
- Cl^- ions content: ≤ 0.10%
- Na_2O equivalent: ≤ 1.0%
- Dry extract (halogen): 21.5% ± 1%
- Dry extract (EN 480-8): 21.7% ± 1%

Packaging

- Bulk
- Drums of 60 L
- Plastic barrels of 215 L
- Cubitainers of 1000 L

Conformity

CHRYSO® Fluid Optima 203 is a plasticizer – water reducer which conforms to CE marking. The appropriate declaration can be found on our internet site.
CHRYSO® Fluid Optima 203 also conforms to NF 085 certification, which technical specifications are those applied in the non harmonized part of the **NF EN 934-2**.
CHRYSO® Fluid Optima 203 also conforms to **ASTM C494 – Types A/F/G** standards.
Adresse AFNOR – 11 avenue F. de Pressensé – 93571 Saint Denis La Plaine Cedex

Application

Domains of application

- Ready-mix concrete
- High performance and very high performance concrete
- Plastic or fluid concrete
- Self-compacting concrete

Method of use

Dosage: 0.3 to 3.0 kg for 100 kg of cement.

CHRYSO®Fluid Optima 203 may be added in the mixing water or later directly on concrete.

When used as a "plasticizer", it is necessary to mix at high speed for 1 minute per m^3 of concrete (with a minimum length of 6 minutes).

Precautions

- Avoid prolonged exposure to high temperatures.
- Store away from frost.
- Should the product freeze, it will recover its properties after thawing and agitating.
- Store in plastic containers, PVC excepted.
- Shelf life: 12 months.

CHRYSO : 19, place de la Résistance - 92446 Issy les Moulineaux cedex France - Tél. : 01 41 17 18 19 - Fax : 01 41 17 18 80

Entreprise certifiée AFAQ ISO 9001

B.3 Accelerator: Xel 650

CHRYSO
CHEMICAL SOLUTIONS FOR THE CONSTRUCTION MATERIALS INDUSTRY

CHRYSO®Xel 650

Set Accelerator

DESCRIPTION
CHRYSO®Xel 650 is a specific non chloride formulation that promotes initial hydration of cements, particularly at low temperature. The set is accelerated and compressive strength develops rapidly.

CHRYSO®Xel 650 is slightly alkaline.

Characteristics

- Nature : liquid
- Density : 1.45 ± 0.01
- Colour : yellow / orange
- pH : 6 ± 1
- Freezing point : about -15°C
- Cl^- ions content : nil to BS 5075
- Na_2O equiv. : ≤ 2.7%
- Dry extracts : 60% ± 2.6%

Packaging

Bulk
Barrels : 215 Litres
Drums : 60 Litres

Conformity
CHRYSO®Xel 650 is a set accelerator which conforms to NF-EN 934-2.

METHOD OF USE
Applications

- All types of cement
- Shuttered concrete
- Pre-stressed concrete
- Precast elements
- Ready mix concrete.
- Pouring of concrete in cold weather

Directions for use
Dosage : 0.4 to 2.5 kg per 100 kg of cement. A 1.5% dosage of the product to the weight of cement is commonly used.
CHRYSO®Xel 650 is completely miscible in water. It must be added to the mixing water.
The optimum dosage of **CHRYSO®Xel 650** can only be established after trial tests, taking into account local conditions affecting the workability of the mix and the mechanical properties required from the concrete.

Precautions

- Do not mix with acidic products.
- If frozen refer to the Chryso technical department for information.
- The shelf life of **CHRYSO®Xel 650** is 18 months.

Tests
Example of results obtained according to the methods defined in the NF-EN 480-1 European certification. Type of concrete : Cement grade 42.5
(SSB : 3200 - 4000 cm2/g and C_3A : 7-11%).
Tests carried out for equal consistency.

	Water T°C	Initial set	Final set	Time taken to set
Control	0,5 à 5°C	650 min	1380 min	730 min
1.7% wt/wt	0,5 à 5°C	300 min	778 min	478 min
CHRYSOXEL 650	0,5 à 20°C	200 min	345 min	145 min

SAFETY

CHRYSO®Xel 650 is classified "Harmful". Whilst handling, it is obligatory to have skin and eye protection, avoid prolonged inhalation of the fumes. Refer to safety data sheet.

B.4 CEM I 52.5N with 15% fly ash: Rapidcem

CEMENT

Strength Performance

Rapidcem - Performance curves

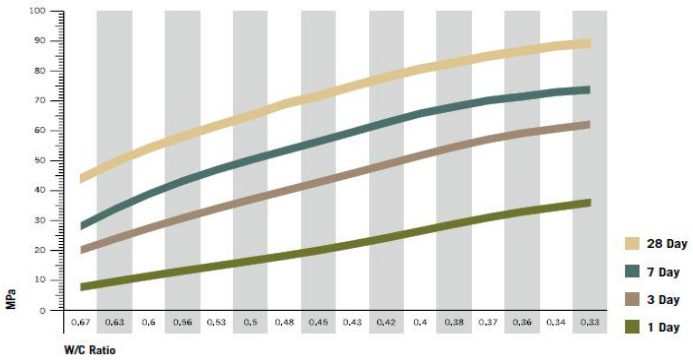

Typical Applications

Incorporating the benefit of Lafarge's unequalled technical resources, Rapidcem adds value to our customers' businesses. Typical applications are:

- Culverts and precast concrete products in general
- Poles and spun concrete pipes
- Concrete roof tiles
- On site blending of high strength custom mixes
- Prestressed floor slabs
- Prestressed railway sleepers

Quality

Rapidcem complies with the chemical and physical requirements of SANS 50197 (EN197) for a Class 52,5N cement.

PHYSICAL PROPERTIES		
Property	**Rapidcem***	**EN 197 SANS 50197 Requirement**
2 day *compressive strength*	> 28,5 MPa	≥ 20,0 MPa
28 day *compressive strength*	> 58,0 MPa	≥ 52,5 MPa
Initial set	160 minutes	≥ 45 minutes
Soundness	< 1,0 mm	< 10mm

**Average test results*

CHEMICAL PROPERTIES		
SO_3	2,60% m/m	≤ 4,0% m/m
Cl^-	0,07% m/m	≤ 0,10% m/m

Technical Services

Rapidcem is fully supported by Lafarge Cement's Quality Department Southern Africa, which is a SANAS accredited Civil Engineering testing facility.

Contact us

For further information on Rapidcem, please contact us:
Toll-free: 0800 110 104 or **Call Centre: 011 257 3085**

Lafarge Cement Head Office
Buildings 3&4 Country Club Estate,
21 Woodlands Drive, Woodmead, 2191
Tel: (011) 257 3100
Fax: (011) 257 3052

www.lafarge.co.za

LAFARGE

B.5 High Aluminate Cement: Ciment Fondu

Product data sheet

Reference PDS-US-CF-8/06

Ciment Fondu®

Updated 8/23/2006

1 General Characteristics

All calcium aluminate cements possess the general properties of **good refractoriness** and **high early strength** when used alone as the principal hydraulic binder. The latter property is often used in combination with other minerals such as calcium sulfate and/or Portland cement to produce high early strengths and/or shrinkage compensation through the formation of ettringite.

Composed mainly of calcium aluminates, CIMENT FONDU® can be used as the primary binder or in combination with other reactive minerals. These combinations comprise the binder in many construction products such as self-leveling floor products, fast setting patch materials, non shrink grouts and tile installation products.

CIMENT FONDU® additions to Portland cement will accelerate the initial set from hours to minutes depending on the type and mill of manufactured Portland cement.

CIMENT FONDU® is a refractory cement that can be used as the primary binder in mortars and concretes exposed to high temperatures. Due to a significant iron oxide content, CIMENT FONDU® should not be used in applications where reducing atmospheres are present.

CIMENT FONDU® is recommended for applications requiring rapid hardening properties, resistance to abrasion and mechanical shock, resistance to chemical attack and exposure to intermediate temperatures.

Calcium aluminate cements do not release Calcium Hydroxide as a hydration product when used as the sole hydraulic compound in a formulation. This imparts good refractoriness, chemical resistance and eliminates the major cause of efflorescence.

As a binder, CIMENT FONDU® reacts with most organic and mineral additives to achieve exceptional flow with high early compressive strength.

CIMENT FONDU® is a very dark gray color. Colorimetry data is available on request.

CIMENT FONDU® does not contain any additives.

CIMENT FONDU® does not contain crystalline silica.

2 Specifications

CIMENT FONDU® produced and distributed in North America adheres to the following specifications:

Chemical constituents (% by XRF chemistry)			
Al_2O_3	CaO	SiO_2	Fe_2O_3
≥ 37.0	≤ 39.8	≤ 6.0	≤ 18.5

- Blaine fineness: 3600-4400 cm^2/g (ASTM C204)

Physical Properties (using EN-196 sand mortar)

- Flow at 15 min: ≥ 30% (ASTM C1437)
- Vicat Initial Set: ≥120 min.
- Vicat Final Set: ≤ 240 min

Modified ASTM C191 - Needle weight is 1000g, needle diameter is 1.16 mm, samples immersed in water.

- Compressive strength (ASTM C349)
  6 hr ≥ 2900 psi (20.0 MPa)
  24 hr ≥ 4900 psi (33.8 MPa)

For detailed test procedures, please contact a Kerneos Technical or Quality Manager.

Kerneos Inc.
1316 Priority Lane Chesapeake, VA 23324
Phone: (757) 284-3200 - FAX: (757) 284-3300

kerneos ALUMINATE TECHNOLOGIES

ISO 9001

3 Additional Physical properties

- Bulk density: 1.16 – 1.37 g/cm^3 (72.4 – 85.5 lb/ft^3)
- Specific gravity: approx. 3.24
- Residue at 90 microns (+170 mesh): < 8%
- Pyrometric cone equivalent - ASTM C24 on neat cement paste: 8-9 (≈ 2320° F or 1271° C)
- Heat of hydration

6h	340 kJ/kg
24h	445 kJ/kg
5d	445 kJ/kg

Minor constituents (% by XRF Chemistry)			
TiO_2	MgO	SO_3	K_2O+Na_2O
< 4.0	< 1.5	< 0.4	< 0.4

- Principal mineralogical phase: calcium aluminate CA
- Secondary phases: $C_{12}A_7$, C_2S, Ferrites, C_4AF

C = CaO A = Al_2O_3 S = SiO_2 F = Fe_2O_3

4 Packaging & Shelf Life

CIMENT FONDU® is available palletized in 94 lb bags or 3000 lb. super sacks. It is also available in bulk semi-tanker or rail car.

CIMENT FONDU® packaging is designed to protect it from humidity. However, as with all hydraulic binders, it is recommended that CIMENT FONDU® not be placed outdoors or in direct contact with the ground. When correctly stored in dry conditions, the properties of CIMENT FONDU® will remain within specification limit for at least 6 months. In most cases, its properties will be retained for over a year.

Mineralogy

KERNEOS LIMITED WARRANTY
Kerneos warrants that this product, at the time of shipment, conforms to the Specifications set forth in section 2 of this Product Data Sheet. All other information provided in this Product Data Sheet is for guidance only. ALL OTHER WARRANTIES, INCLUDING WITHOUT LIMITATION THE WARRANTIES OF MERCHANTABILITY AND FITNESS FOR A PARTICULAR PURPOSE, ARE EXCLUDED. Kerneos' sole obligation and the sole and exclusive remedy under this limited warranty shall be the replacement of any nonconforming product, or, at Kerneos' option, the refund of the purchase price. No warranty is given for any technical advice or recommendations provided by Kerneos. Buyer waives all claims under this limited warranty unless it has given written notice of nonconformity within 30 days of delivery.

Kerneos Inc.
1316 Priority Lane Chesapeake, VA 23324
Phone: (757) 284-3200 - FAX: (757) 284-3300

kerneos ALUMINATE TECHNOLOGIES

ISO 9001

B. 6 Condensed Silica Fume: Microfume

Microfume® Refractories

FerroPem
FerroAtlántica

Amorphous and stable light grey silicon oxide powder, obtained by filtering the dust extracted from the production of silicon metal in an electric arc furnace. **Microfume® Refractories** has a stable pH and a low impurity level and is perfectly adapted to the requirements of refractory castables. Its use improves the flow, the mechanical properties (especially hot strength), and durability (via permeability reduction).

Physical and chemical characteristics

Analysis**	Typical	Limits	
		Min	Max
SiO_2 (%)	96	94	98
Total C (%)	2.0	1.5	2.5
Free Si (%)	0.12	0.1	0.16
Total CaO (%)	0.68	0.5	1.5
SO_3 (%)	0.25	0.15	0.37
Na_2O (%)	0.18	0.10	0.25
K_2O (%)	0.45	0.35	0.60
Cl- (%)	0.015	<0.01***	0.03
Al_2O_3 (%)	< 0.1***	<0.1***	0.2
Fe_2O_3 (%)	< 0.1***	< 0.1***	< 0.1***
MgO (%)	0.2	< 0.1***	0.3
H_2O (%)	0.45	0.1	1.0
pH	6.5	6.3	6.7
Loss on Ignition (at 950°C during 1h) (%)	1.8	1.0	3.0
Specific surface (BET) (m^2/g)	22.5	20	25
Brightness L*	47	45	50

** % by weight of dry mass. *** Lower limit detection

Packaging	Bulk in trucks or in big-bags. Others packaging on request.
Storage	Dry storage. Avoid contact with moisture.
Handling	Product totally amorphous. Material Safety Data Sheet available on *http://www.fdsc.fr/fp*.
Application	Low and Medium-Low Cement Refractory Castables, vibrated or Self Consolidating Concrete (SCC).
Origin	France.
Quality Control	Complies with the ISO 9001norm.
Environment	Complies with the ISO 14001norm.
Safety	Complies with the OHSAS 18001norm.

FERROPEM
517, avenue de la Boisse – F-73025 Chambéry – France.
Contact our sales representative for technical information and support:
Tel: +33 (0)4 79 68 31 35 / Fax: +33 (0)4 79 68 31 32
E-mail: microfume@pemsil.com
Website: www.ferroatlantica.es

Sept 2010